CROSS-PHASE MODULATION IN RUBIDIUM-87

Gary F. Sinclair

A Thesis Submitted for the Degree of PhD
at the
University of St. Andrews

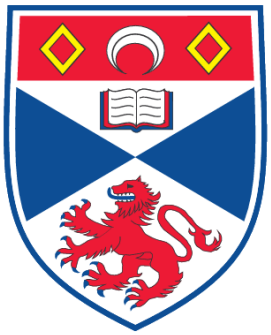

2009

Cross-Phase Modulation in Rubidium-87

Gary F. Sinclair

PhD Thesis

School of Physics and Astronomy,

University of St Andrews,

St Andrews,
United Kingdom

26th February, 2009

Contents

Abstract

This thesis explores the theoretical foundations of cross-phase modulation (XPM) between optical fields in the N-configuration atom. This is the process by which the refractive index experienced by one field can be modulated by controlling the intensity of another. The electro-optical version of this effect was first discovered by John Kerr in 1875 and found applications in photonics as a means of very rapidly modulating the phase and intensity of electromagnetic fields. Due to recent advances in experimental techniques there has been growing interest in generating nonlinear optical interactions in coherently prepared atomic ensembles.

The use of coherently prepared media brings the possibility of achieving a much larger cross-phase modulation than is possible using classical materials. This is particularly useful when trying to create large optical nonlinearities between low-intensity electromagnetic fields. Much of the current research into cross-phase modulation is directed towards realising potential applications in the emerging field of quantum information processing. Above all, the possibility of constructing an all-optical quantum computer has been at the heart of much research and controversy in the field.

In this thesis the theory of steady-state, transient and pulsed cross-phase modulation is developed. Moreover, care has been taken to relate all research back to experimentally feasible situations. As such, the relevance of the theory is justified by consideration of the situation present in rubidium-87. Due to the close relationship between XPM in the N-configuration atom and electromagnetically induced transparency in the Λ-atom, many similarities and insights act as link between these two fields. Indeed, it is frequently demonstrated that the key to understanding the

various properties of XPM in the N-configuration atom is by comparison with the situation in the corresponding Λ-atom equivalent.

Declarations

I, Gary Sinclair, hereby certify that this thesis, which is approximately 23'000 words in length, has been written by me, that it is the record of work carried out by me and that it has not been submitted in any previous application for a higher degree.

Signature of candidate:

Date: 26/02/2009

I was admitted as a research student in September, 2005 and as a candidate for the degree of Doctor of Philosophy in September, 2005; the higher study for which this is a record was carried out in the University of St Andrews between 2005 and 2009.

Signature of candidate:

Date: 26/02/2009

I hereby certify that the candidate has fulfilled the conditions of the Resolution and Regulations appropriate for the degree of Doctor of Philosophy in the University of St Andrews and that the candidate is qualified to submit this thesis in application for that degree.

Signature of supervisor:

Date: 26/02/2009

In submitting this thesis to the University of St Andrews I understand that I am giving permission for it to be made available for use in accordance with the regulations of the University Library for the time being in force, subject to any copyright

vested in the work not being affected thereby. I also understand that the title and abstract will be published, and that a copy of the work may be made and supplied to any bona fide library or research worker, that my thesis will be electronically accessible for personal or research use, and that the library has the right to migrate my thesis into new electronic forms as required to ensure continued access to the thesis. I have obtained any third-party copyright permissions that may be required in order to allow such access and migration.

Signature of candidate:

Date: 26/02/2009

The following is an agreed request by candidate and supervisor regarding the electronic publication of this thesis:
Access to Printed copy and electronic publication of thesis through the University of St Andrews.

Signature of candidate:

Signature of supervisor:

Date: 26/02/2009

Publications and Conferences

Journal Publications

1. *Cross-Kerr interaction in a four-level atomic system*, G.F. Sinclair and N. Korolkova, Phys. Rev. A, **76**, 033803, (2007).

2. *Effective cross-Kerr Hamiltonian for a non-resonant four-level atom*, G.F. Sinclair and N. Korolkova, Phys. Rev. A, **77**, 033843, (2008).

3. *Time-dependent cross-phase modulation in rubidium-87*, G.F. Sinclair, Phys. Rev. A, **79**, 023815, (2009).

Conference Presentations

1. Continuous Variable Quantum Information Processing Workshop (CVQIP 05), Copenhagen, 2005. Poster presentation.

2. Frontiers in Quantum Optics, 2006, St Andrews. Oral presentation.

3. Continuous Variable Quantum Information Processing Workshop (CVQIP 06), St Andrews, 2006. Poster presentation.

4. International Conference on Coherent and Nonlinear Optics (ICONO/LAT 2007), Minsk, Belarus, 2007. Oral presentation.

5. Quantum Information in Scotland (QUISCO), Edinburgh, 2008. Poster presentation.

6. Quantum Information in Scotland (QUISCO), St Andrews, 2008. Poster presentation.

7. 17^{th} International Laser Physics Workshop (LPHYS 08), Trondheim, Norway, 2008. Poster presentation.

8. Photon 08 (Photon 08/QEP-18), Edinburgh, 2008. Poster presentation.

Acknowledgements

There a several people who deserve to be thanked for supporting me during my PhD in St Andrews. Firstly, I would like to thank my family who have offered me unqualified support in everything that I do. Secondly, I would like to thank my fellow students: Andrew Berridge, Steve Hill, Victor Maltcev, David Menzies, Jill Morris and Anthony Yeates. Throughout my time in St Andrews they have provided excellent company, entertainment and assistance. My office mate, David Menzies, deserves a particular mention for his ceaseless banter and entertaining physics, and non-physics, discussions. I would also like to thanks my friends who, after graduating and departing St Andrews several years ago, continue to offer their kind friendship and free accommodation every time I come to visit! Among these are Catherine Assheton-Stones, David Emery, Gordon Munro, Joseph Neizer and Chris Williams.

I would also like to thank my supervisor, Natalia Korolkova, for making this PhD possible. For his academic support I would also like to thank Malcolm Dunn. And finally, I would like to acknowledge the financial support of the Scottish Universities Physics Alliance during these $3^1/_2$ years.

Introduction

The study of optics has occupied some of the greatest physicists in history and has been associated with many of its most significant discoveries. Newton's *Opticks* [1], published in 1704, laid many of the foundations of the subject. Among the most famous of Newton's insights was the decomposition of white light into a continuous colour spectrum, as demonstrated by his prism experiments. Further study of birefringent "Iceland Crystal" also led him to postulate the existence of two "sides", or polarisations, of light. Newton's principle aim in *Opticks* was to explore the properties of light, rather than to explain their causes. Nonetheless, throughout his work there is a clear preference for a corpuscular theory of light.

To find the first explanation of light in terms of propagating waves we must turn to *Traité de la lumiere* [2], the 1690 work of Huygens. In this book light is correctly understood as being of a wave-like nature. The text is also notable for a particularly beautiful account of the determination of the velocity of light by astronomical observations. Nonetheless, it was only much later in 1803 that Young's [3] elegant diffraction experiments conclusively presuaded scientific opinion in favour of the wave theory of light.

The invention of the *modern* theory of light must be attributed to Maxwell and his great unification of light, electricity and magnetism under one mathematical framework. Since their conception, Maxwell's equations have played a central role in the development of physics. For instance, the introduction of Einstein's "quantum" of light to resolve the black-body radiation problem and the null-result of the Michelson-Morley experiment led to quantum mechanics and special relativity respectively. Although both of these theories necessitated great shifts in our physical

paradigms, these shifts occurred whilst leaving the original framework of electromagnetism largely intact. Indeed, in the case of special relativity a much greater insight into the original equations is offered by their new relativistic interpretation.

Despite the extensive history and development of the theory of light, this remains an active and exciting field of research. Modern (quantum) optics is nowadays used to investigate nonclassical physics, and has found applications in many branches of technology. More recently, considerable resources have been directed towards the development of all-optical quantum computing and quantum cryptography, the latter of which is now a commercially available technology.

The research presented in this thesis explores the phenomena of cross-phase modulation in a gas of cold rubidium atoms. This is the process by which the refractive index experienced by one electromagnetic field is modulated by controlling the intensity of a second field. The realisation of such an interaction at the quantum-mechanical level has been proposed as one possible route towards optical quantum computing. However, on a more fundamental level the study of such nonlinear optical phenomena are crucial to the continued development of our understanding of light and matter. As with Newton, we also investigate the *properties* of optical phenomena with the long-term aim of extending our *understanding* of light itself.

Chapter 1

Introduction to Quantum Optics

Quantum optics is the study of electromagnetism at the quantum-mechanical level. Since the foundations were laid by Dirac in 1927 [4] a wealth of quantum-optical phenomena have been explored. Among these are spontaneous emission [5], the Lamb shift [6] and the Casimir force [7]. These early experimental justifications for the quantisation of the electromagnetic field can be explained, at least qualitatively, by a semi-classical plus fluctuations model. Using a stochastic model the atoms are treated quantum-mechanically and fluctuations are added to the classical fields.

More recently a whole range of completely nonclassical features of light have been investigated. These include squeezed vacuum states [8], sub-Poissonion statistics [9] and quantum teleportation via entangled states [10]. The non-classical characteristics of the electromagnetic field demonstrated by these experiments provide further compelling evidence of field quantisation. In addition, the realisation that these properties can be profitably used has been exploited in the emerging discipline of *quantum information*. Indeed, many exciting applications of quantum optics have been proposed in the fields of quantum information and computing. At present applications have already been demonstrated in ghost-imaging [11], quantum lithography [12] and quantum cryptography [13] and the possibility of optical quantum computing continues to be explored [14, 15].

This chapter describes the basic theoretical framework of non-relativistic quantum optics, beginning with quantisation of the Maxwell equations. Particular em-

phasis is placed on the interaction of classical and quantum fields with linear and nonlinear materials.

1.1 Classical Electrodynamics

1.1.1 The Maxwell Equations in Dielectric Media

The development of electromagnetism as a unified theory is due to the work of J.C. Maxwell. The field equations that now bear his name are given by [16]

$$\begin{aligned} \nabla \cdot \mathbf{D} &= \rho, \qquad \nabla \times \mathbf{H} = \mathbf{J} + \frac{\partial \mathbf{D}}{\partial t}, \\ \nabla \cdot \mathbf{B} &= 0, \qquad \nabla \times \mathbf{E} = -\frac{\partial \mathbf{B}}{\partial t}. \end{aligned} \tag{1.1}$$

In dielectric media the free currents and charges vanish ($\mathbf{J} = \mathbf{0}, \rho = \mathbf{0}$). However, these four equations alone do not yet provide a complete description of classical electrodynamics. Rather, it is still necessary to form *constitutive relations* between the derived fields $\mathbf{D}$,$\mathbf{H}$ and the fundamental fields $\mathbf{E}$, $\mathbf{B}$. The derived fields are introduced as a convenient way to macroscopically account for the response of atomic charges and currents to the applied electromagnetic field, which in turn provides a back-action on $\mathbf{E}$ and $\mathbf{B}$ themselves.

Originally the constitutive relations were derived from the classical Lorentzian theory [17] of light-matter interactions. This theory proposed that dielectric materials consist of bound point charges that couple to the applied electromagnetic field. Although simple, this model successfully accounts for almost all low-intensity interactions with bulk materials. However, the advent of quantum mechanics and the laser brought the possibility of, and requirement for, a more sophisticated theory of light-matter interactions: quantum optics.

The most general form of constitutive relations in a dielectric medium are given by the relationships

$$\mathbf{D} = \mathbf{D}[\mathbf{E}, \mathbf{B}], \qquad \mathbf{H} = \mathbf{H}[\mathbf{E}, \mathbf{B}]. \tag{1.2}$$

The square brackets indicate that the relations may depend on the previous values of the fundamental fields (e.g. magnetic hysteresis). When the constitutive relations are simple non-hysteretic functions we can write the displacement current $\mathbf{D}$ and magnetic field $\mathbf{H}$ as

$$\mathbf{D} = \epsilon_0 \mathbf{E} + \mathbf{P}, \tag{1.3}$$

$$\mathbf{H} = \frac{1}{\mu_0}\mathbf{B} - \mathbf{M}. \tag{1.4}$$

Here $\mathbf{P}$ and $\mathbf{M}$ are the polarisation and magnetisation induced by the fields $\mathbf{E}$ and $\mathbf{B}$. In many non-magnetic dielectric materials it is found that $\mathbf{P} = \mathbf{P}(\mathbf{E})$ and $\mathbf{M} = \mu_0 \mathbf{B}$, where μ_0 is the permeability of free space. Nonetheless, other important relationships are possible. For instance, a wide range materials exist for which a molecular, crystalline or magnetically-induced isotropy results in constitutive relations of the mixed form $\mathbf{P} = \mathbf{P}(\mathbf{E}, \mathbf{B})$ and $\mathbf{M} = \mathbf{M}(\mathbf{E}, \mathbf{B})$. Chiral materials such as an aqueous sugar solution and certain coherently prepared atomic vapours exhibit these relationships, the latter of which has been suggested as a route towards negative refraction [18, 19].

For the work in this thesis it is sufficient to assume constitutive relations of the non-mixed, non-hysteretic and non-magnetic form: only the polarisation will vary nonlinearly with the applied electric field. To form solutions of the Maxwell equations we consider a linearly polarised transverse wave propagating along the z-axis. One can derive the wave equation for the non-zero component of the electric field within the paraxial approximation:

$$\left(\frac{\partial^2}{\partial t^2} - c^2 \frac{\partial^2}{\partial z^2} \right) E(z,t) = -\mu_0 c^2 \frac{\partial^2}{\partial t^2} P(z,t). \tag{1.5}$$

The real-valued solution to this equation $E(z,t)$ and the polarisation source terms are given in terms of their Fourier components [20] by

$$E(z,t) = \frac{1}{2} \sum_n \left(E_n e^{i(k_n z - \omega_n t)} + E_n^* e^{-i(k_n z - \omega_n t)} \right), \tag{1.6}$$

$$P(z,t) = \frac{1}{2} \sum_n \left(P_n e^{i(k_n z - \omega_n t)} + P_n^* e^{-i(k_n z - \omega_n t)} \right), \tag{1.7}$$

where the sum is taken over the discrete number of field modes considered. The simplest relationship between the polarisation and electric field Fourier components

is that of a linear dependence. Almost all materials exhibit this dependence in the weak excitation limit, although in some of the most remarkable and useful quantum systems it is possible to suppress this response [21]. In general the proportionality constant, known as the electrical susceptibility $\chi^{(1)}$, will be frequency dependent.

$$P_n = \epsilon_0 \chi^{(1)}(\omega_n;\omega_n) E_n. \tag{1.8}$$

Substitution of the polarisation back into the source term of the wave equation results in the dispersion relation

$$\frac{k_n^2 c^2}{\omega_n^2} = 1 + \chi^{(1)} = (\eta + i\kappa)^2 \tag{1.9}$$

where we have introduced two new parameters η and κ, whose physical interpretation will soon be explained [22]. To model an absorptive material the electrical susceptibility must be a complex quantity, $\chi^{(1)} = \chi'^{(1)} + i\chi''^{(1)})$. By solving the dispersion relation (1.9) for the parameters η and κ in terms of the real and imaginary parts of the electrical susceptibility it is found that

$$\eta^2 - \kappa^2 = 1 + \chi'^{(1)}, \tag{1.10}$$

$$2\eta\kappa = \chi''^{(1)}. \tag{1.11}$$

The interpretation of η and κ as the refractive index and absorption (extinction coefficient) becomes apparent on substitution of k in terms of η and κ back into each of the Fourier components of (1.6). We find that the electric field can be expressed as

$$E(z,t) = \sum_n \left(E_n \exp\left[i\omega_n \left(\frac{\eta}{c} z - t \right) - \frac{\kappa\omega_n}{c} z \right] + c.c. \right) \tag{1.12}$$

Frequently we are interested in more complex response functions where the linear susceptibility is accompanied by several other higher-order terms. From the electrical susceptibility the constitutive relations of the Maxwell equations are determined. In addition, the susceptibility can also be related to the physically measurable quantities of refractive index and absorption.

In the following section we turn to the problem of determining exactly how light and matter interact. Given this interaction mechanism ways must be found to

solve the equation of motion for the atomic system and hence deduce its electrical susceptibility.

1.1.2 The Electric Dipole Interaction

We now turn to deriving the form of the interaction between a classical electromagnetic field and a particle of charge e. The Hamiltonian operator of an electron bound by an atomic potential $V(\mathbf{r})$ and immersed in a external electromagnetic field is given by

$$\hat{H} = \frac{1}{2m}\left(\hat{p} - e\mathbf{A}(\mathbf{r},t)\right)^2 + e\Phi(\mathbf{r},t) + V(\mathbf{r}). \tag{1.13}$$

Here $\Phi(\mathbf{r},t)$ and $\mathbf{A}(\mathbf{r},t)$ are the scalar and vector potentials or the external field and $\hat{p} - e\mathbf{A}(\mathbf{r},t)$ is the canonical momentum of a charged particle [23]. The introduction of electromagnetic potentials greatly facilitates the solution of many problems in electromagnetism, the most useful of which are the standard scalar and vector potentials Φ and $\mathbf{A}$. The fundamental fields are related to these potentials by

$$\mathbf{B} = \nabla \times \mathbf{A}, \tag{1.14}$$

$$\mathbf{E} = -\nabla\Phi - \frac{\partial \mathbf{A}}{\partial t}. \tag{1.15}$$

The two homogenous Maxwell equations are automatically satisfy by the form of the scalar and vector potentials. The inhomogeneous Maxwell equations give rise to evolution equations for the potentials. These are:

$$\nabla^2\Phi + \frac{\partial}{\partial t}(\nabla \cdot \mathbf{A}) = 0, \tag{1.16}$$

$$\nabla^2\mathbf{A} - \frac{1}{c^2}\frac{\partial^2 \mathbf{A}}{\partial t^2} - \nabla\left(\nabla \cdot \mathbf{A} + \frac{1}{c^2}\frac{\partial \Phi}{\partial t}\right) = 0, \tag{1.17}$$

when in a space free from charges and currents. Thus, we arrive at two coupled partial differential equations of motion for the potential functions. At first sight these two equations appear at least as difficult to solve as the original Maxwell equations. However, a considerable simplification is possible. Although we have reduced the six components of the fundamental fields down to four components of the potentials, the exact choice of potential functions are still somewhat arbitrary.

That is, the electromagnetic field is invariant under any *gauge transformation* to the potentials of the form

$$\Phi' = \Phi - \frac{1}{c}\frac{\partial \Lambda}{\partial t}, \tag{1.18}$$

$$\mathbf{A}' = \mathbf{A} + \nabla \Lambda, \tag{1.19}$$

where Λ is a scalar function. Depending on the particular situation a definite gauge may be chosen to simplify the potential evolution equations. In nonrelativistic quantum optics it is most convenient to work within the Coulomb gauge, for which $\nabla \cdot \mathbf{A}'(\mathbf{r}, t) = 0$. This gauge condition is satisfied if $\nabla^2 \Lambda = -\nabla \cdot \mathbf{A}$. Since the gauge condition is of the form of Poisson's equation a transformation can always be found that satisfies the Coulomb gauge condition. Applying the gauge condition to the equations of motion (1.16) we find that $\nabla^2 \Phi' = 0$. This has the trivial solution $\Phi' = 0$. From (1.17) we obtain

$$\nabla^2 \mathbf{A}' - \frac{1}{c}\frac{\partial^2 \mathbf{A}'}{\partial t^2} = 0. \tag{1.20}$$

Thus, the vector potential satisfies a homogeneous wave equation. We will return to this wave equation when quantising the electromagnetic field. By transforming into the Coulomb gauge we have eliminated the scalar potential and have reduced the Hamiltonian to the form

$$\hat{H} = \frac{1}{2m}\left(\hat{p} - e\mathbf{A}'(\mathbf{r}, t)\right)^2 + V(\mathbf{r}). \tag{1.21}$$

A much greater simplification is possible if we also admit one important approximation. In quantum optics we are commonly working with electromagnetic radiation of wavelength around that of visible light ($\lambda \approx 10^{-7}$m), whereas atomic dimensions are typically of the order of $10^{-10}m$. It is therefore common to employ the *dipole approximation*, where we assume that spatial variations of the electromagnetic field on the atomic scale are negligible. The scalar and vector potentials can then be treated as constants over the atomic dimensions. We now use this approximation and perform one further gauge transformation given by

$$\Phi'' = -\frac{1}{c}\frac{\partial \Lambda'}{\partial t}, \qquad \mathbf{A}'' = \mathbf{A}' + \nabla \Lambda', \tag{1.22}$$

where $\Lambda'(\mathbf{r},t) = -\mathbf{A}'(\mathbf{r},t)\cdot\mathbf{r}$ and $\nabla(-\mathbf{A}'(\mathbf{r},t)\cdot\mathbf{r}) \approx -\mathbf{A}'(\mathbf{r},t)$ By doing so, we find that the Hamiltonian can be written as

$$\hat{H} = \frac{\hat{p}^2}{2m} + V(\mathbf{r}) - e\mathbf{E}\cdot\mathbf{r}. \tag{1.23}$$

Here the interaction between the field and the charged particle has been reduced to a single term: $H_I = -e\mathbf{E}\cdot\mathbf{r}$ known as the dipole interaction. We note that although the Hamiltonian was derived by transforming into the gauge (1.22) the quantity $\mathbf{E}(\mathbf{r},\mathbf{t})$, and therefore the interaction term, is gauge independent.

1.2 Field Quantisation

1.2.1 The Electromagnetic Field Hamiltonian

The theory presented above amounts to a *semiclassical* approximation. Whereas the charged particle is described using quantum mechanics it interacts with a classical electromagnetic field. Many phenomena in quantum optics can be described semiclassically, and indeed many more when a semiclassical plus vacuum fluctuations model in employed. However, to understand the full wealth of experimental observations it proves necessary to quantise the electromagnetic field as well.

In the Coulomb gauge the electromagnetic field is completely described by the vector potential alone. Solutions to the wave equation (1.20) are given by the transverse waves

$$\mathbf{A}(\mathbf{r},t) = \sum_{\mathbf{k},s} \mathbf{e}_{\mathbf{k},s}\left(A_{\mathbf{k},s}e^{i(\mathbf{k}\cdot\mathbf{r}-\omega t)} + A^*_{\mathbf{k},s}e^{-i(\mathbf{k}\cdot\mathbf{r}-\omega t)}\right). \tag{1.24}$$

Here $\mathbf{e}_{\mathbf{k},s}$ are a pair of orthogonal polarisation vectors that are perpendicular to the wave propagation ($\mathbf{k}\cdot\mathbf{e}_{\mathbf{k},s} = 0$). We have chosen to solve the wave equation in an cube of volume L^3 with periodic boundary conditions. It is assumed that the cube is free of charges or currents and that the atom-field interaction volume is negligibly small compared to the quantisation volume of the cube. In this case there exist a discrete set of allowed wavevectors that are given by $\mathbf{k} = (2\pi/L)(m_x, m_y, m_z), \{m_\alpha \in [0,\infty)\}$. By using (1.14) and (1.15) we find that the electric and magnetic field components

are given by

$$\mathbf{E}(\mathbf{r},t) = i\sum_{\mathbf{k},s}\omega_{\mathbf{k}}\mathbf{e}_{\mathbf{k},s}\left(A_{\mathbf{k},s}e^{i(\mathbf{k}\cdot\mathbf{r}-\omega t)} - A^*_{\mathbf{k},s}e^{-i(\mathbf{k}\cdot\mathbf{r}-\omega t)}\right), \tag{1.25}$$

$$\mathbf{B}(\mathbf{r},t) = i\sum_{\mathbf{k},s}(\mathbf{k}\times\mathbf{e}_{\mathbf{k},s})\left(A_{\mathbf{k},s}e^{i(\mathbf{k}\cdot\mathbf{r}-\omega t)} - A^*_{\mathbf{k},s}e^{-i(\mathbf{k}\cdot\mathbf{r}-\omega t)}\right). \tag{1.26}$$

Using these solutions we wish to calculate the Hamiltonian of the electromagnetic field. Classically the total energy of the electromagnetic field in a volume $\mathcal{V}$ is given by the integral over the energy density. In the absence of dielectric material this is

$$H = \frac{1}{2}\int_{\mathcal{V}}\left(\epsilon_0\mathbf{E}\cdot\mathbf{E} + \frac{1}{\mu}\mathbf{B}\cdot\mathbf{B}\right)d\mathcal{V}. \tag{1.27}$$

By substitution of the solutions for $\mathbf{E}$ and $\mathbf{B}$ given above, it is found that

$$H = 2\epsilon_0\mathcal{V}\sum_{\mathbf{k},s}\omega^2_{\mathbf{k}}A_{\mathbf{k},s}A^*_{\mathbf{k},s}. \tag{1.28}$$

At this point we can gain further insight into the nature of the electromagnetic field modes by re-writing the field amplitudes $A_{\mathbf{k},s}$ in terms of the quadrature components

$$A_{\mathbf{k},s} = \frac{1}{2\omega_{\mathbf{k}}(\epsilon_o\mathcal{V})^{1/2}}\left(\omega_{\mathbf{k}}q_{\mathbf{k},s} + ip_{\mathbf{k},s}\right), \tag{1.29}$$

$$A^*_{\mathbf{k},s} = \frac{1}{2\omega_{\mathbf{k}}(\epsilon_o\mathcal{V})^{1/2}}\left(\omega_{\mathbf{k}}q_{\mathbf{k},s} - ip_{\mathbf{k},s}\right). \tag{1.30}$$

This results in the Hamiltonian taking the form of a summation over an infinite set independent classical harmonic oscillators:

$$H = \frac{1}{2}\sum_{\mathbf{k},s}\left(p^2_{\mathbf{k},s} + \omega^2_{\mathbf{k}}q^2_{\mathbf{k},s}\right). \tag{1.31}$$

The recognition that each field mode is equivalent to a harmonic oscillator enables us to canonically quantise the conjugate classical variables p and q. It is important to note that since no products of the classical variables appear in the Hamiltonian there will be no ambiguity when replacing the c-numbers with the corresponding non-commuting q-numbers operators, $(p,q)\rightarrow(\hat{p},\hat{q})$. The position and momentum operators are assumed to satisfy the well-known quantisation condition

$$[\hat{q}_{\mathbf{k},s},\hat{p}_{\mathbf{k},s}] = i\hbar\delta_{\mathbf{k},\mathbf{k}'}\delta_{s,s'}, \tag{1.32}$$

where all other commutators vanish. It is now possible to rewrite the quantum-mechanical Hamiltonian in terms of the ladder operators defined by

$$\hat{a}_{\mathbf{k},s} = \frac{1}{(2\hbar\omega_{\mathbf{k}})^{1/2}} \left(\omega_{\mathbf{k}} \hat{q}_{\mathbf{k},s} + i\hat{p}_{\mathbf{k},s}\right), \tag{1.33}$$

$$\hat{a}^{\dagger}_{\mathbf{k},s} = \frac{1}{(2\hbar\omega_{\mathbf{k}})^{1/2}} \left(\omega_{\mathbf{k}} \hat{q}_{\mathbf{k},s} - i\hat{p}_{\mathbf{k},s}\right). \tag{1.34}$$

The definition of these operators is almost identical to (1.29) and (1.30) except that the quadrature components $(\hat{p}, \hat{q})$ no longer commute. Indeed, the Hamiltonian (1.28) could not be quantised directly because of the ambiguity when trying to quantise products of classical variables whose quantum-mechanical equivalents do not commute. When written in terms of the ladder operators we find that the Hamiltonian is similar to (1.29), other than for the existence of an infinite zero-point energy. That is

$$\hat{H} = \sum_{\mathbf{k},s} \hbar\omega_{\mathbf{k}} \left(\hat{a}^{\dagger}_{\mathbf{k},s} \hat{a}_{\mathbf{k},s} + \frac{1}{2}\right). \tag{1.35}$$

The infinite zero-point energy, although appearing problematic at first, causes remarkably few concerns. Since only differences between energy states are observable it is largely ignorable in most calculations. Nonetheless, the existence of a infinite zero-point "background" has been verified by the experimental demonstrations of the Casimir effect [24] and could be used in conjunction with negative refractive index materials to demonstrate *quantum levitation* [25].

1.2.2 Quantum States of the Field

In classical electrodynamics it is often convenient to solve the wave-equation (1.5) in terms of Fourier components. Classically the state of a single-mode field is completely described by one complex frequency amplitude. However, the quantum state of the electromagnetic field, even for a single frequency mode, is much more complicated: this gives rise to the rich diversity of nonclassical effects observed in quantum optics. Thus, the quantum state must be specified with respect to an infinite set of basis states. Certain choices of basis states prove particularly useful. The most straightforward of these are the eigenstates of the Hamiltonian (1.35). For a single

mode field we have

$$\hat{H}|n\rangle = \hbar\omega\left(\hat{n} + \frac{1}{2}\right)|n\rangle = E_n|n\rangle, \tag{1.36}$$

where $\hat{n} = \hat{a}^\dagger\hat{a}$ and

$$E_n = \left(n + \frac{1}{2}\right)\hbar\omega. \tag{1.37}$$

These states are known as *Fock-* or *number-states* and range in energy from a lower bound of $E_0 = \hbar\omega/2$ to infinity in steps of $\hbar\omega$. A state $|n\rangle$ is interpreted as representing n photons delocalised throughout the quantisation volume. Notably, the bounding of the Fock-state spectrum from below is responsible for the impossibility of forming conjugate phase and number operators [26, 27].

The n-photon eigenstate can be generated from the vacuum by repeated application of the creation operator $\hat{a}^\dagger$:

$$|n\rangle = \frac{(\hat{a}^\dagger)^n}{\sqrt{n!}}|0\rangle. \tag{1.38}$$

We also note that the set of eigenstates of (1.35) form a complete and orthonormal basis.

$$\sum_{n=0}^{\infty}|n\rangle\langle n| = 1, \qquad \langle n|m\rangle = \delta_{n,m}. \tag{1.39}$$

Another useful set of basis states are the *coherent states*. These are commonly defined as eigenstates of the annihilation operator $\hat{a}|\alpha\rangle = \alpha|\alpha\rangle$ and are expressed in terms of the Fock basis by

$$|\alpha\rangle = \exp\left(-|\alpha|^2/2\right)\sum_{n=0}^{\infty}\frac{\alpha^n}{\sqrt{n!}}|n\rangle. \tag{1.40}$$

The coherent state has an average number of photons $\langle n\rangle = |\alpha|^2$ and a Poissonian distribution.

$$p(n) = \frac{\langle\hat{n}\rangle^n e^{-\langle\hat{n}\rangle}}{n!}. \tag{1.41}$$

Once again we note that the coherent states form a complete set. However, although these states form a basis they are not orthogonal. The basis is therefore termed "over-complete". The overlap of coherent states is given by

$$|\langle\alpha|\alpha'\rangle|^2 = \exp\left(-|\alpha - \alpha'|^2\right). \tag{1.42}$$

Clearly coherent states with significantly different eigenvalues α have an exponentially vanishing inner product. The coherent states are also significant because they are generated by the radiation of a classical dipole oscillator. For a free oscillating dipole we expect equal excitation of the electric and magnetic field components due to the equipartition of energy between the field degrees of freedom. Indeed, were the annihilation and creation operators to become c-numbers we would expect them to describe counter-rotation vectors of constant magnitude (in the Heisenberg picture). The quantum-mechanical version in the Schrödinger picture corresponds to a complete (and constant) knowledge of α - that is an eigenstate of the annihilation operator $\hat{a}$. These two definitions are therefore identical.

1.3 Nonlinear Dielectrics

1.3.1 Classical Description

It was realised early in the development of electromagnetic theory that light-rays are able to cross paths undisturbed [1, 2]. This essential feature of light in free space means that interactions between fields are impossible to generate without the use of a nonabsorbing, nonlinear medium. With the demonstration of the laser by Maiman in 1960 [28] began a rapid exploration of nonlinear optics. However, even before the availability of high-intensity coherent light sources, some success had been achieved in the field. One of the most important nonlinear interactions between an electric and an electromagnetic field was discovered as early as 1875 by the Scottish physicist John Kerr [29]. This interaction, the electro-optical cross-phase modulation, now bears his name: the *cross-Kerr* effect.

Essentially nonlinear optical interactions occur due to the nonlinear response of materials to an external electromagnetic field. This in turn generates a nonlinear back-action on the fields themselves. Whereas previously it was sufficient to assume that the material polarisation was proportional to the applied field, in general we will have to take into account higher-order effects. We begin by considering a classical

material, such as an optical fibre, for which the polarisation is given by

$$P(t) = P^{(1)}(t) + P^{(2)}(t) + P^{(3)}(t) + ... \tag{1.43}$$

where $P^{(n)}(t) = \epsilon_0 \chi^{(n)} E(t)^n$. For centrosymmetric materials the second-order polarisation term must vanish in the dipole approximation due to the inversion symmetry [20]. We suppose that the material is driven by an electric field composed of two frequency components

$$E(t) = \frac{1}{2} E_a \exp[i(k_a z - \omega_a t)] + \frac{1}{2} E_b \exp[i(k_b z - \omega_b t)] + \text{c.c.} \tag{1.44}$$

In this case the third-order polarisation of the material displays a wide variety of effects. Namely

$$\begin{aligned}
P^3(t) &= \epsilon_0 \chi^{(3)} E(t)^3 \qquad (1.45)\\
&= \epsilon_0 \chi^{(3)} \left\{ \left(\frac{3}{8}|E_a|^2 + \frac{3}{4}|E_b|^2 \right) E_a \exp[i(k_a z - \omega_a t)] \right.\\
&+ \left(\frac{3}{8}|E_b|^2 + \frac{3}{4}|E_a|^2 \right) E_b \exp[i(k_b z - \omega_b t)]\\
&+ \frac{1}{8} E_a^3 \exp[3i(k_a z - \omega_a t)] + \frac{1}{8} E_b^3 \exp[3i(k_b z - \omega_b t)]\\
&+ \frac{3}{8} E_a^2 E_b \exp\left[(2i(k_a z - \omega_a t) + i(k_b z - \omega_b t)\right]\\
&+ \frac{3}{8} E_b^2 E_a \exp\left[2i(k_b z - \omega_b t) + i(k_a z - \omega_a t)\right]\\
&+ \frac{3}{8} E_a^{*2} E_b \exp\left[-2i(k_a z - \omega_a t) + i(k_b z - \omega_b t)\right]\\
&+ \left. \frac{3}{8} E_b^{*2} E_a \exp\left[-2i(k_b z - \omega_b t) + i(k_a z - \omega_a t)\right] \right\}
\end{aligned}$$

These terms represent the parametric processes that occur in a fibre: the self- and cross-Kerr nonlinearities, third-harmonic generation and four-wave mixing (FWM). In general the $\chi^{(3)}$ nonlinearity is seen to generate a large number of interacting effects. However, other than the self- and cross-Kerr nonlinearities all other processes will normally make a negligible contribution due to phase-matching requirements. Consider the third-harmonic generation at a frequency $\omega' = 3\omega_a$. The polarisation induced at the frequency $\exp[i(k'z - \omega' t)]$ will have the amplitude

$$P_{\omega'} = \frac{1}{8} E_a^3 \exp[i(3k_a - k')z]. \tag{1.46}$$

Since we cannot suppose that the optical fibre will have a linear dispersion relation then generally $k' \neq 3k_a$. This results in neighbouring points on the optical fibre radiating at frequency $3\omega_a$, but out-of-phase with each other. For optimal frequency conversion it is necessary to phase-match the radiating dipoles by working between suitable points on the dispersion profile of the fibre [30]. Alternatively one can employ a secondary non-parametric process (e.g. stimulated Raman scattering) as is done in supercontinuum generation [31].

This generally leaves only SPM and XPM simultaneously present in the fibre. Unfortunately, the strength of the nonlinearity generated in an optical fibre is relatively small. Consider the nonlinear refractive index coefficient related to the intensity of the field ($\delta\eta_{NL} = \eta_I^{(2)} I$). This is given by [30]

$$\eta_I^{(2)} = \frac{A_{eff}\lambda\gamma}{2\pi}, \tag{1.47}$$

where A_{eff} is the effective area of the fibre core, λ is the wavelength of light and γ is the nonlinearity parameter. Typical values for a microstructured optical fibre are $A_{eff} = \pi r^2, r = 0.8\mu$m, $\gamma = 95\text{W}^{-1}\text{km}^{-1}$, $\lambda = 800$nm and $\eta^{(0)} = 1.47$. This results in a nonlinear index of $\eta_I^{(2)} \approx 2.4\text{m}^2\text{W}^{-1}$. To convert this to the nonlinear index related to the square of the amplitude $\delta\eta_{NL} = \eta^{(2)}|E|^2$ we use the conversion factor to find

$$\eta^{(2)} = \frac{\epsilon_0 c \eta^{(0)} \eta_I^{(2)}}{2} \approx 4.7 \times 10^{-23}\text{m}^2\text{V}^{-2}. \tag{1.48}$$

With this we can calculate the nonlinear electric susceptibility of a typical microstructured optical fibre:

$$\chi^{(3)} = \frac{8\eta^{(0)}\eta^{(2)}}{3} \approx 1.9 \times 10^{-22}\text{m}^2\text{V}^{-2}. \tag{1.49}$$

We will find in later calculations that the coherent interaction with rubidium-87 in the N-configuration atom provides a much larger nonlinearity. In addition we are able to isolate the cross-phase modulation on its own. Thus, although optical fibres provide a convenient and robust method of generating optical nonlinearities, we are motivated to find alternative systems in which a single, stronger nonlinearity can be isolated.

When only the self-Kerr and cross-Kerr nonlinearities are present the third-order material polarisation at a frequency ω_a is given by

$$P_a^{(3)} = \epsilon_0 \frac{3}{2}\chi^{(3)}(\omega_a;\omega_b,-\omega_b,\omega_a)|E_b|^2E_a + \tag{1.50}$$

$$\epsilon_0 \frac{3}{4}\chi^{(3)}(\omega_a;\omega_a,-\omega_a,\omega_a)|E_a|^2E_a. \tag{1.51}$$

For convenience we abbreviate the notation for the self- and cross Kerr susceptibilities such that $\chi_s^{(3)}(\omega_a) = \chi^{(3)}(\omega_a;\omega_a,-\omega_a,\omega_a)$ and $\chi_c^{(3)}(\omega_a) = \chi^{(3)}(\omega_a;\omega_c,-\omega_c,\omega_a)$. The linear and non-linear polarisation terms are substituted into the wave equation and on Fourier transforming the result we find the dispersion relation

$$\frac{c^2k_a^2}{\omega_a^2} = 1 + \chi^{(1)}(\omega_a) + \frac{3}{4}\chi_s^{(3)}(\omega_a)|E_a|^2 + \frac{3}{2}\chi_c^{(3)}(\omega_a)|E_b|^2. \tag{1.52}$$

In this case the plane-waves of the Fourier decomposition are clearly still valid solutions of the non-linear wave equation because frequency conversion processes have been excluded. The form of this dispersion relation is important, since it presents the possibility that the linear dispersion associated with $\chi^{(1)}(\omega)$ term could be cancelled by the non-linear terms. In this case, it is possible to find non-dispersive localised excitations of the nonlinear field - commonly known as *solitons* [32]. For example, an important example is the bright/dark solitons supported by the self-phase modulation present in optical fibres with anomalous/normal dispersion [33, 34].

The refractive index and absorption can be calculated by solving the equations

$$\eta_\alpha^2 - \kappa_\alpha^2 = \mathcal{R}e\left\{\frac{c^2k_\alpha}{\omega_\alpha}\right\}, \qquad 2\eta_\alpha\kappa_\alpha = \mathcal{I}mg\left\{\frac{c^2k_\alpha}{\omega_\alpha}\right\}. \tag{1.53}$$

Given the situation (to be considered later) where only the cross-Kerr interaction remains, we find that the refractive index and absorption experienced by the electric field E_a are given by

$$\eta_a = 1 + \frac{3}{4}|E_b|^2\mathcal{R}e\left\{\chi_c^{(3)}(\omega_a)\right\}, \tag{1.54}$$

$$\kappa_a = \frac{3}{4}|E_b|^2\mathcal{I}mg\left\{\chi_c^{(3)}(\omega_a)\right\}. \tag{1.55}$$

From this we can see that the cross-Kerr interaction results in a contribution to the refractive index and absorption of one field that is dependent on the intensity of the

other. This relationship is reciprocal and is often taken as defining the cross-Kerr interaction. When a linear response is also present and the system is lossless, then the refractive index experienced by the field α is

$$\eta_a = \eta_\alpha^{(0)}(\omega_a) + \eta_\alpha^{(2)}(\omega_a, \omega_\beta)|E_\beta|^2, \tag{1.56}$$

where $\alpha, \beta \in \{a, b\}, \beta \neq \alpha$. Given that $\chi_c^{(3)}$ is small, the zeroth- and second-order refractive index terms are found to be

$$\eta_\alpha^{(0)}(\omega_\alpha) = \left(1 + \chi^{(1)}(\omega_\alpha)\right)^{1/2}, \tag{1.57}$$

$$\eta^{(2)}(\omega_\alpha, \omega_\beta) = \frac{3}{4\eta_\alpha^{(0)}}\chi^{(3)}(\omega_\alpha, \omega_\beta, -\omega_\beta, \omega_\alpha). \tag{1.58}$$

The nonlinear refractive index contribution will also give rise to a phase shift of the incident plane wave (α) of angle

$$\Delta\phi_{NL} = k_0 l \left(\frac{3}{4}|E_\beta|^2 \mathcal{R}e\left\{\chi_c^{(3)}\right\}\right), \tag{1.59}$$

where l is the interaction length and k_0 is the magnitude of the free-space wave vector.

1.3.2 Quantum-Mechanical Description

So far the effect of the cross-Kerr nonlinearity has been considered in a purely classical context. That is, the quantities considered are all measurable for classical fields. Let us now consider the effect of the cross-Kerr nonlinearity on quantum states of the light field. The Hamiltonian of the cross-Kerr nonlinearity is given by [35]

$$\hat{H} = \hbar K \hat{n}_a \hat{n}_b. \tag{1.60}$$

We can derive this Hamiltonian using a method very similar to the quantisation of the free electromagnetic field. In this case we consider the energy shift of the atom due to the electric-dipole interaction with two orthogonal electromagnetic fields subject to the cross-Kerr interaction. The total energy is given by the volume integral over the electric field energy density

$$H = \frac{1}{2}\int_{\mathcal{V}} \mathbf{E} \cdot \mathbf{D} d\mathcal{V}. \tag{1.61}$$

Here the electric field is assumed to consist of two components $\mathbf{E}(\mathbf{r},t) = \mathbf{E}_a(\mathbf{r},t) + \mathbf{E}_b(\mathbf{r},t)$, which are given by

$$\mathbf{E}_\alpha(\mathbf{r},t) = i\omega_\alpha \mathbf{e}_\alpha \left[A_\alpha e^{i(\mathbf{k}\cdot\mathbf{r}-\omega_\alpha t)} - A_\alpha^* e^{-i(\mathbf{k}\cdot\mathbf{r}-\omega_\alpha t)}\right], \tag{1.62}$$

where $\mathbf{e}_a \cdot \mathbf{e}_b = 0$. The polarisation is given by the cross-Kerr interaction only

$$\mathbf{P}(\mathbf{r},t) = \frac{3}{2}\epsilon_0 \chi^{(3)} |\mathbf{E}(\omega_b)|^2 \mathbf{E}_a(\mathbf{r},t) + \frac{3}{2}\epsilon_0 \chi^{(3)} |\mathbf{E}(\omega_a)|^2 \mathbf{E}_b(\mathbf{r},t). \tag{1.63}$$

The nonlinear susceptibility is assumed to be real, and therefore lossless. Now, we choose to integrate the electric field energy density of a volume $\mathcal{V}$. For each of the fields we find the interaction energy is given by

$$H = 6\epsilon_0 \mathcal{V} \chi^{(3)} \omega_a^2 \omega_b^2 A_a A_a^* A_b A_b^*. \tag{1.64}$$

It is now possible to construct the quantum-mechanical Hamiltonian by using the relationships (1.29-1.30) and (1.33-1.34). After dropping terms associated with the zero-point energy we find that each of the electromagnetic fields will experience an interaction with the atom of the form

$$\hat{H}_I = \frac{-3\hbar^2 \omega_a \omega_c \chi^{(3)}}{2\epsilon_0 \mathcal{V}} \hat{n}_a \hat{n}_c. \tag{1.65}$$

The interaction strength is therefore clearly given by

$$K = -\frac{3\hbar \omega_a \omega_c \chi^{(3)}}{2\epsilon_0 \mathcal{V}}. \tag{1.66}$$

We now ask what effect will this Hamiltonian have on quantum states of the field. Consider the evolution of two electromagnetic fields, both of which are in Fock states. If $|\psi(0)\rangle = |n_a\rangle \otimes |n_b\rangle$ then at a later time the combined state is given by

$$|\psi(t)\rangle = e^{iKn_a n_b t} |n_a\rangle \otimes |n_b\rangle. \tag{1.67}$$

Thus, the Fock state experiences a phase shift that is proportional to the product of the photon numbers. This simple interaction forms the basis of many applications of the cross-Kerr effect in quantum information/optics.

Chapter 2

Introduction to Quantum Electronics

In the first chapter we developed a quantum-mechanical description of light in the presence of a dielectric material. This is the domain of quantum optics. Very closely related, and nowadays seldom differentiated, is the topic of this chapter: *quantum electronics*. Whereas quantum optics focuses on the optical fields, quantum electronics considers the effect of photons on the quantum state of electrons from which matter is composed. An understanding of these atom-field interactions has led to important technological developments such as the laser, optical amplifiers and laser cooling.

2.1 The Schrödinger Equation

One of the most common problems in life is working out what will happen next. Given that we can estimate the initial state of a system and know approximate rules for its evolution, then we can determine its configuration at a later time.

However, in many of the sciences the discovery of the evolutionary rules remains an outstanding problem. Even when these laws are known estimating the initial conditions or evaluating the result is often impractical. Nonetheless no discipline has developed a greater quantitative understanding than that achieved in physics.

Fortunately in the case of quantum optics, the systems studied can often be modelled with remarkable accuracy using quite straightforward methods.

As physicists we appeal to the framework of mathematics and physical intuition to form equations from which predictions can be made. In the case of quantum mechanics the starting point of our investigations is usually the Schödinger equation

$$i\hbar\frac{\partial}{\partial t}|\psi(t)\rangle = \hat{H}|\psi(t)\rangle, \tag{2.1}$$

where $\hat{H}$ is the Hamiltonian, or "total energy operator". The Hamiltonian defines the energy eigenstates

$$\hat{H}|\phi_n(0)\rangle = E_n|\phi_n(0)\rangle. \tag{2.2}$$

The Hamiltonian has particular significance in both classical and quantum mechanics. In addition to giving the energy the Hamiltonian also generates the evolution of the system via either the classical Hamilton-Jacobi equation [23] or the Schödinger equation. This dual role means that the eigenstates of the Hamiltonian are also steady states of the probability distribution. The number of eigenstates of the Hamiltonian is equal to the dimension of the quantum system. The evolution of each is simply given by

$$|\phi_n(t)\rangle = \exp(-iE_nt/\hbar)|\phi_n(0)\rangle. \tag{2.3}$$

Since these eigenstates form a basis for solutions of the Schrödinger equation, then the evolution of any pure quantum state can be decomposed in terms of these functions. This provides a powerful and straightforward method for determining solutions of the Schrödinger equation.

2.2 Interaction Pictures

Using the description of quantum dynamics given above results in the time evolution of the system being described by the state vector. This is known as the Schrödinger picture. However, it is often convenient to transform the dynamical equations into other "pictures" where the evolution is contained wholly or partly within the operators [36]. These are known as the Heisenberg and interaction pictures respectively.

We will have many occasions to transform into an interaction picture during this thesis.

To transform into an interaction picture we suppose that the Hamiltonian can be split into two parts

$$\hat{H}_{SP}(t) = \hat{H}'_{SP}(t) + \hat{H}''_{SP}(t) \tag{2.4}$$

Commonly, the first term, $\hat{H}'_{SP}$, will be time-independent and is responsible for producing phase changes in the chosen basis states, whereas the second term, $\hat{H}''_{SP}(t)$, represents interactions between these. The interaction picture is defined by the transformation

$$|\psi_{IP}(t)\rangle = \hat{U}^{-1}(t)|\psi_{SP}(t)\rangle. \tag{2.5}$$

Here $\hat{U}(t)$ is the unitary operator that generates the time evolution associated with $H'_{SP}(t)$. When this part of the Hamiltonian is time-independent we have

$$\hat{U}(t) = \exp\left[\frac{-i\hat{H}'_{SP}t}{\hbar}\right]. \tag{2.6}$$

In this interaction picture the wavefunction now obeys the equation of motion

$$i\hbar\frac{\partial}{\partial t}|\psi_{IP}(t)\rangle = \hat{H}_{IP}|\psi_{IP}(t)\rangle, \tag{2.7}$$

where $\hat{H}_{IP} = \hat{U}^{-1}(t)\hat{H}''_{SP}\hat{U}(t)$ is the representation of the Hamiltonian in the interaction picture. The operators transform as $\hat{\Omega}_{IP}(t) = \hat{U}^{-1}(t)\hat{\Omega}_{SP}\hat{U}(t)$ and are found to obey the equation of motion

$$\frac{\partial}{\partial t}\hat{\Omega}_{IP}(t) = \frac{i}{\hbar}\left[\hat{H}'_{SP}(t), \Omega_{IP}(t)\right]_-. \tag{2.8}$$

2.3 Dressed States

It is well-known that the energy levels of an atom are solutions of the time-independent Schrödinger equation describing electrons bound by a spherically symmetric potential. For a single electron atom we have [37]

$$\hat{H}_0(r)|\phi(\mathbf{r})\rangle = E|\phi(\mathbf{r})\rangle. \tag{2.9}$$

However, when an external perturbation is applied then the energy levels of the free atom cease to be eigenstates of the total Hamiltonian $\hat{H}(\mathbf{r}) = \hat{H}_0(r) + \hat{V}(\mathbf{r})$. That is

$$\left[\hat{H}_0(r) + \hat{V}(\mathbf{r})\right] |\phi(\mathbf{r})\rangle \neq E|\phi(\mathbf{r})\rangle. \tag{2.10}$$

Commonly this occurs due to one or more electromagnetic fields perturbing the atom via the electric-dipole interaction discussed in Chapter 1. Nonetheless, often it is still possible to find eigenstates (or at least approximations to them) of the total Hamiltonian. The atom is said to be *dressed* by the fields and the new eigenstates of the total Hamiltonian are named the *dressed states*.

One of the simplest exactly solvable examples is given by the two-level atom interacting with a single field mode. In an interaction picture the Hamiltonian is [26]

$$\hat{H}_{IP} = \hbar\Delta\sigma_{22} + \hbar g\left(\sigma_{21}\hat{a} + \sigma_{12}\hat{a}^\dagger\right), \tag{2.11}$$

where $\Delta = \omega_2 - \omega_1 - \omega$ is the detuning of the electromagnetic field and $\sigma_{ij} = |i\rangle\langle j|$ are the atomic transition operators. In general the solution space will be spanned by a tensor product between the infinite set of field states and the two states of the atom given by

$$|\psi(t)\rangle = \sum_{i=1}^{2}\sum_{n=0}^{\infty} c_{i,n}|i\rangle_A \otimes |n\rangle. \tag{2.12}$$

By inspection of the Hamiltonian we see that only pairs of states will couple to each other. That is, the infinite set of subspaces $\{|1\rangle_A \otimes |n+1\rangle, |2\rangle_A \otimes |n\rangle\}, n \in [0, \infty)\}$ are invariant under the operation of the Hamiltonian. We therefore restrict our analysis to within one such resonant manifold [38]. The eigenstates of (2.11) are found to be

$$|C_\pm\rangle = \frac{1}{N_\pm}\left(\Omega|1\rangle + 2\lambda_\pm|2\rangle\right), \tag{2.13}$$

where $|1\rangle = |1\rangle_A \otimes |n+1\rangle, |2\rangle = |2\rangle_A \otimes |n\rangle$ and $N_\pm$ are the normalisation constants. Here $\Omega = g\sqrt{n+1}$ is called the Rabi-frequency and gives the interaction strength in frequency units. The corresponding eigenvalues are

$$\lambda_\pm = \frac{1}{2}\left(\Delta \pm \sqrt{\Delta^2 + \Omega^2}\right). \tag{2.14}$$

Any initial pure state can be decomposed in terms of the two dressed states and is easily shown to evolve as

$$|\psi(t)\rangle = c_-(0)e^{-i\lambda_- t}|C_-\rangle + c_+(0)e^{-i\lambda_+ t}|C_+\rangle. \tag{2.15}$$

As an example consider the atom initially in the upper state, with $n+1$ photons in the field mode. Then the initial condition $|\psi(0)\rangle = |2\rangle$ expressed in terms of the dressed basis is found to be

$$c_-(0) = -\frac{N_-}{2\tilde{\Omega}}, \qquad c_+(0) = \frac{N_+}{2\tilde{\Omega}}, \tag{2.16}$$

where $\tilde{\Omega} = \sqrt{\Delta^2 + \Omega^2}$. By substitution of these initial conditions into the general solution (2.15) the well-known Rabi-solution to the dynamics is deduced:

$$|\psi(t)\rangle = \frac{e^{-i\Delta t/2}}{\tilde{\Omega}} \left\{ -i\Omega \sin\left(\frac{\tilde{\Omega}t}{2}\right)|1\rangle + \left[\tilde{\Omega}\cos\left(\frac{\tilde{\Omega}t}{2}\right) - i\Delta\sin\left(\frac{\tilde{\Omega}t}{2}\right)\right]|2\rangle \right\}. \tag{2.17}$$

It is straightforward to show that $\tilde{\Omega}$ is the frequency at which population oscillations occur between the upper and lower atomic states. When driven by a classical field we have $\Omega = -pE/\hbar$ and identical population oscillations are observed [39]. However, when the two-level atom is driven by coherent state (generally considered the most classical state) then the atom is shown to undergo periodic decay and revival of the oscillations [40, 41]. This occurs due to interference between the sinusoidal oscillations corresponding to the various Fock state components of the coherent state, as shown in (1.40).

Another feature of the two-state atom without a classical analogue is the existence of zero-field Rabi oscillations. In the semi-classical model an atom prepared in the upper atomic state will remain there so long as no external classical field is applied. However, when the interaction with a single field mode is modelled quantum-mechanically it is seen that an atom initially prepared in the upper atomic state with no photons present will still experience population oscillations. This is due to the non-vanishing vacuum Rabi-frequency $\Omega = g\sqrt{1}$ and is an example of *reversible* spontaneous emission. Both of these quantum-mechanical features of the

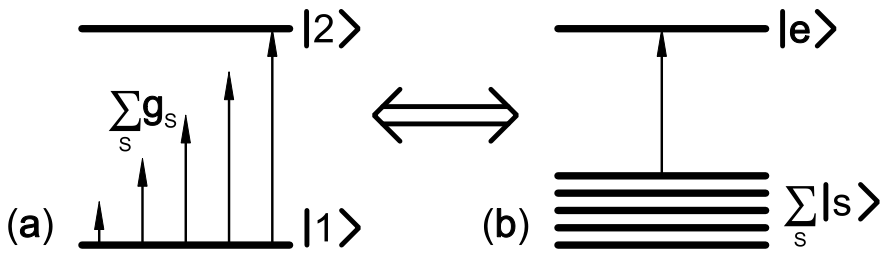

Figure 2.1: (a) The two-level atom interacting with a set of electromagnetic field modes. (b) When the atom is initially in the excited state and couples to the ground state via an ensemble of vacuum modes the system is equivalent to semi-classical photoionisation to a continuum.

Rabi-oscillations have been observed at microwave frequency using rubidium atoms highly excited into Rydberg states [41].

For transitions at optical frequencies however, it is observed that an excited atom will rapidly decay into the lower atomic level. This is in contrast to the reversible population oscillations predicted by the single-mode model described above. We now turn to the problem of accurately modelling the real atomic dynamics of atoms with transitions at optical frequencies. We find that the discrepancy between the theory and experiment can be corrected by including the interaction of the atom with a continuum of field modes.

2.4 Weisskopf-Wigner Theory

At optical frequencies spontaneous emission often plays the dominant role in the dynamics of atomic systems. As shown previously, the simple two-level atom interacting with a single field mode is unable to account for the experimentally observed decay. The first successful method of explaining spontaneous emission was proposed by Weisskopf and Wigner in 1930 [5]. Following their method we show that by including the coupling to a continuum of free-space electromagnetic field modes the

rate of decay can be deduced.

The Hamiltonian of a two-level atom interacting with a infinite set of field modes is given by

$$H = \hbar\omega_1\sigma_{11} + \hbar\omega_2\sigma_{22} + \hbar\sum_s \omega_s\hat{a}_s^\dagger\hat{a}_s + \hbar\sum_s g_s(\sigma_+\hat{a}_s + \sigma_-\hat{a}_s^\dagger), \tag{2.18}$$

where we have removed the zero-point energy associated with each field mode. We now restrict the atom to the situation where only one photon is present in one of the field modes while the atom is in the ground state. The restricted basis can be written as

$$|s\rangle = |1\rangle_A \otimes |\ldots, 0, 1, 0, \ldots\rangle, \tag{2.19}$$

$$|e\rangle = |2\rangle_A \otimes |0, 0, \ldots, 0\rangle, \tag{2.20}$$

where $s \in [0, \infty)$ labels which of the infinite set of field modes the photon is in. Within this basis the Hamiltonian becomes

$$H = \hbar\omega_2\sigma_{ee} + \hbar\sum_s(\omega_1 + \omega_s)\sigma_{ss} + \hbar\sum_s g_s(\sigma_{s+} + \sigma_{s-}), \tag{2.21}$$

where $\sigma_{s+} = |e\rangle\langle s|$. This Hamiltonian describes an excited state, $|e\rangle$, coupled to a infinite set of lower levels, $|s\rangle$. The set of energy levels $|s\rangle$ represent the atom in the ground state with one photon of frequency ω_s. Thus, we have transformed our Hamiltonian into the form of a classical photoionisation problem. To take account of the infinite set of field modes we change the summation into a three dimensional integral over the density of states:

$$\sum_s \longrightarrow \int \mathcal{D}(\boldsymbol{\omega}_s)d^3\boldsymbol{\omega}_s. \tag{2.22}$$

The integral is taken over all possible field modes. Here $\mathcal{D}(\boldsymbol{\omega}_s)$ is the density of states, which in free space is frequency independent, isotropic and is found to be $\mathcal{D}(0) = 2V/(2\pi c)^3$. It is important to recall that the dipole coupling element is a function of both the frequency and orientation of each field mode with respect to the atomic dipole moment. That is

$$g(\boldsymbol{\omega}_s) = \frac{\mathbf{p}\cdot\hat{\mathbf{e}}_{\boldsymbol{\omega}_s}\epsilon_{\omega_s}}{\hbar} = g(\omega_s)\cos(\theta), \tag{2.23}$$

where θ is the angle between the atomic dipole and the polarisation of the field mode $\boldsymbol{\omega}_s$. Transforming into an interaction picture we get the form of a Hamiltonian describing the coupling between a single bound state and an isotropic continuum of free space modes:

$$H = \hbar \int \Delta_s \sigma_{ss} \mathcal{D}(0) d^3\boldsymbol{\omega}_s + \hbar \int g(\boldsymbol{\omega}_s)(\sigma_{s+} + \sigma_{s-}) \mathcal{D}(0) d^3\boldsymbol{\omega}_s, \tag{2.24}$$

where $\Delta_s = \omega_1 - \omega_2 + \omega_s$. We assume that the solution to the dynamics is of the form

$$|\psi(t)\rangle = c_e(t)|e\rangle + \int c_s(t)|s\rangle \mathcal{D}(0) d^3\boldsymbol{\omega}_s. \tag{2.25}$$

This results in the infinite set of coupled equations for the time-dependent coefficients:

$$\dot{c}_e(t) = -i \int g(\boldsymbol{\omega}_s) c_s(t) \mathcal{D}(0) d\boldsymbol{\omega}_s, \tag{2.26}$$

$$\dot{c}_s(t) = -i\Delta_s c_s(t) - i g(\boldsymbol{\omega}_s) c_e(t). \tag{2.27}$$

We now formally integrate the equation (2.27) and substitute this into the differential equation (2.26). This transforms the two coupled differential equations into a single integro-differential equation for the coefficient $c_e(t)$. Once the angular integrations have been performed we find

$$\dot{c}_e(t) = \frac{-p^2}{6\pi^2 c^3 \hbar \epsilon_0} \int_0^\infty d\omega_s \omega_s^3 \int_0^t dt' c_e(t') e^{i\Delta_s(t'-t)}. \tag{2.28}$$

So far this equation is exact. However, we now note that for large values of Δ_s the time integral makes a vanishing contribution, varying approximately as $\propto 1/\Delta_s$. Since only frequencies around resonance contribute significantly, we can make the approximation $\omega_s^3 = \omega_{21}^3$. Therefore

$$\dot{c}_e(t) = \frac{-p^2 \omega_{21}^3}{6\pi^2 c^3 \hbar \epsilon_0} \int_{\omega_1 - \omega_2}^\infty d\Delta_s \int_0^t dt' c_e(t') e^{i\Delta_s(t'-t)}. \tag{2.29}$$

When the integral over the detunings is evaluated we obtain

$$\int_{\omega_1-\omega_2}^\infty d\Delta_s e^{i\Delta_s(t'-t)} = \pi\delta(t'-t) + i\mathcal{P}. \tag{2.30}$$

The term $\mathcal{P}$ is a principle value integral that leads to an energy shift of the state $|e\rangle$. This is due to the dressing of the bare state by the continuum of vacuum modes

with non-zero Rabi-frequency and is closely related to the Lamb shift in hydrogen [6, 17]. Normally the energy shift is very small and is absorbed into the definition of the natural frequency ω_{21}. In fact, this is an elementary example of the method of renormalisation often used in quantum field theory. Evaluating the time integral we find that the decay rate of the excited state is

$$\dot{c}_e(t) = \frac{-p^2\omega_{21}^3}{6\pi c^3\hbar\epsilon_0}c_e(t). \tag{2.31}$$

This is easily solved to give the observed exponential decay of the excited atomic state:

$$c_e(t) = \exp(-\Gamma t/2)c_e(0), \tag{2.32}$$

where the spontaneous decay rate has the value

$$\Gamma = \frac{p^2\omega_{21}^3}{3\pi\epsilon_0\hbar c^3}. \tag{2.33}$$

We note that the spontaneous decay rate of the excited state is proportional to the cube of the transition frequency. This explains why decay rates of the order 10Hz are possible at microwave frequencies, as opposed to 10MHz at optical frequencies. Spontaneous emission can also be reduced by decreasing the number of field modes present, as is often done by placing the atom in a high Q-factor cavity.

Commonly spontaneous emission is explained as arising due to stimulated emission of the atom by the vacuum field modes. It should be noted however, that the calculation above makes no direct reference to the zero-point fluctuations of the vacuum fields. These fluctuations are in fact neglected at the very beginning of the calculation. Indeed, were this explanation complete one would expect spontaneous absorption of vacuum fluctuations to occur also, contrary to experimental evidence. In has therefore been suggested that a more classical interpretation of spontaneous emission should be employed [17]. For instance, when in an excited state the atom's own non-vanishing electromagnetic field ($\Omega \neq 0$) should be viewed as causing a radiative reaction that results in decay. This explanation is directly analogous to the classical Lorentzian theory of radiative decay.

2.5 Master Equations

In practice the problem of determine the dynamics of an ensemble of multilevel atoms coupling to a continuum of field modes in arbitrary photon number states is quite intractable. In addition, often the motion of the atoms, and the associated collisional and Doppler broadening, should be included in the analysis. Generally, spontaneous emission is only one of several decoherence mechanisms present. A more straightforward, and approximate method of accounting for all the degrees of freedom of the ensemble must be found. We represent the interaction between an atom and its environment by forming the density matrix equation of motion:

$$\dot{\hat{\rho}} = -\frac{i}{\hbar}[\hat{H}, \hat{\rho}]_- - \hat{D}(\hat{\rho}(t)), \tag{2.34}$$

where $\hat{D}$ is the decoherence operator. Our choice of decoherence operator depends on the decay and dephasing mechanisms which we expect to be present in the system, and the ease by which the resulting differential equations can be solved. One of the most general forms of decoherence operator is the Lindblad form [42]

$$\hat{D}(\hat{\rho}(t)) = \frac{1}{2}\sum_m \gamma_m \left([\hat{\rho}\hat{L}_m^\dagger, \hat{L}_m]_- + [\hat{L}_m^\dagger, \hat{L}_m\hat{\rho}]_- \right). \tag{2.35}$$

Here γ_m gives the rate of each decay or dephasing process described by the operators $\hat{L}_m$. For example, a spontaneous emission from an atomic level $|2\rangle$ to $|1\rangle$ is generated by the operator $\hat{L} = \sigma_{12}$. Similarly, a pure dephasing between two atomic levels is represented by $\hat{L} = \frac{1}{\sqrt{2}}(\sigma_{22} - \sigma_{11})$. Such a dephasing could occur due to an elastic collision between atoms.

However, an alternative form of decoherence operator also exists, which although less general, produces a master equation that is much easier to solve. This master equation is

$$\dot{\hat{\rho}}(t) = -\frac{i}{\hbar}[\hat{H}, \rho(t)]_- - \frac{1}{2}[\Gamma, \rho(t)]_+, \tag{2.36}$$

for which the decay matrix $\Gamma = \mathrm{diag}\{\Gamma_1, \Gamma_2 \ldots\}$. The main disadvantage of this form of master equation is that only spontaneous decay and decay induced dephasing can be modelled by it. For example, elastic collisions that induce dephasing, but not

atomic transitions, cannot be included by this mechanism. Similarly, no account can be made for the drift of atoms in and out of the interaction region. This is particularly significant for systems such as the atomic lambda system, which contains a pair of nearly degenerate ground states. According to the Maxwell-Boltzmann distribution there will be an appreciable probability for the atom occupying either ground state. Therefore, in a thermal gas there will be a constant drift of coherently prepared atoms out of the laser beam, and a drift of (almost maximally) mixed states into the interaction region. However, given a sufficiently low density gas (few collisions, with buffer gas present) prepared at low temperature (lower drift rate, less mixing and fewer collisions), it is possible to model an atomic system accurately using the master equation (2.36). This is particular significant since solutions to this equation are much easier to derive than solutions using the full Lindblad method. Consider the Schrödinger equation, where the Hamiltonian is no longer necessarily Hermitian:

$$\frac{\partial}{\partial t}|\psi\rangle = -\frac{i}{\hbar}\hat{H}|\psi\rangle, \qquad \equiv \qquad \frac{\partial}{\partial t}\langle\psi| = -\frac{i}{\hbar}\langle\psi|\hat{H}^{\dagger}. \tag{2.37}$$

If we form the density matrix equation of motion $\hat{\rho} = |\psi\rangle\langle\psi|$, we find

$$\dot{\hat{\rho}} = -\frac{i}{\hbar}\left(\hat{H}\hat{\rho} - \hat{\rho}\hat{H}^{\dagger}\right). \tag{2.38}$$

Now, we choose the non-Hermitian Hamiltonian to be of the form

$$\hat{H} = \hat{H}_o - \frac{i\hbar}{2}\hat{\Gamma}, \tag{2.39}$$

where $\hat{\Gamma}$ is represented by the diagonal decay matrix given above. Then we can rewrite the density operator equation of motion as

$$\dot{\hat{\rho}} = -\frac{i}{\hbar}[\hat{H}_o, \hat{\rho}]_- - \frac{1}{2}[\hat{\Gamma}, \hat{\rho}]_+. \tag{2.40}$$

Clearly, this is exactly the same form as the master equation given above (2.36). By solving the Schrödinger equation and making the substitution (2.39), where the eigenvalues of $\hat{H}_o$ become complex, we have also formed solutions to the master equation. We note that this is more that just a mathematical coincidence. From examination of the Weisskopf-Wigner theory we have seen that the energy shift and

decay can be understood as modifications to the real and imaginary parts of the eigenenergy of the excited state. In addition, as was shown in section 1.3 there exists a relationship between the Hamiltonian and the electric susceptibility. Thus, the Kramer-Krönig relations between the real and imaginary parts of the susceptibility at least suggest that a similar relationship may exist for the transition energies.

One further caveat of the simple master equation (2.36) is that although it can model decay and decay induced dephasing, it cannot produce a cascade of population between energy levels. A very simple example of this is given by a system for which the matrix representation of the Hamiltonian is diagonal. In this case the diagonal elements of $[H, \rho]_-$ vanish and their evolution is dictated by the decay only:

$$\dot{\rho}_{pp}(t) = \left(-\frac{1}{2}[\Gamma, \rho(t)]\right)_{pp} = -\Gamma_{pp}\rho_{pp}(t). \tag{2.41}$$

The solution is given by the exponential decay $\rho_{pp}(t) = \exp(-\Gamma_{pp}t)\rho(0)$. That is, the population that decays from each atomic level is simply "lost" from the system and does not cascade. We interpret this as the atom spontaneously decaying into a state outwith our Hilbert space. The decaying behaviour is exactly that predicted by the Weisskopf-Wigner theory, although in many case the actual rate will vary significantly from the W.-W. result. This is due to multilevel effects that arise when energy levels are nearly degenerate and the simple two-level model presented above is no longer valid [36].

2.6 Electromagnetically Induced Transparency

One of the most striking examples of the quantum nature of light is the double-slit interference pattern generated over time by an ensemble of individual photons. Similarly, the quantum-mechanical nature of matter is elegantly demonstrated by the corresponding single-electron experiment [43]. However, it is also possible to demonstrate the quantum-interference of electronic states by using electrons bound within the atom. This was first recognised by Fano in 1961 when considering the process of *autoionisation* [44], by which two two pathways exist for ionisation of an atom

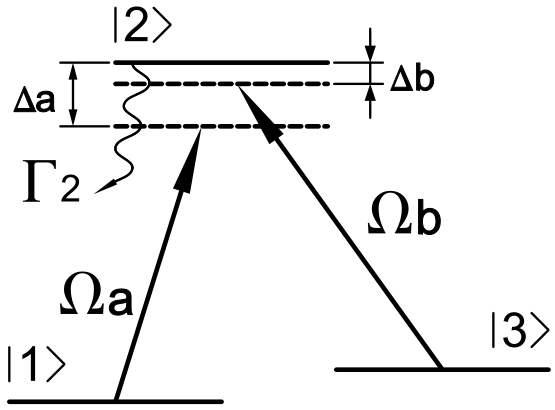

Figure 2.2: The atomic lambda system (Λ-system). Two ground states are coupled to a single excited state that decays at the rate Γ_2.

to occur. More recently, the realisation that intra-atomic quantum interference can produce dramatic effects has been exploited in the phenomena of electromagnetically induced transparency (EIT).

It is well known that a classical electromagnetic field interacting with a quantum-mechanical two-level atom will experience a Lorentzian absorption profile. That is, the electric susceptibility for a density of N/V atoms in the ground state is given by [39]

$$\chi(\Delta) = \frac{Np^2}{\hbar\epsilon_0 V}\frac{\Delta + i\gamma}{\Delta^2 + \gamma^2}, \tag{2.42}$$

where $\Delta - i\gamma$ is the complex detuning predicted by the Weisskopf-Wigner theory. However, there is nothing particularly quantum-mechanical about this result. In fact the same response can be derived by considering the electron as a point charge trapped within a damped harmonic oscillator [17]. The true quantum-mechanical nature of bound-state electrons only becomes manifest when multiple excitation pathways exist and quantum interference can occur. This is analogous to interference occurring in the double-slit experiment.

We consider an atom consisting of two ground states coupled to a decaying excited state (Fig. 2.2). This configuration is often called the *lambda* system (Λ system). The most straightforward method of understanding the Λ system is to

consider the dressed states of the Hamiltonian [45]. Working within an interaction picture and for a semi-classical approximation (or when we restrict ourselves to within one resonant manifold [38]) the Hamiltonian has the matrix representation

$$H = \hbar \begin{pmatrix} 0 & \Omega_a/2 & 0 \\ \Omega_a/2 & \Delta_a & \Omega_b/2 \\ 0 & \Omega_b/2 & \Delta_a - \Delta_b \end{pmatrix}, \tag{2.43}$$

where $\Omega_\alpha, \alpha \in \{a, b\}$ are the Rabi-frequencies of both fields and $\Delta_a = \omega_2 - \omega_1 - \omega_a, \Delta_b = \omega_2 - \omega_3 - \omega_b$ are the detunings. The characteristic polynomial that defines the eigenvalues ($E_n = \hbar\lambda_n$) is

$$4\lambda^3 - 4\lambda^2(2\Delta_a - \Delta_b) - \lambda\left[\Omega_a^2 + \Omega_b^2 - 4\Delta_a(\Delta_a - \Delta_b)\right] + (\Delta_a - \Delta_b)\Omega^2 = 0. \tag{2.44}$$

The eigenvalues can be found by depressing the cubic polynomial and then using a cosine substitution [36]. However, it is more instructive to consider the situation when the fields are *Raman-resonant* with the two photon transition between the ground states ($\Delta_a - \Delta_b = 0$). Then the eigenvalues are easily found to be

$$\lambda_D = 0, \qquad \lambda_\pm = \frac{1}{2}\left(\Delta_a \pm \sqrt{\Delta_a^2 + \bar{\Omega}^2}\right), \tag{2.45}$$

with $\bar{\Omega}^2 = \Omega_a^2 + \Omega_b^2$. The corresponding eigenstates are

$$|D\rangle = \frac{1}{\bar{\Omega}}\left(\Omega_b|1\rangle - \Omega_a|3\rangle\right), \tag{2.46}$$

$$|\Phi_\pm\rangle = \frac{1}{N_\pm}\left(\Omega_a|1\rangle + \Omega_b|3\rangle + 2\lambda_\pm|2\rangle\right). \tag{2.47}$$

The eigenstate $|D\rangle$ is called the *dark state* of the Λ system. It is non-interacting, or *dark*, to the electromagnetic fields since the density matrix elements ρ_{21} and ρ_{23} vanish. This can be explained by the destructive interference between excitation from both ground states. That is, the population is shared among the ground states so as to maintain balanced but anti-phase excitations.

Since $|D\rangle$ is an eigenstate and only contains components of the radiatively stable ground states, we expect that an atom prepared in any mixture of the dressed states to *relax* into the equilibrium dark state. By this method an optically thick gas of

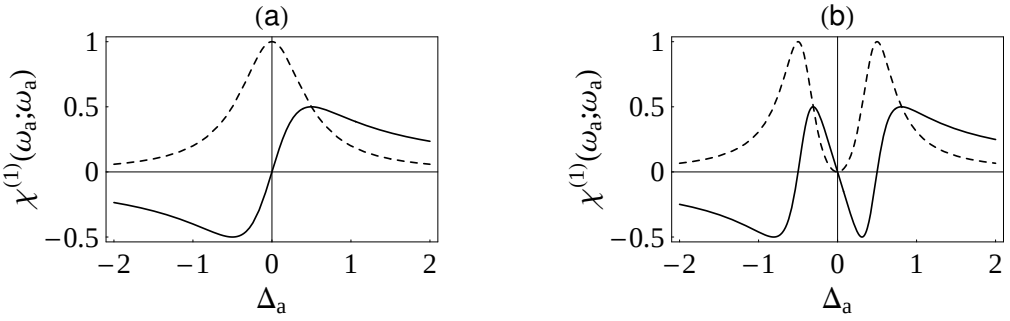

Figure 2.3: The form of the linear electric susceptibilities for (a) two-level atom and (b) the atomic lambda system.

Λ-atoms can be rendered transparent by the addition of a second Raman-resonant field and the subsequent relaxation into the dark state.

This procedure is called electromagnetically induced transparency (EIT) and was first suggested in 1989 by Harris and Imamoğlu [46] when investigating the possibility of lasing without inversion (LWI). Since then the field of gas-phase nonlinear optics has flourished due to the creation of several successful and promising EIT based schemes. In practice transparency is usually achieved in an atom illuminated by one weak (Ω_a) and one strong (Ω_b) field. These are usually named the *probe* and *pump* fields respectively. Within this approximation the linear electric susceptibility experienced by the probe field is

$$\chi^{(1)}(\omega_a;\omega_a) = \frac{4N(\Delta_a - \Delta_b)|p_{12}|^2}{\hbar\epsilon_0 V\left[4(\Delta_a - \Delta_b)(\Delta_a - i\gamma_1) - \Omega_b^2\right]}. \tag{2.48}$$

This electric susceptibility is compared with the two-level case in Fig.(2.3). We note that due to the presence of the atomic dark-state on resonance, the Lorentzian absorption profile has been split into two components. These are called the Autler-Townes components and were observed by spectroscopic analysis of an optically thin gas in 1955 [47].

Many of the most exciting applications of EIT rely on the region of large normal dispersion occurring within the EIT transparency window. For instance, it was demonstrated in 1999 that the high dispersion can be used to reduce the group velocity of light to 17ms^{-1} in an ensemble of ultra-cold sodium atoms [48]. Since

then it has been proposed that slow-light, or *dark-state polaritons* [49], could be used to stop and store light pulses to form an optical quantum memory [50]. Indeed, there has already been considerable success in storing light pulses in both rubidium vapour [51], doped solids [52] and even at the single photon level [53].

The rapid change of refractive index around resonance can also give rise to a large cross-phase modulation (XPM) between two electromagnetic fields in the four- and five-level atoms [54, 55]. This effect forms the foundation of the research undertaken in this thesis and is extensively explored in the following chapters. Much of the current interest in the XPM produced in atomic vapours is due to the central role this interaction plays in many quantum information processing protocols [56, 57]. It has also been suggested as a possible quantum logic gate as part of an all-optical quantum computer [58, 15, 14].

Chapter 3

Steady-State Cross-Phase Modulation

In chapter 1 it was demonstrated that cross-phase modulation will occur in any non-linear centrosymmetric classical material. However, by using coherent interactions between light and an ensemble of atoms it is possible to produce a much stronger, and often pure cross-phase modulation. This possibility was first explored when considering the three-level atom in the EIT configuration. The Λ configuration does however have serious limitations which will be discussed below. Nonetheless, by modifying this system to include a fourth atomic level we are able to overcome many of these problems.

The possibility of achieving large cross-Kerr nonlinearities in the four-level atom, known as the N-configuration atom, was first suggested by Schmidt and Imamoğlu in 1996 [54]. It is the investigation of this system in the non-resonant [59, 60] and time-dependent regimes [61] that constitutes my original work in this thesis. Recently it has been suggested that equally strong nonlinearities could also be produced in the Λ atom by using a single-mode cavity to enhance the interaction [62]. This interesting development has yet to be experimentally realised, but appears to provide another viable method for the generation of large XPM in atomic systems.

3.1 XPM in the Λ System

To show that cross-phase modulation can be produced in a Λ atom we begin by working in the EIT limit. In this case the ground states of the Λ atom are coupled to the excited state by the pump (Ω_b) and probe fields (Ω_a), see fig. 2.2. The electric susceptibility experienced by the weak probe field Ω_a is

$$\chi = \frac{4N(\Delta_a - \Delta_b)|p_{12}|^2}{\hbar\epsilon_0 V\left[4(\Delta_b - \Delta_a)(\Delta_a - i\gamma) - \Omega_b^2\right]}. \tag{3.1}$$

Here, the susceptibility has been calculated to first-order in Ω_a and to all orders in Ω_b. We now make the approximation that the control field Ω_b is strongly detuned, in particular we have $\Omega_b \ll (\Delta_b - \Delta_a)(\Delta_a - i\gamma)$. Then the susceptibility can be Taylor expanded in Ω_b to give linear and XPM terms:

$$\chi^{(1)}(\omega_a;\omega_a) = \frac{N|p_{12}|^2}{\hbar\epsilon_0 V(\Delta_a - i\gamma)}, \tag{3.2}$$

$$\chi^{(3)}(\omega_a;\omega_a,\omega_b,-\omega_b) = \frac{N|p_{12}|^2|p_{34}|^2}{4\hbar^3 V(\Delta_a - i\gamma)^2(\Delta_a - \Delta_b)}. \tag{3.3}$$

The linear term is found to be the usual Lorentzian absorption for an atom in the ground state and the nonlinear term is the cross-phase modulation which we required (Fig. 3.1). However, this configuration has a serious drawback: the XPM is maximal when the probe field is close to resonance with the Lorentzian absorption peak (see fig.(2.3a)). The essential problem of with XPM in the Λ atom is that the XPM is obscured by strong Lorentzian absorption. Unfortunately this cannot be mitigated by working off-resonance since the XPM term decays faster than the linear absorption.

Recent demonstrations of the XPM generated in the three-level atom have chosen to operate on resonance of the probe field [63]. In this case the nonlinear susceptibility simplifies to

$$\chi^{(3)}(\omega_a,\omega_a,\omega_b,-\omega_b) = \frac{4N|p_{12}|^2|p_{23}|^2}{\hbar^3 V\gamma^2\Delta_b}. \tag{3.4}$$

In this expression we can see that the strength of the XPM nonlinearity is limited by the square of the decay rate of the excited state, γ^2. For a typical alkali metal this decay rate is of the order of tens of MHz and severely limits the strength of

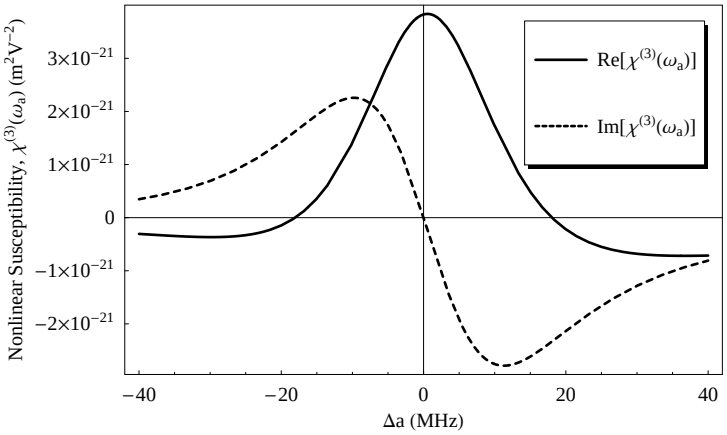

Figure 3.1: The cross-phase modulation $\chi^{(3)}$ nonlinear electric susceptibility generated in the Λ-atom.

the cross-Kerr nonlinearity that can be achieved. For values typical of rubidium-87 and for a control field detuned by 100MHz we find that the XPM produced is only slightly larger than that created in a microstructured optical fibre (e.g. in fibre $\chi^{(3)} \approx 10^{-22}\mathrm{m}^2\mathrm{V}^{-2}$).

3.2 XPM in the N-System

The possibility of achieving a large cross-Kerr nonlinearity in the four-level atom was first proposed by Schmidt and Imamoğlu in 1996 [54]. In the configuration that they suggested three electromagnetic fields were envisaged to interact with an ensemble of atoms in the N configuration (fig. 3.2). This was analysed in the steady-state regime for a resonant Λ subsystem. By using the well-known sodium D-line transitions they proposed that the required four-level atom could be experimentally realised. In keeping with recent experimental demonstrations [64] we will apply the theory developed in this thesis to an ensemble of rubidium-87 atoms trapped within a MOT. The calculations in the following chapter are drawn from the papers [59, 60] and represent original work of the candidate.

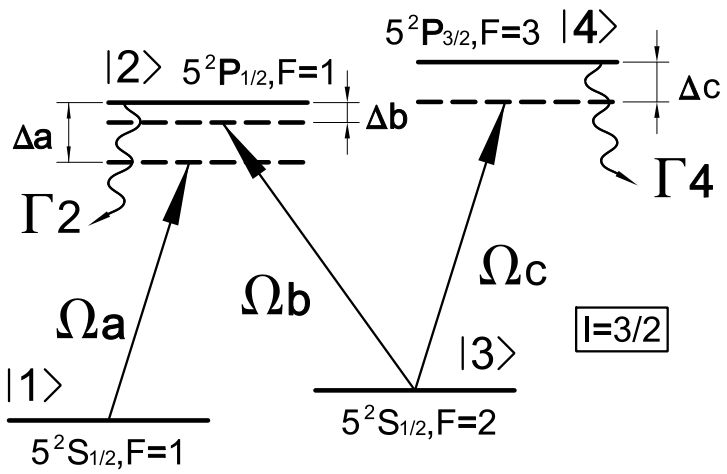

Figure 3.2: The four-level ^{87}Rb atom. We consider transitions between the hyperfine components of the rubidium D lines.

3.2.1 A Simple Model

We begin by presenting a very intuitive explanation of XPM in the N-configuration atom. In this way we show that the XPM is a direct consequence of the electromagnetically induced transparency response of the Λ subsystem.

As discussed in section 2.6 electromagnetically induced transparency can be interpreted as the trapping of the atom in a dark state. This occurs due to spontaneous emission from the excited state rapidly populating the dark superposition of the ground states given by

$$|D\rangle = \frac{1}{\bar{\Omega}} \left(\Omega_b|1\rangle - \Omega_a|3\rangle\right). \tag{3.5}$$

Since the state is non-interacting with the fields the eigenenergy of this state can be shown to vanish ($E_D = 0$, with a suitable choice of zero-point). In the EIT limit the small amount of atomic population in the ground state $|3\rangle$ has the value

$$\rho_{33} \approx \frac{\Omega_a^2}{\Omega_b^2}. \tag{3.6}$$

We now introduce the third field Ω_c that weakly couples to the excited state $|4\rangle$. The weak coupling is due to the large (complex) detuning from resonance $|\Delta_c - i\Gamma_4/2| \gg 0$. From second-order perturbation theory we know that the mixing of the energy

levels will produce a Stark-shift of the state $|3\rangle$ equal to

$$\Delta E_3 \approx -\frac{\hbar\Omega_c^2}{4(\Delta_c - i\Gamma_4/2)}. \tag{3.7}$$

Thus we expect that the energy shift of the dark state in the EIT limit will be given by the product of the population in $|3\rangle$ and the energy shift of the level. We therefore obtain

$$\Delta E_D = -\frac{\hbar\Omega_a^2\Omega_c^2}{4(\Delta_c - i\Gamma_4/2)\Omega_b^2}. \tag{3.8}$$

The product between the electromagnetic fields Ω_a and Ω_c indicates that XPM will occur. By substitution of the energy contribution into the right hand side of (1.64) we find that the cross-Kerr susceptibility for an ensemble of atoms (number density N/V) is given by

$$\chi^{(3)}(\omega_a; \omega_a, \omega_c, -\omega_c) = \frac{2N|p_{12}|^2|p_{34}|^2}{3\epsilon_0 V\hbar^3(\Delta_c - i\Gamma_4/2)\Omega_b^2}. \tag{3.9}$$

This is indeed the correct answer when the Λ subsystem is resonant. We note that the strength of the cross-phase modulation is proportional to the inverse of the pump intensity ($\propto 1/\Omega_b^2$). This is limited however by the requirement that we operate within the EIT regime, for which Ω_b is couples much more strongly that probe fields.

From this simple EIT based argument we can see that the XPM is produced due to the Stark-shift of the small amount of population coherently trapped in the $|3\rangle$ component of the dark state. By viewing the Stark-shift due to the weak field Ω_c as breaking the Raman-resonance of the EIT system, we can also derive XPM directly from the EIT linear susceptibility.

3.2.2 A Full Calculation

We now undertake a more rigorous calculation of the cross-phase modulation in the N-configuration atom. In what follows we remove the requirement that any of the fields are resonant. In addition to XPM we will therefore expect to find linear and self-phase modulation contributions to the electric susceptibility. So that perturbation theory can be used, we also require that the electric fields Ω_a and

Ω_c only weakly excite the atom, whereas Ω_b is a strong pump field. Given these constraints it is expected that a cross-Kerr nonlinearity will arise between the weak probe fields and for the effective Hamiltonian experienced by these fields to be of the form (1.60).

We begin by modelling a single atom interacting with three continuous-wave monochromatic electromagnetic fields. Both the atom and the three fields are treated quantum mechanically. All possible states of the atom are spanned by the four eigenstates $|1\rangle_A, |2\rangle_A, |3\rangle_A$, and $|4\rangle_A$. Similarly, the state of each electromagnetic field mode 'x' can be expanded in the Fock basis $\{|n_x\rangle : n_x \in [0, \infty)\}$.

The state space of the atom and three fields is spanned by the tensor product between the basis vectors of the individual components. That is, the state of the atom and three fields can be expanded in a basis of the form

$$|\psi\rangle = \sum_{i=1}^{4} \sum_{\substack{n_a=0 \\ n_b=0 \\ n_c=0}}^{\infty} c_{i,n_a,n_b,n_c} |i\rangle_A \otimes |n_a\rangle \otimes |n_b\rangle \otimes |n_c\rangle. \tag{3.10}$$

To clarify the notation we will henceforth omit the tensor product symbols and use the shorthand

$$|i\rangle_A \otimes |n_a\rangle \otimes |n_b\rangle \otimes |n_c\rangle = |i, n_a, n_b, n_c\rangle. \tag{3.11}$$

As shown in Chapter 1, the electromagnetic fields couple to the atom by the electric-dipole interaction. Considering only energy-conserving terms (the rotating wave approximation), the total Hamiltonian is written in the Schrödinger picture as

$$\hat{H}_{sp} = \sum_{i=1}^{4} E_i \hat{\sigma}_{i,i} + \hbar \sum_{k=\{a,b,c\}} \omega_k \hat{a}_k^\dagger \hat{a}_k + g_k \hat{\sigma}_k \hat{a}_k + g_k^* \hat{\sigma}_k^\dagger \hat{a}_k^\dagger. \tag{3.12}$$

This is an extension of the Jaynes-Cummings Hamiltonian [26] to a three-mode and four-level atom in the N configuration. Here ω_k is the angular frequency of the electromagnetic field mode 'k'; $\hat{a}_k^\dagger$ and $\hat{a}_k$ are the creation and annihilation operators and g_k and $\hat{\sigma}_k$ are the coupling strengths and atomic-transition operators for the allowed electric-dipole transitions. The coupling strengths are defined in terms of the electric-dipole transition-matrix elements $p_{ij} = e_A \langle i|r|j\rangle_A$ by

$$g_a = \frac{p_{21}\epsilon_a}{\hbar}, \qquad g_b = \frac{p_{23}\epsilon_b}{\hbar}, \qquad g_c = \frac{p_{43}\epsilon_c}{\hbar}. \tag{3.13}$$

Here, $\epsilon_x = \left(\frac{\hbar\omega_x}{2\epsilon_0 V}\right)^{1/2}$ are chosen so that the energy density integral over the mode volume V gives the total energy in the electromagnetic field [39]. The atomic transition operators are defined as

$$\hat{\sigma}_a = |2\rangle_{AA}\langle 1|, \qquad \hat{\sigma}_b = |2\rangle_{AA}\langle 3|, \qquad \hat{\sigma}_c = |4\rangle_{AA}\langle 3|. \tag{3.14}$$

It is convenient to transform the Hamiltonian into the interaction picture where the atomic levels are separated by the multi-photon detunings. This is done by writing the non-coupling terms of the Hamiltonian in terms of the 'conversion' operator invariants of the Hamiltonian. In this interaction picture we obtain the Hamiltonian

$$\hat{H} = \hbar\left(\delta_1\hat{\sigma}_{22} + \delta_2\hat{\sigma}_{33} + \delta_3\hat{\sigma}_{44}\right) + \hbar\sum_{k=\{a,b,c\}} g_k\hat{\sigma}_k\hat{a}_k + g_k^*\hat{\sigma}_k^\dagger\hat{a}_k^\dagger. \tag{3.15}$$

The multi-photon detunings are defined as

$$\begin{aligned} \delta_1 &= \Delta_a = (\omega_2 - \omega_1) - \omega_a, \\ \delta_2 &= \Delta_a - \Delta_b = (\omega_3 - \omega_1) - (\omega_a - \omega_b), \\ \delta_3 &= \Delta_a - \Delta_b + \Delta_c = (\omega_4 - \omega_1) - (\omega_a - \omega_b + \omega_c). \end{aligned} \tag{3.16}$$

By considering the action of the Hamiltonian on basis vectors from the set $\{|i, n_a, n_b, n_c\rangle\}$ one can show that the system will evolve within a four-dimensional resonant-manifold [38]. For instance, the state $|1, n_a, n_b, n_c\rangle$ couples only to the states:

$$\begin{gathered} |2, n_a - 1, n_b, n_c\rangle, \\ |3, n_a - 1, n_b + 1, n_c\rangle, \\ |4, n_a - 1, n_b + 1, n_c - 1\rangle. \end{gathered} \tag{3.17}$$

Since every basis vector in the expansion (3.10) can be written as a state belonging to a resonant manifold of the form (3.17), we need only consider the behaviour of the system within one such four-dimensional subspace. It is therefore possible to further simplify our notation by saying that

$$\begin{aligned} |1\rangle &= |1, n_a, n_b, n_c\rangle, & |2\rangle &= |2, n_a - 1, n_b, n_c\rangle, \\ |3\rangle &= |3, n_a - 1, n_b + 1, n_c\rangle, & |4\rangle &= |4, n_a - 1, n_b + 1, n_c - 1\rangle. \end{aligned} \tag{3.18}$$

Thus, by $|1\rangle$ we mean the state for which the atom is in the state $|1\rangle_A$ and the field modes "a", "b" and "c" are in the number states $|n_a\rangle, |n_b\rangle$ and $|n_c\rangle$ respectively.

When performing calculations it is helpful to express the Hamiltonian in matrix form. All matrices in this section are written with respect to the canonical basis $|1\rangle = [1,0,0,0]^\dagger$, etc. The Hamiltonian therefore has the representation

$$H = \hbar \begin{bmatrix} 0 & \Omega_a^*/2 & 0 & 0 \\ \Omega_a/2 & \delta_1 & \Omega_b/2 & 0 \\ 0 & \Omega_b^*/2 & \delta_2 & \Omega_c^*/2 \\ 0 & 0 & \Omega_c/2 & \delta_3 \end{bmatrix}, \tag{3.19}$$

where the Rabi-frequencies Ω_x are the interaction energies in frequency units and are defined as

$$\Omega_a = 2g_a\sqrt{n_a}, \qquad \Omega_b = 2g_b\sqrt{n_b+1}, \qquad \Omega_c = 2g_c\sqrt{n_c}. \tag{3.20}$$

We note that the Rabi-frequencies are taken as complex numbers. Although this is not necessary when investigating the steady-state behaviour, it will prove useful for comparison with later transient and time-dependent calculations. The form of the Hamiltonian (3.19) is particularly convenient since it is identical to that used in semi-classical calculations. Writing the Hamiltonian in this way is possible since spontaneous emission has been neglected and each state evolves within a single resonant manifold. Otherwise, transitions could be made to non-resonant manifolds and it would be insufficient to model each manifold in isolation.

Dressed States and the Effective Hamiltonian

We now use non-degenerate perturbation theory to calculate dressed states of the atom. From these we can determine the steady-state electric susceptibilities experienced by the fields. In particular, we hope to show that a cross-Kerr nonlinearity will arise between the weak probe fields Ω_a and Ω_c.

We begin by splitting the Hamiltonian into three parts: $\hat{H}_0, \hat{V}_a$ and $\hat{V}_c$. $\hat{H}_0$ consists of the four energy levels, where the states $|2\rangle$ and $|3\rangle$ are coupled by the field Ω_b. This system represents an exactly solvable two-level subsystem with two additional uncoupled levels. $\hat{V}_a$ is the weak coupling from $|1\rangle$ to $|2\rangle$ due to the field Ω_a and $\hat{V}_c$ is the coupling between $|3\rangle$ and $|4\rangle$ produced by Ω_c. The strength

of the perturbations is parameterised by a single variable each: $\xi_a = |\Omega_a|/2$ and $\xi_c = |\Omega_c|/2$, whereas the structure is determined by the matrix operators $\hat{V}_a$ and $\hat{V}_c$. This is depicted in the bare atomic basis by Fig. 3.2. Splitting the Hamiltonian in this way we obtain

$$\hat{H} = \hat{H}_0 + \xi_a \hat{V}_a + \xi_c \hat{V}_c. \tag{3.21}$$

The Hamiltonian $\hat{H}_0$ of the two-level subsystem has the matrix representation

$$H_0 = \begin{bmatrix} 0 & 0 & 0 & 0 \\ 0 & \delta_1 & \Omega_b/2 & 0 \\ 0 & \Omega_b^*/2 & \delta_2 & 0 \\ 0 & 0 & 0 & \delta_3 \end{bmatrix}. \tag{3.22}$$

The two perturbations $\hat{V}_a$ and $\hat{V}_c$ have the representations

$$V_a = \begin{bmatrix} 0 & e^{-i\phi_a} & 0 & 0 \\ e^{i\phi_a} & 0 & 0 & 0 \\ 0 & 0 & 0 & 0 \\ 0 & 0 & 0 & 0 \end{bmatrix}, \qquad V_c = \begin{bmatrix} 0 & 0 & 0 & 0 \\ 0 & 0 & 0 & 0 \\ 0 & 0 & 0 & e^{-i\phi_c} \\ 0 & 0 & e^{i\phi_c} & 0 \end{bmatrix}, \tag{3.23}$$

where $\phi_a = arg(\Omega_a)$ and $\phi_c = arg(\Omega_c)$.

To use perturbation theory we must first determine the eigenstates of the exactly solvable system $\hat{H}_0$. These are given by the uncoupled states $|1\rangle$ and $|4\rangle$ and the dressed states of the two-level subsystem:

$$|\phi_1^{(0,0)}\rangle = |1\rangle, \tag{3.24}$$

$$|\phi_2^{(0,0)}\rangle = |C_-\rangle = \frac{1}{N_-}(\Omega_b|2\rangle + 2(\lambda_- - \delta_1)|3\rangle), \tag{3.25}$$

$$|\phi_3^{(0,0)}\rangle = |C_+\rangle = \frac{1}{N_+}(\Omega_b|2\rangle + 2(\lambda_+ - \delta_1)|3\rangle), \tag{3.26}$$

$$|\phi_4^{(0,0)}\rangle = |4\rangle. \tag{3.27}$$

Here, $N_\pm$ are the normalisation constants for the two-level subsystem eigenstates. The corresponding eigenenergies are given by

$$\lambda_1^{(0,0)} = 0, \tag{3.28}$$

$$\lambda_2^{(0,0)} = \lambda_- = \frac{1}{2}\left((\delta_1+\delta_2) - \sqrt{(\delta_1-\delta_2)^2+|\Omega_b|^2}\right), \tag{3.29}$$

$$\lambda_3^{(0,0)} = \lambda_+ = \frac{1}{2}\left((\delta_1+\delta_2) + \sqrt{(\delta_1-\delta_2)^2+|\Omega_b|^2}\right), \tag{3.30}$$

$$\lambda_4^{(0,0)} = 0. \tag{3.31}$$

Since we are perturbing the atom with two independent interactions V_a and V_c, we expect the eigenenergies and eigenstates to be expressed as Taylor series in both ξ_a and ξ_c. The eigenenergy and eigenstates are therefore assumed to have the form

$$E_n = \sum_{i,j=0}^{\infty} \xi_a^i \xi_c^j E_n^{(i,j)}, \tag{3.32}$$

$$|\phi_n\rangle = \sum_{i,j=0}^{\infty} \xi_a^i \xi_c^j |\phi_n^{(i,j)}\rangle, \tag{3.33}$$

where $E_n^{(i,j)}$ ($\phi_n^{(i,j)}$) is the term of E_n (ϕ_n) i order in V_a and j order in V_c. It also proves convenient to expand the eigenstate corrections in terms of the unperturbed basis states:

$$|\phi_n^{(i,j)}\rangle = \sum_{s=0}^{\infty} a_n^{s(i,j)} |\phi_s^{(0,0)}\rangle. \tag{3.34}$$

By substituting these series solutions into the eigenvalue equation for the Hamiltonian $\hat{H}|\phi_n\rangle = E_n|\phi_n\rangle$ we deduce the expression

$$a_n^{m(p,q)} E_m^{(0,0)} + \langle\phi_m^{(0,0)}|V_a|\phi_n^{(p-1,q)}\rangle + \langle\phi_m^{(0,0)}|V_c|\phi_n^{(p,q-1)}\rangle = \sum_{i=0}^{p}\sum_{j=0}^{q} E_n^{(i,j)} a_n^{m(p-i,q-j)}. \tag{3.35}$$

From (3.35) equations for the $a_n^{m(p,q)}$ and $E_n^{(p,q)}$ terms can be found, other than when $m = n$. In this case we must examine the normalisation of the eigenstate $\langle\phi_n|\phi_n\rangle = 1$ to derive the expression

$$\sum_{i=0}^{p}\sum_{j=0}^{q}\sum_{s=1}^{4} a_n^{*s(i,j)} a_n^{s(p-i,q-j)} = 0, \tag{3.36}$$

from which the $a_n^{n(p,q)}$ terms can be deduced. In practice it will be sufficient during the calculations to expand the eigenstates to third-order and eigenenergy to fourth-order. The relevant formulae are listed in appendix A.

We have now finished "setting-up" the system and are prepared to calculate the approximate dressed states of the atom. However, only the modification caused to

the bare atomic state $|1, n_a, n_b, n_c\rangle$ will be of interest. We expect this, because it is the only radiatively stable state of the unperturbed system. When the strong coupling field "b" is turned on, we expect the atom to rapidly relax from any mixed state into this pure *dark-state*. Indeed, when the atom is perturbed by the fields "a" and "c" we expect $|\phi_1\rangle$, the perturbed counterpart of $|1\rangle$, to remain the most radiately stable dressed state. It is interesting to note that even when considering only the unitary dynamics of the system we require spontaneous emission to establish the atom in an initial pure state.

To fourth-order it is found that the eigenenergy of the state $|\phi_1\rangle$ is found to be

$$\lambda_1 \approx \xi_a^2 \lambda_1^{(2,0)} + \xi_a^4 \lambda_1^{(4,0)} + \xi_a^2 \xi_c^2 \lambda_1^{(2,2)}, \tag{3.37}$$

where the eigenvalue corrections are

$$\lambda_1^{(2,0)} = -\frac{\delta_2 |\Omega_a|^2}{4\delta_1\delta_2 - |\Omega_b|^2}, \tag{3.38}$$

$$\lambda_1^{(4,0)} = \frac{\delta_2(4\delta_2^2 + |\Omega_b|^2)|\Omega_a|^4}{(4\delta_1\delta_2 - |\Omega_b|^2)^3}, \tag{3.39}$$

$$\lambda_1^{(2,2)} = -\frac{|\Omega_b|^2|\Omega_a|^2|\Omega_c|^2}{4\delta_3(4\delta_1\delta_2 - |\Omega_b|^2)^2}. \tag{3.40}$$

Similarly, the approximate eigenstate $|\phi_1\rangle$ is given in the bare atomic basis to third-order by

$$\begin{aligned} |\phi_1\rangle = & \left[1 - \frac{|\Omega_a|^2(4\delta_2^2 + |\Omega_b|^2)}{2(\delta_1\delta_2 - |\Omega_b|^2)^2}\right]|1\rangle + \left[\frac{-2\Omega_a\delta_2}{4\delta_1\delta_2 - |\Omega_b|^2} + \frac{3|\Omega_a|^2\Omega_a\delta_2(4\delta_2^2 + |\Omega_b|^2)}{(4\delta_1\delta_2 - |\Omega_b|^2)^3}\right]|2\rangle + \\ & \left[\frac{\Omega_a\Omega_b^*}{4\delta_1\delta_2 - |\Omega_b|^2} - \frac{|\Omega_a|^2\Omega_a\Omega_b^*(8\delta_1\delta_2 + 12\delta_2^2 + |\Omega_b|^2)}{2(4\delta_1\delta_2 - |\Omega_b|^2)^3}\right]|3\rangle - \\ & \frac{\Omega_a\Omega_b^*\Omega_c}{2\delta_3(4\delta_1\delta_2 - |\Omega_b|^2)}|4\rangle. \end{aligned} \tag{3.41}$$

Since eigenstates of the Hamiltonian are also solutions of the time-independent Schrödinger equation the evolution of $|\phi_1\rangle$ is described by

$$|\phi_1(t)\rangle = \exp(-i\lambda_1 t)|\phi_1(0)\rangle. \tag{3.42}$$

Recalling the definition of the Rabi frequencies (3.20) we may express each of the eigenvalue terms (3.38),(3.39) and (3.40) in terms of photon numbers. Moreover,

since the eigenstate $|\phi_1\rangle$ is given to zeroth order by $|1, n_a, n_b, n_c\rangle$ then we can replace the photon numbers with their corresponding photon-number operators, when acting on this state. This is possible because the state $|1, n_a, n_b, n_c\rangle$ is an eigenstate of the photon-number operators $\hat{n}_x$ with eigenvalues n_x. Therefore

$$|\phi_1(t)\rangle = \exp\left(-i\left\{L\hat{n}_a + S\hat{n}_a^2 + K\hat{n}_a\hat{n}_c\right\}t\right)|\phi_1(0)\rangle, \tag{3.43}$$

where we have defined

$$L = -\frac{\delta_2|g_a|^2}{\delta_1\delta_2 - |g_b|^2(n_b+1)}, \tag{3.44}$$

$$S = \frac{\delta_2(\delta_2^2 + |g_b|^2(n_b+1))|g_b|^4}{(\delta_1\delta_2 - |g_b|^2(n_b+1))^3}, \tag{3.45}$$

$$K = \frac{-|g_a|^2|g_b|^2|g_c|^2(n_b+1)}{\delta_3(\delta_1\delta_2 - |g_b|^2(n_b+1))^2}. \tag{3.46}$$

The coupling strengths g_x and multi-photon detunings are defined in equations (3.16) and (3.13) respectively. From the form of the evolution (3.43) we can see that this is generated by the effective Hamiltonian

$$\hat{H}_{eff} = \hbar\left(L\hat{n}_a + S\hat{n}_a^2 + K\hat{n}_a\hat{n}_c\right). \tag{3.47}$$

The coefficients L, S and K represent the linear, self-Kerr and cross-Kerr responses of the atom. The linear and self-Kerr energy contributions are due to the fields Ω_a and Ω_b coupling between the states $|1\rangle, |2\rangle$ and $|3\rangle$: this constitutes a Λ subsystem. However, the cross-Kerr response arises because of the adiabatic Stark shift of the atomic level $|3\rangle$. As shown previously by using the "simple model" for a resonant Λ subsystem, this will result in a cross-Kerr nonlinearity.

It is well known that when the two-photon transition from $|1\rangle$ to $|3\rangle$ is resonant ($\delta_2 = 0$), then there is no linear or self-Kerr interaction. This is due to the atom relaxing into the *darkstate* of the Λ subsystem (see section 2.6). In this state the atom is non-interacting, or *dark*, to the applied fields. Therefore the linear- and self-Kerr responses vanish ($L = S = 0$) and the evolution of the system reduces to a pure cross-Kerr interaction. On Raman-resonance the cross-Kerr coefficient has the value

$$K = -\frac{|g_a|^2|g_c|^2}{\delta_3|g_b|^2(\hat{n}_b+1)}. \tag{3.48}$$

The effective Hamiltonian (3.47) then has the form of Eq. (1.60). That is

$$\hat{H}_{eff} = \hbar K \hat{n}_a \hat{n}_c. \tag{3.49}$$

For an ensemble of rubidium atoms prepared in the collective atomic ground state $|\{1\}, n_a, n_b, n_c\rangle$ the effective Hamiltonian is given again by (3.49), where

$$K = \frac{-N|g_a|^2|g_c|^2}{\delta_3|g_b|^2(\hat{n}_b + 1)} \tag{3.50}$$

and N is the number of atoms in the interaction volume. The enhancement of the coupling strength by a factor of N is due to the additive nature of the energy for each non-interacting atom.

Electric Susceptibility

We now calculate the absorption that accompanies the linear, Kerr and cross-Kerr responses of the atom. To do so, we consider the macroscopic material polarisation at both the probe field frequencies.

$$P(t) = \frac{1}{2} \sum_{n=\{a,c\}} P_n e^{-i\omega_n t} + P_n^* e^{i\omega_n t}. \tag{3.51}$$

We expect that the component of polarisation at the frequency ω_a will display linear, self-Kerr and cross-Kerr contributions. Up to third-order we therefore have

$$\begin{aligned} P_a &= \epsilon_0 \chi^{(1)}(\omega_a; \omega_a) E_a + \frac{3}{4} \epsilon_0 \chi^{(3)}(\omega_a; \omega_a, -\omega_a, \omega_a) |E_a|^2 E_a & (3.52) \\ &\quad + \frac{3}{2} \epsilon_0 \chi^{(3)}(\omega_a; \omega_c, -\omega_c, \omega_a) |E_c|^2 E_a. & (3.53) \end{aligned}$$

We note that the electric fields are related to the Rabi-frequencies by

$$E_a = -\frac{\Omega_a \epsilon_a}{g_a}, \qquad E_c = -\frac{\Omega_c \epsilon_c}{g_c}. \tag{3.54}$$

It is expected that the macroscopic polarisation (3.51) will be related the microscopic state of the atom. We begin by constructing the density matrix corresponding to the approximate eigenstate $|\phi_1\rangle$ (3.41):

$$\rho = |\phi_1\rangle\langle\phi_1|. \tag{3.55}$$

In particular, the atom interacts with the electromagnetic fields via the off-diagonal elements of the density matrix. In the interaction picture these are time-independent and are given by

$$\rho_{21} = \langle 2|\rho|1\rangle, \tag{3.56}$$

$$\rho_{43} = \langle 4|\rho|3\rangle. \tag{3.57}$$

So far the system has been described by the unitary evolution of the Schrödinger equation. To model the spontaneous decay of the upper atomic levels ($|2\rangle$ and $|4\rangle$) we take the multi-photon detunings of the eigenstate (3.41) as complex [65]. As shown in section 2.5 this makes the evolution of the non-Hermitian Hamiltonian equivalent to the density matrix master equation (2.36). Thus, the detunings are transformed such that

$$\delta_1 \to \delta_1 - i\gamma_1, \qquad \delta_3 \to \delta_3 - i\gamma_3. \tag{3.58}$$

Here $\gamma_1 = \Gamma_2/2$ and $\gamma_3 = \Gamma_4/2$ where Γ_x is the spontaneous decay rate of the atomic level $|x\rangle$. It is now possible to equate the material polarisation with that described by the off-diagonal density matrix elements in the Schödinger picture. If we have a dilute ensemble of non-interacting trapped atoms then the material polarisation scales as the number of atoms per unit volume. Therefore, the polarisation is related to the off-diagonal density matrix elements by

$$P(t) = \frac{N}{V}\left(\rho_{12}p_{21} + \rho_{34}p_{43} + c.c.\right), \tag{3.59}$$

where $p_{ij} = e_A\langle i|r|j\rangle_A$ are the dipole matrix elements. By Taylor expanding the off-diagonal density matrix elements in terms of the fields Ω_a and Ω_c we find expressions for the linear, self-Kerr and cross-Kerr electric susceptibilities. For the $|1\rangle \leftrightarrow |2\rangle$ transition the linear susceptibility is

$$\chi^{(1)}(\omega_a;\omega_a) = \frac{4N\delta_2\omega_a|p_{12}|^2}{\hbar\epsilon_0 V[4\delta_2(\delta_1 - i\gamma) - |\Omega_b|^2]}. \tag{3.60}$$

The self-Kerr susceptibility is found to be somewhat more complicated, and is given by

$$\chi^{(3)}(\omega_a;\omega_a,-\omega_a,\omega_a) = \frac{32|p_{12}|^4 N\delta_2(4\delta_2^2 + |\Omega_b|^2)}{3\epsilon_0\hbar^3 V} \times \tag{3.61}$$

$$\frac{[16\gamma_1^2\delta_2^2 - (4\delta_1\delta_2 - |\Omega_b|^2)[4i\gamma_1\delta_2 + 4\delta_1\delta_2 - |\Omega_b|^2]]}{(4\gamma_1\delta_2 - 4i\delta_1\delta_2 + i|\Omega_b|^2)^2(-4i\gamma_1\delta_2 + 4\delta_1\delta_2 - |\Omega_b|^2)^3}.$$

By taking terms of ρ_{21} of first-order in Ω_a and second-order in Ω_c we obtain the cross-Kerr susceptibility:

$$\chi^{(3)}(\omega_a; \omega_c, -\omega_c, \omega_a) = \frac{2N|p_{12}|^2|p_{34}|^2|\Omega_b|^2}{3\epsilon_0\hbar^3 V(\delta_3 - i\gamma_3)(4\delta_2(i\gamma_1 - \delta_1) + |\Omega_b|^2)^2}. \tag{3.62}$$

For the $|3\rangle \rightarrow |4\rangle$ transition we find that only the third-order cross-Kerr susceptibility is present. Thus, by taking terms in ρ_{43} of second-order in Ω_a and first-order in Ω_c we find that the XPM experienced by the field Ω_c is given by

$$\chi^{(3)}(\omega_c; \omega_a, -\omega_a, \omega_c) = \frac{2N|p_{12}|^2|p_{34}|^2}{3\epsilon_0\hbar^3(\delta_3 - i\gamma_3)[4(\delta_1 - i\gamma_1)\delta_2 - |\Omega_b|^2][4(\delta_1 + i\gamma_1)\delta_2 - |\Omega_b|^2]}. \tag{3.63}$$

It is interesting to note that in general the fields Ω_a and Ω_c will experience *different* cross phase modulations. Only on Raman-resonance do we find that the XPM is reciprocal. In this case the third-order XPM susceptibility experience by both probe fields is given by

$$\chi^{(3)}(\omega_a|\omega_c) = \frac{2N|p_{12}|^2|p_{34}|^2}{3\epsilon_0\hbar^3 V(\Delta_c - i\Gamma_4/2)|\Omega_b|^2}. \tag{3.64}$$

We note that this is exactly the XPM derived previously using the simple model in subsection 3.2.1. However, previously we were only able to derive the XPM experienced by the probe field Ω_a, when the Λ subsystem was resonant. Using the full model explored in this section we have removed these limitations.

3.2.3 Experimental Parameters

We now turn to evaluating our theory for a realistic physical system: an ensemble of rubidium-87 atoms. The energy level structure is depicted in figure (3.3), showing only the hyperfine sublevels used. The decay rates and transition strengths for the D1 and D2 lines are given in table (3.2.3) and are found in Steck's spectroscopic data [66]. In passing, we note that the decay rate for the D1 line is very close to that predicted by the Weisskopf-Wigner theory (predicted: 35.9MHz, observed: 36.1MHz). However, the D2 line deviates significantly (predicted: 76.0MHz, observed: 38.1MHz). This can be explained by the small energy separation between

the four upper-level hyperfine components of the D2 line. In this case the two-level model is a poor approximation, and should be extended to include the effect of nearly degenerate levels [36].

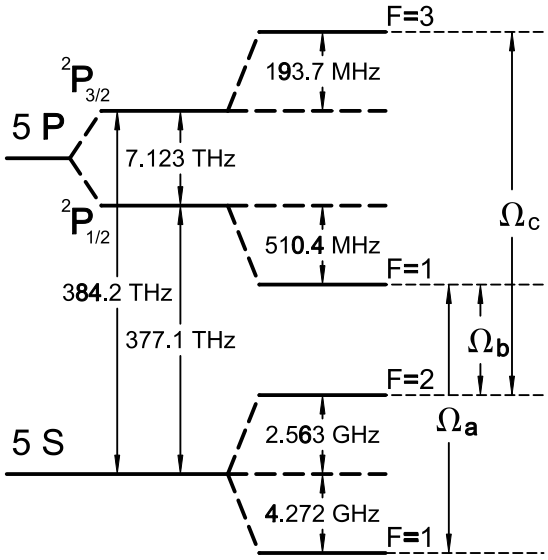

Figure 3.3: The energy level structure of rubidium 87 showing the hyperfine sublevels used.

The data book [66] also provides the transition strengths for the fine structure D lines. However, the experimental implementation of the four-level atom proposed requires the use of hyperfine transitions. It is therefore necessary to derive the dipole matrix elements for each of the hyperfine components. From [67] we find the relative line intensities for a quartet. These are enumerated in table (3.2.3) and can easily be converted into fractions of the total line intensity.

For a two-level atom, the absorption or emission line intensity is given by the imaginary part of the linear electric susceptibility [39]:

$$\mathrm{Img}\left[\chi^{(1)}\right] = -\frac{|p|^2\gamma}{\hbar\epsilon_0(\Delta^2+\gamma^2)}(\rho_{11}-\rho_{22}) \tag{3.65}$$

Assuming that the decay rate of the hyperfine sublevels are equal, then the line intensity is proportional to the square of the dipole matrix element: $I \propto |p|^2$. Hence, by taking the square root of the fractional line intensities of each component, the

fractional dipole matrix elements can be derived. These are likewise enumerated in table (3.2.3). From these calculations we find that the dipole matrix elements have the values

$$p_a = 0.25 \times 2.534 \times 10^{-29} = 6.335 \times 10^{-30} \text{ Cm}, \tag{3.66}$$

$$p_b = 0.56 \times 2.534 \times 10^{-29} = 1.419 \times 10^{-29} \text{ Cm}, \tag{3.67}$$

$$p_c = 0.66 \times 3.584 \times 10^{-29} = 2.365 \times 10^{-29} \text{ Cm}. \tag{3.68}$$

In addition to the dipole matrix elements and decay rates we also require some knowledge of the experimental set-up, such as the field intensities used, number of atoms trapped, etc. For these, we use parameters from a recent experimental demonstration of XPM in rubidium [64]. That is, we have $N = 10^9$ atoms contained within a 3 mm radius sphere, trapped by a MOT. The probe fields are supposed to be focused to a radius significantly narrower that the trapped cloud, so that the fields propagate through a cylinder of trapped atoms. The electromagnetic fields are chosen to have the Rabi-frequencies $\Omega_a = 0.2$ MHz, $\Omega_b = 4$ MHz and $\Omega_c = 3$ MHz. These correspond to the approximate photon numbers, $n_a = 3$, $n_b = 221$ and $n_c = 44$. The fields Ω_a and Ω_b are on-resonance, whereas the field Ω_c is detuned by $\Delta_c = 100$ MHz. On evaluation of the cross-Kerr constant K, as given by (3.50), we find that $K = -4.607 \times 10^8$. This corresponds to a phase-shift of the Fock state by $\theta = -1.12$ rad,

$$|\{1\}, n_a, n_b, n_c\rangle \rightarrow \exp(-i\theta)|\{1\}, n_a, n_b, n_c\rangle. \tag{3.69}$$

This is of the order required by many quantum information processing protocols that require large phase-shifts with relatively few (often single) photons. Next, we evaluate the optical phase shift caused to the field Ω_a. The phase shift it given by (1.59) and has the value

$$\Delta\phi_{NL} = 0.1 \text{ rad}. \tag{3.70}$$

Employing the experimental parameters listed above we also evaluate the linear (3.60), self-Kerr (3.62) and cross-Kerr susceptibilities (3.62, 3.63). Figure (3.4) shows the distinctive EIT response of the atom to the Ω_a probe field. Notable features are the narrow transparency window on resonance ($\Delta_a = \Delta_b = 0$) and

Decay rates:	
$D1 : (5^2S_{1/2} \rightarrow 5^2P_{1/2})$	$2\gamma_1 = \Gamma_{D1} = 38.11 \times 10^6 s^{-1}$
$D2 : (5^2S_{1/2} \rightarrow 5^2P_{3/2})$	$2\gamma_2 = \Gamma_{D2} = 36.10 \times 10^6 s^{-1}$

Dipole matrix elements:	
$D1 : (5^2S_{1/2} \rightarrow 5^2P_{1/2})$	$\langle J = 1/2 \vert er \vert J' = 1/2 \rangle = 2.534 \times 10^{-29}$Cm
$D2 : (5^2S_{1/2} \rightarrow 5^2P_{3/2})$	$\langle J = 1/2 \vert er \vert J' = 3/2 \rangle = 3.584 \times 10^{-29}$Cm

Nuclear angular momentum I=3/2

Table 3.1: Rubidium 87 Data

D1	J=1/2		**D2**	J=1/2	
	F=1	F=2		F=1	F=2
			J'=3/2, F'=0	14.3	
J'=1/2, F'=1	20	100	F'=1	35.7	7.1
F'=2	100	100	F'=2	35.7	35.7
			F'=3		100

Table 3.2: Relative line intensities for the D1 and D2 lines.

D1	J=1/2		**D2**	J=1/2	
	F=1	F=2		F=1	F=2
			J'=3/2, F'=0	0.25	
J'=1/2, F'=1	0.25	0.56	F'=1	0.39	0.18
F'=2	0.56	0.56	F'=2	0.39	0.39
			F'=3		0.66
	$\times 2.534 \times 10^{-29}$ Cm			$\times 3.584 \times 10^{-29}$ Cm	

Table 3.3: Fraction of the dipole matrix elements for the D1 and D2 lines.

steep normal dispersion associated with slow-light propagation. The self-Kerr susceptibility experienced by the field Ω_a is plotted in figure (3.5). Again, due to the dark-state trapping on resonance the refractive and absorptive components of the nonlinearity vanish on resonance. However, the transparency window of the SPM is significantly narrower than for the linear response. Nonetheless, by choosing the field strengths such that $\Omega_c \gg \Omega_a$ the self-phase modulation is approximately an order-of-magnitude less that the cross-phase modulation.

Figure (3.6) shows the cross-phase modulation experienced by both probe fields when the Λ subsystem is resonant ($\Delta_a = \Delta_b = 0$). We note that on resonance ($\Delta_c = 0$) there is a large absorption and the refractive component of the susceptibility vanishes. However, by increasing the detuning of the field Ω_c it is possible to reach a regime where the ratio of refractive to absorptive nonlinearity is much more favourable. Typically we work with a detuning of $\Delta_c = 100$ MHz for which

$$\frac{\mathrm{Re}[\chi_c^{(3)}(\Delta_c = 10^8)]}{\mathrm{Im}[\chi_c^{(3)}(\Delta_c = 10^8)]} \approx 5. \tag{3.71}$$

In this region, the refractive nonlinearity ($\chi^{(3)} \approx 10^{-7}\mathrm{m}^2\mathrm{V}^{-2}$) is many orders of magnitude larger than that generated in microstructured optical fibre ($\chi^{(3)} \approx 10^{-21}\mathrm{m}^2\mathrm{V}^{-2}$) or the Λ atom ($\chi^{(3)} \approx 10^{-22}\mathrm{m}^2\mathrm{V}^{-2}$).

3.3 Chapter Summary

In this chapter we have investigated the generation of cross-phase modulation in the N-configuration atom. By using the remarkable properties of electromagnetically induced transparency it is possible to generate a very large cross-Kerr nonlinearity. In general the light fields coupling to the atom will experience a linear response, self-phase and cross-phase modulation. However, by adjusting the detunings of the electromagnetic fields it is possible to isolate a large refractive nonlinearity, with vanishing absorption.

The generation of this nonlinearity can be understood as arising due to the perturbation caused to the Λ atom dark-state. When the fields coupling to the Λ atom

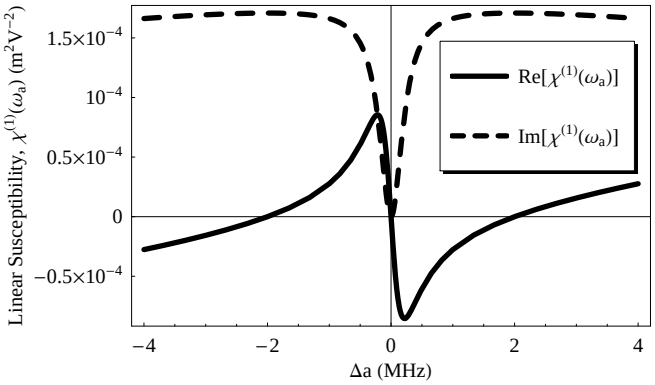

Figure 3.4: The real and imaginary components of the linear electric susceptibility experienced by the field "a" plotted versus the detuning of the probe field "a" (Δ_a) for a resonant pump field "b"

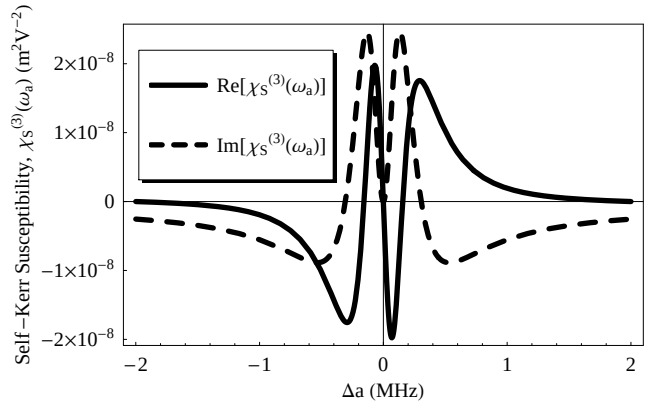

Figure 3.5: The real and imaginary components of the electric susceptibility experienced by the field "a" plotted versus the detuning of the probe field "a" (Δ_a) for a resonant pump field "b"

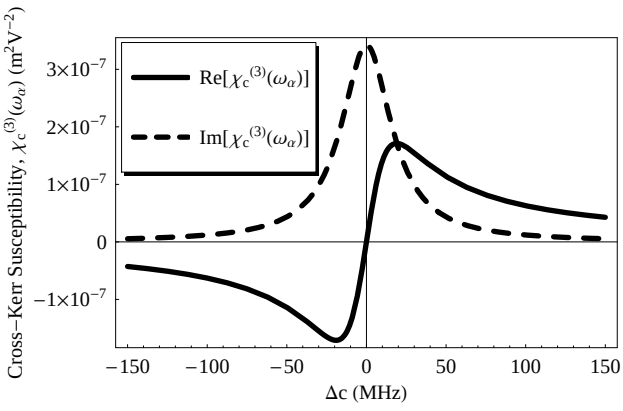

Figure 3.6: The real and imaginary components of the electric susceptibility experienced by the field "α", $\alpha \in \{a, c\}$ plotted versus the detuning of the probe field "c" (Δ_c) for a resonant probe "a" and resonant pump "b".

are resonant ($\Delta_a = \Delta_b = 0$) then the atom becomes transparent (non-absorptive and non-refractive) to the fields. This is the well-known effect of electromagnetically induced transparency. By introducing a third weak field it is possible to perturb the dark-state so as to Stark-shift one of the Λ atom ground states. This breaks the resonance requirement of the dark state ($\Delta_b \neq 0$) and introduces nonlinear absorption and refraction into the atom. However, by increasing the detuning of the field it is seen that the absorption decays much more rapidly than the refraction (fig. 3.6). We are therefore able to produce a large refractive cross-Kerr nonlinearity.

The theory is also shown to be consistent with recent experimental demonstrations of a large XPM generated in rubidium-87. The values of the nonlinear coupling strength is calculated for an ensemble of 10^9 rubidium atoms and is seen to be many orders of magnitude larger than that generated in the Λ atom or microstructured optical fibres. Indeed, the nonlinearity is of ample magnitude to suggest the feasibility of several XPM based quantum-information processing protocols.

Chapter 4

Transient Cross-Phase Modulation

In the previous chapter the steady-state cross-phase modulation that occurs in a N-configuration atom was investigated. Often it is necessary, and indeed interesting, to consider the effect of applying time-dependent fields to atomic systems. In this chapter we consider one of the most straightforward time-dependent situations: coherent transients.

Mathematically transient solution are important when studying the time-dependent behaviour of a system for which the initial state is *not* one of steady states. In this case, we expect damping to gradually relax the system towards its long-term behaviour. In the case of coherent atomic interactions the transient behaviour is induced by a sudden change in either the intensity or detuning of an applied electromagnetic field.

4.1 Λ-System Transients

In recent years there has been growing interest in the transient behaviour of the three-level atom. This has been driven by several motivations. In some cases there has simply being a desire to gain a deeper understanding of coherent interactions [68]. Nonetheless, the incentive for much of the research has been from potential applications. For instance, recent research has suggested that the transient induced by rapidly sweeping the detuning of a probe field could be used to make low in-

tensity field measurements [69]. However, the greatest incentive towards the study of transient EIT has been due to the relationship between this and quantum information storage. For example recent work employing a room-temperature vapour of rubidium-87 has determined the non-radiative decay of the hyperfine components of the $5S_{1/2}$ ground state [70]. An accurate knowledge of this as a function of temperature is vital in determining the maximum storage time in dark-state quantum memory schemes [50]. Again, this experiment was based on controlling the detuning of the EIT field (in this case an instantaneous shift was made) and observing the resultant fluctuations in the sample transmission.

Considerable effort has also been expended on investigations of intensity-induced transients. Commonly these have involved suddenly turning-on or off the fields. One of the earliest works on EIT transients involved predicting a large absorption of the probe field when suddenly turned on [68]. This also occurs in the N-configuration atom, in which we will later study transient XPM. More recently work has concentrated on the turn-on and turn-off characteristics of the control field. These investigation have been motivated by the close relationship to dark-state polariton based quantum memory schemes [71]. In addition the recent experimental demonstrations of transient lasing without inversion (LWI) in the three- [72] and four-level systems [73] have also provided further incentive for the studying this field. Indeed, in the three-level scheme transient LWI for a weak probe field was demonstrated even without the need for incoherent pumping.

Despite the wide variety of effects investigated in these papers they all share some fundamental time-dependent characteristics, intrinsic to the Λ system. This can be understood by considering the three-level atom on two-photon (or Raman) resonance. In this case the Hamiltonian can be written as

$$H = \begin{bmatrix} 0 & \Omega_a/2 & 0 \\ \Omega_a/2 & \Delta & \Omega_b/2 \\ 0 & \Omega_b/2 & 0 \end{bmatrix}. \tag{4.1}$$

We now introduce a new ordered basis:

$$|-\rangle \;=\; \frac{1}{\bar{\Omega}}\left(\Omega_b|1\rangle - \Omega_a|3\rangle\right), \tag{4.2}$$

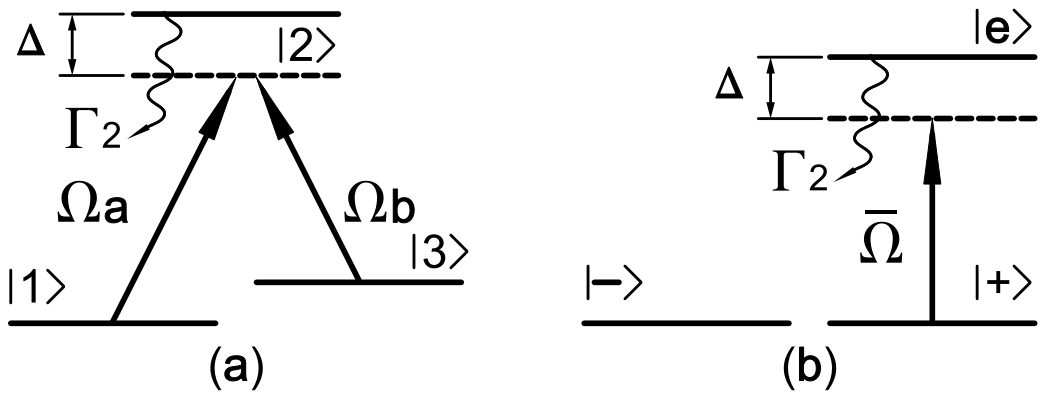

Figure 4.1: The two-photon resonant Λ-atom represented in (a) the bare atomic basis and (b) with respect to the bright/dark ground state superpositions $|\pm\rangle$ and the excited state $|e\rangle$.

$$|+\rangle = \frac{1}{\bar{\Omega}}\left(\Omega_a|1\rangle + \Omega_b|3\rangle\right), \tag{4.3}$$

$$|e\rangle = |2\rangle, \tag{4.4}$$

where $\bar{\Omega}^2 = \Omega_a^2 + \Omega_b^2$. These are the bright ($|+\rangle$) and dark ($|-\rangle$) superpositions of the ground states and the excited state $|e\rangle$. We allow the excited state to decay at a rate Γ_2. Using this new basis the Raman-resonant Hamiltonian can be transformed into the form

$$H = \begin{bmatrix} 0 & 0 & 0 \\ 0 & 0 & \bar{\Omega}/2 \\ 0 & \bar{\Omega}/2 & \Delta \end{bmatrix}. \tag{4.5}$$

Remarkably, we can see that the dark-state has decoupled out of the unitary evolution of the system. In this basis, the Raman-resonant Λ system has been transformed into a decoupled dark-state $|-\rangle$ and a two-level subsystem formed by $|+\rangle$ and $|e\rangle$ coupled by the effective field $\bar{\Omega}$. Using this basis we can now form the density matrix equations of motion for the atom. In particular we find the following equation for the coherence between the bright and excited states:

$$\dot{\rho}_{+e}(t) = \left[-\frac{\Gamma_2}{2} + i\Delta\right]\rho_{+e}(t) + \frac{i}{2}\left[\rho_{++}(t) - \rho_{ee}(t)\right]\bar{\Omega}. \tag{4.6}$$

Now, we choose to work in the regime for which the excited state decays very rapidly

(e.g. in alkali metals this is commonly tens of MHz). Then we can assume that the excited state is never appreciably populated, or $\rho_{ee} \approx 0$. For simplicity we take $\Delta = 0$, in which case we expect the coherence to rapidly reach a quasi-equilibrium given by

$$\rho_{+e}(t) \approx \frac{i\rho_{++}(t)\bar{\Omega}}{\Gamma_2}. \tag{4.7}$$

We can then substitute this result into the equation of motion for the bright state

$$\dot{\rho}_{++}(t) = \frac{i}{2}\left[\rho_{+e}(t) - \rho_{e+}(t)\right]\bar{\Omega}. \tag{4.8}$$

Solving this equation of motion we find that the decay of the bright state is given by

$$\rho_{++}(t) = \rho_{++}(0)\exp\left[-\frac{\bar{\Omega}^2 t}{\Gamma_2}\right]. \tag{4.9}$$

Since the decay of the bright state occurs only by transitions via the excited state, then its relaxation will be relatively slow. For values typical in unsaturated EIT experiments ($\Omega_b \ll \Gamma_2$) the decay rate of the bright state is of the order of less than 1MHz; much less that the excited state decay rate. Thus, when considering the dynamics of the Λ- and N-configuration systems, the dominant time-scale determining the dynamics will be the decay rate of the bright state. Although a detailed discussion of the above papers is unnecessary, the bright state decay rate is seen to dominate all of the physical processes described in the papers above. We expect this since any sudden intensity or detuning variation will cause a proportion of the initial state to reside in the bright superposition of the ground states. It is then the decay of this population that will define the dominant time-scale of the particular process. We will see that this is also true when investigating the dynamics of XPM in the N-configuration atom.

4.2 N-System Transients

Recently there has been growing interest in the transient behaviour of the N-configuration system. Indeed, there has already been a number of theoretical [74]

and experimental [75, 76] investigations into transients of the absorptive and refractive Kerr nonlinearity. We investigate here the situation where the EIT probe field, Ω_a, is suddenly turned on and calculate the transient behaviour of the linear and nonlinear susceptibilities on both probe transitions. The majority of the results in the proceeding section have been published by the candidate in [61], although some of the interpretations are more recent.

To calculate the transient behaviour of the atom when the field Ω_a is suddenly turned on, we first determine the dressed states of the atom - that is, the eigenstates of the Hamiltonian (3.19). As done in chapter 3 we begin by splitting the Hamiltonian into three parts: the two-level subsystem, plus two perturbations (see equation (3.21)). In order to simplify the calculations the perturbations will be applied *consecutively* rather than simultaneously as before. This has the advantage that only two first-order perturbations have to be performed. However, it also means that no information can be deduced about the magnitude or time-dependence of the self-Kerr effect. Nonetheless, since it has already been shown in chapter 3 that with a suitable choice of field strengths the SPM is negligible, we feel justified in making this approximation here.

We perturb the system to first-order by introducing the interaction term $\hat{V}_c$. To avoid degeneracies in the perturbation series we assume that the detuning δ_3 dominates over the other zeroth-order eigenvalues ($\delta_3 \gg \lambda_\pm$). Since this detuning will later be taken to be complex (Weiskopf-Wigner decay), the rapid decay from the state $|4\rangle$ will justify this condition even when $\Delta_c = 0$. We begin by using the unperturbed basis states (3.24)-(3.27). To first-order the new eigenstates of the "intermediate" perturbed Hamiltonian $\hat{H} \approx \hat{H}_0 + \epsilon_c \hat{V}_c$ are

$$|\phi_1\rangle \approx |1\rangle, \tag{4.10}$$

$$|\phi_2\rangle \approx |C_-\rangle - \frac{\Omega_c(\lambda_- - \delta_1)}{\delta_3 N_-}|4\rangle, \tag{4.11}$$

$$|\phi_3\rangle \approx |C_+\rangle - \frac{\Omega_c(\lambda_+ - \delta_1)}{\delta_3 N_+}|4\rangle, \tag{4.12}$$

$$|\phi_4\rangle \approx |4\rangle + \frac{\Omega_c^*(\lambda_- - \delta_1)}{\delta_3 N_-}|C_-\rangle + \frac{\Omega_c^*(\lambda_+ - \delta_1)}{\delta_3 N_+}|C_+\rangle. \tag{4.13}$$

Corresponding to these eigenstates are the second-order eigenvalues

$$\lambda_1 \approx 0, \tag{4.14}$$

$$\lambda_2 \approx \bar{\lambda}_- = \lambda_- - \frac{|\Omega_c|^2(\lambda_- - \delta_1)^2}{\delta_3 N_-^2}, \tag{4.15}$$

$$\lambda_3 \approx \bar{\lambda}_+ = \lambda_+ - \frac{|\Omega_c|^2(\lambda_+ - \delta_1)^2}{\delta_3 N_+^2}, \tag{4.16}$$

$$\lambda_4 \approx \delta_3. \tag{4.17}$$

However, during later calculations it is found that the expansion of the eigenvectors up to first-order is insufficiently accurate in certain parameter ranges. This is because during calculations it is sometimes necessary to determine the small differences between eigenstates, which may vanish to first-order. Nonetheless, we can improve the accuracy by self-consistently adjusting the normalisation constants $N_\pm$ to take account of the Stark-shift of the energy level $|3\rangle$ by the field Ω_c. We do this by performing the substitutions

$$N_\pm^2 \to \bar{N}_\pm^2 = |\Omega_b|^2 + 4(\bar{\lambda}_\pm - \delta_1)^2. \tag{4.18}$$

This modification to the normalisation constants introduces a sufficiently higher-order correction, without over-complicating the calculations. Using perturbation theory simultaneously avoids the requirement to make this somewhat intuitive adjustment, but it does however make the calculations much more lengthy. We note that the correction to the eigenvalues could have been performed in two ways: either by adding on a term to $N_\pm$ proportional to the excitation into the state $|4\rangle$, or by taking account of the Stark-shift to the state $|3\rangle$. In the former case the adjustment would be proportional to $\sim |\Omega_c|^2/\delta_3^2$ and in the later $\sim |\Omega_c|^2/\delta_3$. Since δ_3 is assumed to be large, we see that the later adjustment will produce the largest correction and is therefore used.

We take account of the probe field Ω_a by perturbing the intermediate system $(\hat{H}_0 + \epsilon_c \hat{V}_c)$ with the interaction $\hat{V}_a$. During this calculation the approximate eigenstates (4.10)-(4.13) of the intermediate Hamiltonian are used as our initial eigenbasis. We find that the perturbed eigenstates are given by

$$|\phi_1\rangle \approx |1\rangle - \frac{\Omega_a \Omega_b^*}{2\bar{N}_-\bar{\lambda}_-}|C_-\rangle - \frac{\Omega_a \Omega_b^*}{2\bar{N}_+\bar{\lambda}_+}|C_+\rangle - \frac{\Omega_a \Omega_b^* \Omega_c}{2\delta_3(4\delta_1\delta_2 - \Omega_b^2)}|4\rangle, \tag{4.19}$$

$$|\phi_2\rangle \approx |C_-\rangle + \frac{\Omega_a^*\Omega_b}{2\bar{N}_-\bar{\lambda}_-}|1\rangle - \frac{\Omega_c(\lambda_- - \delta_1)}{\bar{N}_-\delta_3}|4\rangle, \tag{4.20}$$

$$|\phi_3\rangle \approx |C_+\rangle + \frac{\Omega_a^*\Omega_b}{2\bar{N}_+\bar{\lambda}_+}|1\rangle - \frac{\Omega_c(\lambda_+ - \delta_1)}{\bar{N}_+\delta_3}|4\rangle, \tag{4.21}$$

$$|\phi_4\rangle \approx |4\rangle + \frac{\Omega_c^*(\lambda_- - \delta_1)}{\delta_3\bar{N}_-}|C_+\rangle + \frac{\Omega_c^*(\lambda_+ - \delta_1)}{\delta_3\bar{N}_+}|C_+\rangle. \tag{4.22}$$

The eigenenergy corresponding to the dressed state $|\phi_1\rangle$ is found to have the value

$$\lambda_1 \approx -\frac{|\Omega_a|^2\delta_2}{4\delta_1\delta_2 - |\Omega_b|^2}. \tag{4.23}$$

Again, from the dressed state $|\phi_1\rangle$ the steady-state atomic coherences can be again calculated. These can be shown to furnish identical results for the linear and XPM responses as in the previous calculations of chapter 3.

4.2.1 Transient Evolution of the Atom

We now determine the evolution given that at time $t = 0$ the atom is initially in the ground state ($|\psi(0)\rangle = |1\rangle$). At this point the electromagnetic field Ω_a is suddenly turned on and the atom will evolve according to the Schrödinger equation $i\hbar\partial_t|\psi(t)\rangle = \hat{H}|\psi(t)\rangle$. We note that using (4.19) the initial state of the atom can be written as

$$\begin{aligned}|\psi(0)\rangle = |\phi_1\rangle + \frac{\Omega_a\Omega_b}{2\bar{N}_-\bar{\lambda}_-}\left(|C_-\rangle - \frac{\Omega_c(\lambda_- - \delta_1)}{\bar{N}_-\delta_3}|4\rangle\right) + \\ \frac{\Omega_a\Omega_b}{2\bar{N}_+\bar{\lambda}_+}\left(|C_+\rangle - \frac{\Omega_c(\lambda_+ - \delta_1)}{\bar{N}_+\delta_3}|4\rangle\right).\end{aligned} \tag{4.24}$$

In this section we are concerned with the collective behaviour of an ensemble of atoms, in particular the transient absorption and refraction that can be measured by transmission through the ensemble. Presently we are not modelling the dynamics of the laser pulses *inside* the ensemble. For this reason we can assume that the variation in intensity of the electromagnetic field across the ensemble is negligible and that the dipole matrix elements can be adjusted to compensate for the local phase of the field. Making these assumptions lets us take all the Rabi-frequencies to be real for the remainder of this chapter.

We note that in (4.24) the terms $|\phi_1\rangle$ and $|C_\pm\rangle - \dfrac{\Omega_c(\lambda_\pm - \delta_1)}{\bar{N}_\pm \delta_3}|4\rangle$ are eigenvectors to at least first-order. Since the evolution of energy eigenstates are particularly simple, we can show that the evolution of $|\psi(t)\rangle$ must be given by

$$\begin{aligned}
|\psi(t)\rangle \;=\;& \exp(-i\lambda_1 t)|1\rangle + \\
& \frac{\Omega_a\Omega_b}{2\bar{N}_-\bar{\lambda}_-}\left[\exp(-i\bar{\lambda}_- t) - \exp[-i\lambda_1 t]\right]|C_-\rangle + \\
& \frac{\Omega_a\Omega_b}{2\bar{N}_+\bar{\lambda}_+}\left[\exp(-i\bar{\lambda}_+ t) - \exp[-i\lambda_1 t]\right]|C_+\rangle - \\
& \frac{\Omega_a\Omega_b\Omega_c}{2\delta_3}\left[\frac{\lambda_- - \delta_1}{\bar{N}_-^2\bar{\lambda}_-}\exp(-i\bar{\lambda}_- t) + \frac{\lambda_+ - \delta_1}{\bar{N}_+^2\bar{\lambda}_+}\exp(-i\bar{\lambda}_+ t) + \frac{\exp(-i\lambda_1 t)}{4\delta_1\delta_2 - \Omega_b^2}\right]|4\rangle.
\end{aligned} \tag{4.25}$$

Furthermore, due to the equivalence between solutions of the master equation and the non-Hermitian Schrödinger equation (Section 2.5) this solution will also hold when the multi-photon detunings are taken to be complex, as in (3.58).

The evolution (4.25) simplifies considerably by assuming that the system is operating close to Raman-resonance ($\delta_2 \approx 0$). In this case the linear absorption will be small. Then the excitation of atoms into the decaying state $|2\rangle$ will be negligible and over a reasonably long time scale we can make the non-depletion approximation, $\exp[-i\lambda_1 t] \approx 1$. By dropping terms that only contribute to third-order or higher in Ω_c we find that

$$\begin{aligned}
|\psi(t)\rangle \;=\;& |1\rangle + \frac{\Omega_a\Omega_b}{2\bar{N}_-\bar{\lambda}_-}\left[\exp(-i\bar{\lambda}_- t) - 1\right]|C_-\rangle + \frac{\Omega_a\Omega_b}{2\bar{N}_+\bar{\lambda}_+}\left[\exp(-\bar{\lambda}_+ t) - 1\right]|C_+\rangle - \\
& \frac{\Omega_a\Omega_b\Omega_c}{2\delta_3(4\delta_1\delta_2 - \Omega_b^2)} \times \left[1 + \frac{\lambda_+}{\delta_1 + \delta_2 - 2\lambda_+}\exp(-i\bar{\lambda}_- t)\right. \\
& \left. + \frac{\lambda_-}{\delta_1 + \delta_2 - 2\lambda_-}\exp(-i\bar{\lambda}_+ t)\right]|4\rangle.
\end{aligned} \tag{4.26}$$

From the expression (4.26) the time-dependent atomic coherences $\rho_{21}(t)$ and $\rho_{43}(t)$ can be calculated and Taylor expanded in powers of Ω_a and Ω_c. In turn, these furnish the time-dependent linear and cross-Kerr electric susceptibilies. The atomic coherences obtained are

$$\rho_{21}(t) \;=\; \rho_{21}^{(ss)} + \frac{\Omega_a\Omega_b^2}{2}\left[\frac{\exp(-i\bar{\lambda}_- t)}{\bar{N}_-^2\bar{\lambda}_-} + \frac{\exp(-i\bar{\lambda}_+ t)}{\bar{N}_+^2\bar{\lambda}_+}\right], \tag{4.27}$$

$$\rho_{43}(t) \;=\; \rho_{43}^{(ss)} \times \left\{\left[1 + \left(\frac{\lambda_+}{\delta_1 + \delta_2 - 2\lambda_+}\right)\exp(-i\bar{\lambda}_- t)\right.\right.$$

$$+\left(\frac{\lambda_-}{\delta_1+\delta_2-2\lambda_-}\right)\exp(-i\bar{\lambda}_+t)\Big]\times\text{c.c.}\Big\}, \tag{4.28}$$

where $\rho_{21}^{(ss)}$ and $\rho_{43}^{(ss)}$ are the steady-state atomic coherences calculated in chapter 3. These are:

$$\rho_{21}^{(ss)} = -\frac{2\Omega_a\delta_2}{4\delta_1\delta_2-\Omega_b^2}-\frac{\Omega_a\Omega_b^2\Omega_c^2}{2\delta_3(4\delta_1\delta_2-\Omega_b^2)^2}, \tag{4.29}$$

$$\rho_{43}^{(ss)} = -\frac{\Omega_a^2\Omega_b^2\Omega_c}{2\delta_3(4\delta_a\delta_2-\Omega_b^2)(4\delta_1^*\delta_2^*-\Omega_b^2)}. \tag{4.30}$$

To elucidate the underlying physical processes it is useful to work in the unsaturated ($\Omega_b \ll \Gamma_2$) and Raman-resonant ($\delta_2 = 0$) limits. This is also the regime in which experiments will usually be concerned. The expression thus obtained lend themselves to straightforward physical interpretations. For the atomic coherence on the $|1\rangle \leftrightarrow |2\rangle$ transition we find that

$$\begin{aligned}\rho_{21}(t) &= \frac{i\Omega_a}{\Gamma_2}\left[\exp\left(-\frac{\Omega_b^2t}{2\Gamma_2}+i\frac{\Omega_c^2t}{4\delta_3}\right)-\exp\left(-\frac{\Gamma_2t}{2}\right)\right]\\ &\quad -\frac{\Omega_a\Omega_c^2}{2\Omega_b^2\delta_3}\left[1-\exp\left(-\frac{\Omega_b^2t}{2\Gamma_2}\right)\right].\end{aligned} \tag{4.31}$$

The first term of (4.31) clearly represents a transient linear response to the field Ω_a, and the latter term a time-dependent XPM response. For the $|3\rangle \leftrightarrow |4\rangle$ transition we obtain only a time-dependent XPM response of the form

$$\rho_{43}(t) = -\frac{\Omega_a^2\Omega_c}{2\delta_3\Omega_b^2}\left[1-\exp\left(-\frac{\Omega_b^2t}{2\Gamma_2}\right)\right]^2. \tag{4.32}$$

The physical interpretation of these results is explained in the following subsection.

4.2.2 Time-Dependent Electric Susceptibilities

We now calculate the time-dependent electric susceptibilities given that at $t = 0$ the EIT probe field is suddenly turned on. All other fields are switched on throughout the interaction. We consider the situation where the fields Ω_a and Ω_b are Raman-resonant ($\delta_2 = 0$) and the control field is operating well below saturation ($\Omega_b \ll \gamma_1$). The linear susceptibility experienced by the field Ω_a is determined by using the relationship

$$\chi^{(1)}(\omega_a) = \frac{2\rho_{21}^{(1,0)}(t)p_{12}^*}{\epsilon_0 E(\omega_a)}, \tag{4.33}$$

where $\rho_{xy}^{(\alpha,\beta)}$ is the α-order in Ω_a and β-order in Ω_c term of ρ_{xy}. In this case $\rho_{21}^{(1,0)}(t)$ is the first term of (4.31). Thus, the susceptibility is found to be

$$\chi^{(1)}(\omega_a) = \frac{2iN|p_a|^2}{\epsilon_0 V\hbar\Gamma_2}\left[\exp\left(-\frac{\Omega_b^2}{2\Gamma_2}t + i\frac{\Omega_c^2}{4\delta_3}t\right) - \exp\left(-\frac{\Gamma_2}{2}t\right)\right]. \quad (4.34)$$

It can be seen from Fig. 4.2 that when the field Ω_a is turned on, it is subject to a very large transient absorption [68]. The presence of this very large linear term also retrospectively justifies our neglecting higher-order effects, such as the transient SPM.

The form of this transient absorption can readily be explained by the diminishing coherent excitation of atoms from the state $|1\rangle$ into the radiatively decaying state $|2\rangle$. The atom rapidly reaches an equilibrium between coherent excitation and decay, on a timescale of $\sim 1/\Gamma_2$. However, the supply of population to $|2\rangle$ gradually diminishes due to the relaxation of bright superposition of the ground states into the dark-state of the Λ subsystem. Absorption is therefore limited by the gradual establishment of electromagnetically induced transparency at a rate $\sim \Omega_b^2/\Gamma_2$. The relatively long timescale over which relaxation occurs will result in large absorption when using short pulses or rapidly switched fields. This could put constraints on the adiabaticity of schemes based on slow pulse propagation through single or double-EIT [55] configurations.

To gain a more quantitative understanding of the form of (4.34) we work in the bright/dark and excited state basis (4.2)-(4.4). We begin with the equation for the coherence between the dark and excited states on resonance:

$$\dot{\rho}_{-e}(t) = -\frac{\Gamma_2}{2}\rho_{-e}(t) + \frac{i}{2}\bar{\Omega}\rho_{-+}. \quad (4.35)$$

Since the excited state decays rapidly we expect the coherence to relax into a quasi-steady-state over a very short period of time. Setting $\dot{\rho}_{-e} = 0$ we find

$$\rho_{-e}(t) \approx \frac{i\bar{\Omega}}{\Gamma_2}\rho_{-+}(t). \quad (4.36)$$

This solution indicates that the coherence between the dark and excited states follows the ground-state coherence $\rho_{-+}(t)$ to lowest-order. This is a good approximation when the decay Γ_2 is rapid, but does not satisfy the initial conditions of

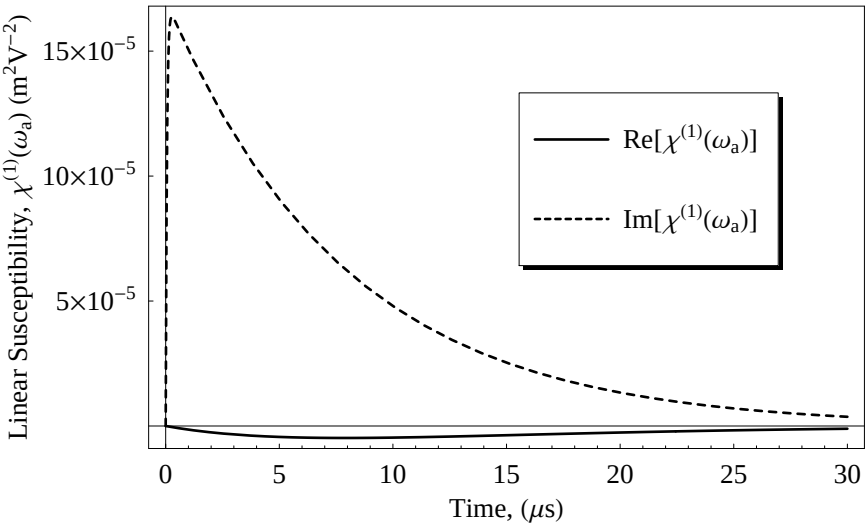

Figure 4.2: The time-dependent linear electric susceptibility experienced by the field Ω_a for a resonant Λ subsystem and $\Omega_b = 3$ MHz. When the field Ω_a is suddenly turned on, it experiences a very large transient absorption.

our problem ($\rho_{-+} = \dfrac{\Omega_a\Omega_b}{\bar{\Omega}^2}, \rho_{-e} = 0$). Therefore, to find a better approximation we must first determine the explicit time-dependence of the ground state coherence. The quasi steady state solution for $\rho_{-e}(t)$ is substituted into the equation for the coherence between the bright and dark superpositions of the ground states, $\dot{\rho}_{-+}(t) = i(\bar{\Omega}/2)\rho_{-e}(t)$. We obtain

$$\rho_{-+}(t) = \rho_{-+}(0)\exp\left(-\frac{\bar{\Omega}^2 t}{2\Gamma_2}\right). \tag{4.37}$$

Again we note that this coherence decays on the timescale of the bright-state relaxation. The final step is to substitute the solution for the ground-state coherence ρ_{-+} back into (4.35) to form a linear uncoupled differential equation for $\rho_{-e}(t)$. We try an Ansatz of the form $\rho_{-e}(t) = A(t)\exp(-\Gamma_2 t/2) + B(t)$, where $A(t)$ and $B(t)$ are slowly varying functions. The solution is found to be

$$\rho_{-e}(t) = \frac{i\Omega_a\Omega_b}{\bar{\Omega}\Gamma_2}\left[\exp\left(-\frac{\bar{\Omega}^2 t}{2\Gamma_2}\right) - \exp\left(-\frac{\Gamma_2 t}{2}\right)\right]. \tag{4.38}$$

Thus, $\rho_{-e}(t)$ rapidly responds to the injection of coherence from $\rho_{-+}(t)$. Due to the relaxation of the bright state as the atom evolves into the atomic dark state we see

that $\rho_{-e}(t)$ slowly decays as the source term $\rho_{-+}(t)$ diminishes. By taking the EIT limit ($\rho_{-e}(t) \rightarrow \rho_{12}(t), \bar{\Omega} \rightarrow \Omega_b$) we recover the linear part of the solution derived previously (4.31).

To calculate the cross-Kerr susceptibilities experienced by the fields Ω_a and Ω_c we use the relationships

$$\chi_c^{(3)}(\omega_a) = \frac{4\rho_{21}^{(1,2)} p_a^*}{3\epsilon_0 E(\omega_a)|E(\omega_c)|^2}, \tag{4.39}$$

$$\chi_c^{(3)}(\omega_c) = \frac{4\rho_{43}^{(2,1)} p_c^*}{3\epsilon_0 E(\omega_c)|E(\omega_a)|^2}. \tag{4.40}$$

Using the second term of (4.31) and (4.32) it is seen that the nonlinear susceptibilities have the values

$$\chi^{(3)}(\omega_a) = \frac{2N|p_a|^2|p_c|^2}{3\epsilon_0 V\hbar^3\delta_3\Omega_b^2}\left[1-\exp\left(-\frac{\Omega_b^2}{2\Gamma_2}t\right)\right], \tag{4.41}$$

$$\chi^{(3)}(\omega_c) = \frac{2N|p_a|^2|p_c|^2}{3\epsilon_0 V\hbar^3\delta_3\Omega_b^2}\left[1-\exp\left(-\frac{\Omega_b^2}{2\Gamma_2}t\right)\right]^2. \tag{4.42}$$

Again, the cross-Kerr interaction becomes established on a timescale equal to the relaxation time of the atom into the dark-state. This is to be expected since the cross-phase modulation occurs in the steady-state due to the adiabatic Stark-shift of the dark-state by the field Ω_c [60].

To explain the form of the transient susceptbilities, or rather the coherence elements $\rho_{21}(t)$ and $\rho_{43}(t)$ associated with these, we again work in the basis (4.2)-(4.4), with the addition of the fourth state $|4\rangle$. We find that the coherence between the dark and excited states is given by

$$\dot{\rho}_{-e}(t) = -\frac{\Gamma_2}{2}\rho_{-e}(t) + \frac{i\bar{\Omega}}{2}\rho_{-+}(t) + \frac{i\Omega_a\Omega_c}{2\bar{\Omega}}\rho_{4e}(t). \tag{4.43}$$

This is identical to (4.35) except for the addition of a source term proportional to $\rho_{4e}(t)$. Since we are working in the unsaturated limit we expect $\rho_{4e}(t) \approx 0$. Therefore, any higher-order XPM effects must arise through modifications to the ground-state coherence (GSC). Taking into account the effect of Ω_c the GSC is now defined by

$$\dot{\rho}_{-+}(t) = \frac{i\bar{\Omega}}{2}\rho_{-e}(t) + \frac{i\Omega_a\Omega_b}{2\bar{\Omega}}\rho_{4+}(t) + \frac{i\Omega_b\Omega_c}{2\bar{\Omega}}\rho_{-4}(t). \tag{4.44}$$

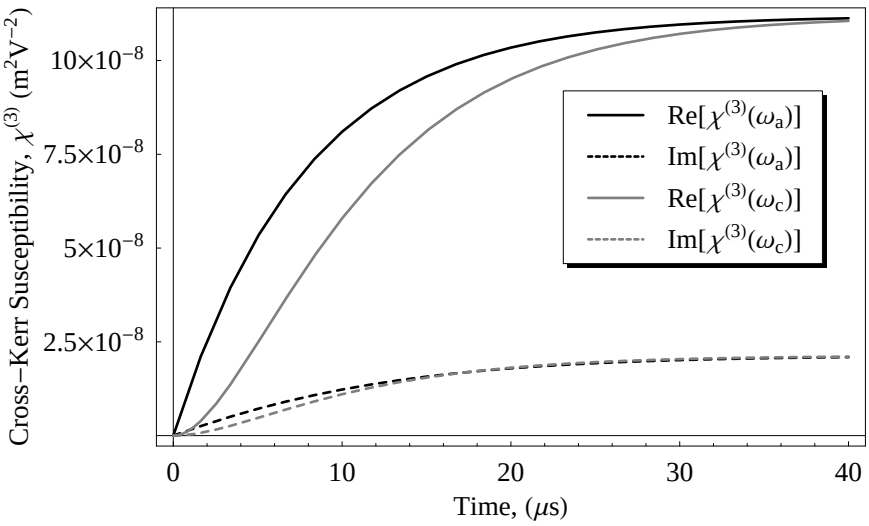

Figure 4.3: The transient cross-Kerr susceptibilities experienced by the fields Ω_a and Ω_c when the field Ω_a is suddenly turned on. Plotted for a resonant Λ subsystem, $\Omega_b = 3$ MHz and $\Delta_c = 100$ MHz.

Again, the assumption is made that coupling between the bright state and $|4\rangle$ will make less of a contribution to the GSC than that due to the dark state coupling to $|4\rangle$. We solve $\rho_{-4}(t)$ in the steady state and use this along with (4.36) to obtain the equation of motion for the GSC:

$$\dot{\rho}_{-+}(t) = -\frac{\bar{\Omega}^2}{2\Gamma_2}\rho_{-+}(t) - \frac{i\Omega_b^2\Omega_c^2}{4\bar{\Omega}^2\delta_3^*}\rho_{-+}(t) + \frac{i\Omega_a\Omega_b^3\Omega_c^2}{4\bar{\Omega}^2\delta_3^*}. \tag{4.45}$$

The first term of this is clearly identical to that derived previously when considering only the Λ subsystem. The two additional terms will give rise to 1) a small change in phase evolution of the GSC and 2) a non-vanishing source term for the GSC due to the coupling of the dark state to $|4\rangle$. Solving (4.45) and substituting the answer into the equation of motion for $\rho_{-e}(t)$ yields

$$\rho_{-e}(t) = \frac{i\Omega_a\Omega_b}{\bar{\Omega}\Gamma_2}\left[\exp\left(-\frac{\bar{\Omega}^2 t}{2\Gamma_2} - \frac{i\Omega_b^2\Omega_c^2 t}{4\bar{\Omega}^2\delta_3^*}\right) - \exp\left(-\frac{\Omega_2 t}{2}\right)\right] \tag{4.46}$$

$$-\frac{\Omega_a\Omega_b^3\Omega_c^2}{2\bar{\Omega}^5\delta_3^*}\left[1 - \exp\left(-\frac{\bar{\Omega}^2 t}{2\Gamma_2}\right)\right]. \tag{4.47}$$

This is related to the coherence $\rho_{12}(t)$ by the relationship

$$\rho_{12}(t) = \frac{\Omega_a}{\bar{\Omega}}\rho_{+e}(t) + \frac{\Omega_b}{\bar{\Omega}}\rho_{-e}(t). \tag{4.48}$$

By taking the EIT limit ($\Omega_a \ll \Omega_b \approx \bar{\Omega}$) we find $\rho_{12}(t) \approx \rho_{-e}(t)$. The $\rho_{+e}(t)$ term gives rise to a higher-order transient self-phase modulation. Taking the complex conjugate of $\rho_{12}(t)$ we recover the result (4.31). The key physical point to note in this derivation is that transient XPM arises due to a perturbation of the Λ atom ground state coherence. This perturbation is generated by a constant injection of coherence by the coupling between the dark state $|-\rangle$ and the excited state $|4\rangle$. Once again, XPM in the N-configuration atom is shown to be intimately linked to coherent population trapping in the atomic dark state.

A similar derivation can be employed to explain the form of the transient XPM on the $\rho_{43}(t)$ transition, with surprising results. We begin by noting that the $\rho_{43}(t)$ matrix element is given by

$$\rho_{43}(t) = \frac{\Omega_b}{\bar{\Omega}}\rho_{4+}(t) - \frac{\Omega_a}{\bar{\Omega}}\rho_{4-}(t). \tag{4.49}$$

We first determine $\rho_{4+}(t)$ from the equation of motion

$$\dot{\rho}_{4+}(t) = -i\delta_3\rho_{4+}(t) + \frac{i\bar{\Omega}}{2}\rho_{4e}(t) + \frac{i\Omega_a\Omega_c}{2\bar{\Omega}}\rho_{-+}(t) - \frac{i\Omega_b\Omega_c}{2\bar{\Omega}}\left[\rho_{++}(t) - \rho_{44}(t)\right]. \tag{4.50}$$

Again we take the low excitation limit $\rho_{44}(t) \approx 0, \rho_{4e}(t) \approx 0$ and use the Λ-atom approximations for $\rho_{-+}(t)$ given by (4.37) and $\rho_{++}(t)$ given by (4.9). Then we obtain

$$\rho_{4+}(t) = \frac{\Omega_a^2\Omega_b\Omega_c}{2\bar{\Omega}^3\delta_3}\exp\left(-\frac{\bar{\Omega}^2 t}{2\Gamma_2}\right)\left[1 - \exp\left(-\frac{\bar{\Omega}^2 t}{2\Gamma_2}\right)\right]. \tag{4.51}$$

We can see from the form of this equation that coupling between the bright state and $|4\rangle$ vanishes at $t = 0$ and as $t \to \infty$. However, it does make a significant transient contribution to the XPM. Essentially this arises due to the different relaxation rates of the bright state, $\rho_{++}(t)$, and the GSC, $\rho_{-+}(t)$. Solving for the $\rho_{4-}(t)$ element to lowest-order we obtain

$$\rho_{4-}(t) = \frac{\Omega_a\Omega_b^2\Omega_c}{2\bar{\Omega}^3\delta_3}\left[\exp\left(-\frac{\bar{\Omega}^2 t}{2\Gamma_2}\right) - 1\right]. \tag{4.52}$$

In contrast to the transient coupling between the bright state and $|4\rangle$, the dark state coupling gradually increases to is maximum value when the atom has fully relaxed. Combining both contributions from the coupling between the dark/bright states as

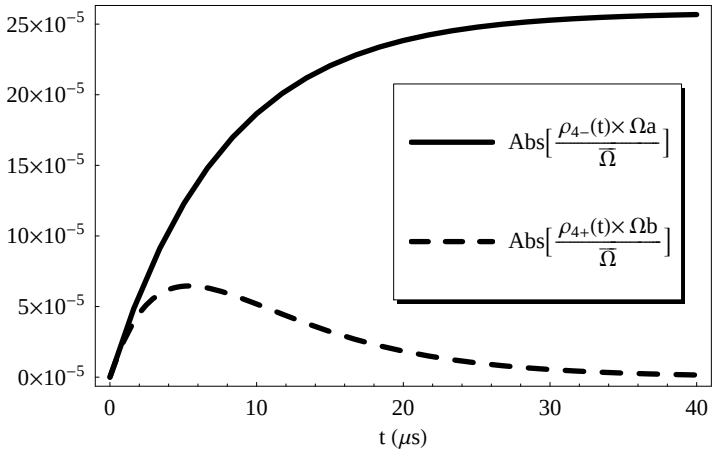

Figure 4.4: Contributions to the $\rho_{43}(t)$ coherence due to the bright and dark states coupling to $|4\rangle$. The coupling between the bright state and $|4\rangle$ makes a significant transient contribution.

the excited state $|4\rangle$ we find that in the EIT limit

$$\rho_{43}(t) = \frac{\Omega_a^2 \Omega_c}{2\Omega_b^2 \delta_3} \left[\exp\left(-\frac{\Omega_b^2 t}{2\Gamma_2} \right) - 1 \right]^2 \tag{4.53}$$

Again, this is identical to (4.32). However, the physical interpretation of the above derivation deviates significantly from what we would expect intuitively. In the steady state we have seen that XPM arises due to the coupling between the dark state $|-\rangle$ and the excited state $|4\rangle$. This behaviour is again found when we consider the transient XPM on the $|1\rangle \leftrightarrow |2\rangle$ transition. However, from an analysis in the partly dressed basis we can see that the $\rho_{43}(t)$ transition experiences a significant, although transient, contribution due to the coupling between the bright and excited states. The contributions from coupling between the dark/bright states and $|4\rangle$ are compared in figure (4.4).

Thus, it is not entirely true to say that XPM occurs due to the perturbation of the Λ-atom dark state: a transient contribution from the bright state coupling is also present.

4.3 Chapter Summary

In this chapter we have investigated the transient behaviour of the atom when the EIT probe field (Ω_a) is suddenly turned on. One of the most striking features is the large and relatively long duration transient absorption of the EIT probe. This occurs due to the finite time required to transfer atomic population from the previously uncoupled state $|1\rangle$ into the new dark state of the Λ subsystem. The rate of this process is limited by the slow relaxation of the bright state superposition of the ground states. Thus, the transient absorption is a precursor of the establishment of electromagnetically induced transparency in the Λ subsystem.

Expressions for the transient cross-phase modulation on the Ω_a and Ω_c probe transitions are also derived. In both cases it is seen that XPM arises on a time scale dictated by the relaxation of the atom into the EIT state. However, the interpretation of these results in terms of the bright/dark state partly dressed basis leads to some surprising results. In the case of the Ω_a transition, XPM is found to be generated by the coupling between the dark state and the excited state $|4\rangle$. This is identical to the explanation of XPM given in the steady state regime (subsection 3.2.1). For the Ω_c transition however, it is seen that the coupling between the bright state and $|4\rangle$ gives a significant transient contribution. Although it is sufficient to view XPM as arising to due the perturbation of the Λ-atom dark state in the steady-state regime, this is not a complete explanation when time-dependent fields are considered.

From the form of the susceptibilities it can also be seen that the rise time is proportional to the magnitude of the nonlinear susceptibility. Thus, larger nonlinearities will take longer to become established. This could have significant implications when trying to achieve strong nonlinear interactions between short optical pulses. Furthermore, since the atom is slow to respond to changes in the probe field, this indicates that there could be limitations and interesting non-adiabatic behaviour of the atom when using short pulses on the EIT probe transition. The non-adiabatic behaviour of the N-configuration atom will be investigated further chapter 5.

Chapter 5

Slowly Pulsed Cross-Phase Modulation

So far we have considered the interaction of an ensemble of identical atoms with spatially and at least piece-wise temporally constant electromagnetic fields. In many respects this is a very reasonable approximation. Consider first the temporal variation of the field.

From the Weisskopf-Wigner theory (2.33), we have seen that the radiative decay rate of a transition at optical frequencies will be on the order of tens of MHz. Typically the pulse duration used in experiments will be of the order of many microseconds, although much shorter is possible. Nonetheless, it would seem reasonable to assume that the atom has sufficient time to relax into a quasi-steady state. As noted in the previous chapter the actual atomic dynamics in the Λ- and N-configuration systems is dictated by the much slower relaxation of the bright-state superposition of the ground states. Therefore, even when using relatively long duration pulses then non-equilibrium effects should be taken into consideration.

A second and related issue is the assumption that the electromagnetic field is constant across the dimensions of the atomic sample. Again, we consider typical parameters: sample length, $l_s = 10^{-3}$m and pulse duration $\tau = 1\mu s$. In free space we would therefore expect the pulse length to be of the order

$$l_p = c \times \tau \approx 300\text{m}. \tag{5.1}$$

Clearly, the pulse length is much greater than the atomic sample length. However, due to the remarkable properties of the Λ atom we will see that pulses propagating through the sample will undergo compression by several orders of magnitude: this is a natural consequence of slow-light propagation in the atomic ensemble. In turn, this turns out to be a non-equilibrium effect of the slow bright-state relaxation rate.

5.1 Slowly Varying Envelope Approximation

During the calculations in this thesis, and indeed for most experiments undertaken, we are able to work within the *slowly-varying envelope approximation*. That is, we assume that variations in the classical field amplitude occur on a length scale much longer than the wavelength of the light. We begin with the Maxwell wave equation:

$$\left(\frac{\partial^2}{\partial t^2} - c^2\frac{\partial^2}{\partial z^2}\right) E(z,t) = \mu_0 c^2 \frac{\partial^2}{\partial t^2} P(z,t). \tag{5.2}$$

The electric and polarisation fields have the form

$$E(z,t) = \frac{E_0(z,t)}{2}\exp[kz - \omega t + \phi(z,t)] + c.c.\,, \tag{5.3}$$

$$P(z,t) = \frac{P_0(z,t)}{2}\exp[kz - \omega t + \phi(z,t)] + c.c.\,. \tag{5.4}$$

where the coefficients $E_0(z,t)$ are real, slowly-varying functions of space and time. The corresponding polarisation terms $P_0(z,t)$ may be complex, since the induced polarisation will generally not be in-phase with the applied electromagnetic field. Making these assumptions we find coupled first-order wave-equations for the amplitude and phase of the electromagnetic field [42]:

$$\left(\frac{\partial}{\partial t} + c\frac{\partial}{\partial z}\right) E_0(z,t) = -\frac{\omega}{2\epsilon_0}\mathrm{Im}\left[P_0(z,t)\right], \tag{5.5}$$

$$E_0(z,t)\left(\frac{\partial}{\partial t} + c\frac{\partial}{\partial z}\right) \phi(z,t) = \frac{\omega}{2\epsilon_0}\mathrm{Re}\left[P_0(z,t)\right]. \tag{5.6}$$

When employing a semi-classical approximation we want to relate the macroscopic polarisation of the material to the off-diagonal elements of the density matrix. In this case we have

$$\mathrm{Im}\left[P_0(z,t)\right] = \frac{2N}{V}\mathrm{Im}[p_{12}\rho_{21}], \tag{5.7}$$

$$\mathrm{Re}\left[P_0(z,t)\right] = \frac{2N}{V}\mathrm{Re}[p_{12}\rho_{21}], \tag{5.8}$$

where N/V is the number density of identical atoms in the atomic ensemble.

Throughout this chapter we analyse the propagation of classical pulses through quantum-mechanical matter: a semi-classical approximation. By doing so we can model a narrow bandwidth pulse as a plane wave modulated by a slowly varying field envelope. It is possible to take a similar approach in the fully quantum-mechanical regime, although the validity of applying this to particular situations is a much more tricky subject. In general, each Fourier component of the field must be taken account of in a multi-modal description of the field [77].

5.2 Pulses in the Two-Level Atom

Determining the pulse propagation in an atomic ensemble involves two steps. First, we solve the density matrix equation of motion (2.34) to obtain the relationship between the instantaneous polarisation and the history of an applied electromagnetic field. Then, the polarisation is substituted into the wave-equations (5.5) and (5.6). This is used to determine a self-consistent solution to the pulse dynamics. In general finding exact solutions is a difficult, if not entirely impossible task.

However, for certain systems exact solutions can be found. An important example arises when we investigate the interaction of a pulse with a two-level atom. This is examined in the following subsection. The analysis of this problem will help elucidate the situations where exact solutions exist and the difficulties encountered when deriving approximate solutions for non-integrable systems.

5.2.1 Self Induced Transparency

For a pulse propagating in the two-level atom it is possible to show that *soliton* solutions exist. Remarkably, these solitonic pulses are able to travel undisturbed through an ensemble of normally absorptive two-level atoms [78]. To show this, we begin by transforming into the *Bloch vector* model of the atom. In this picture, the

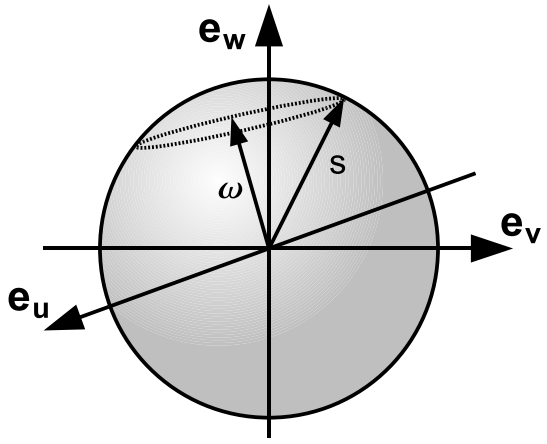

Figure 5.1: The state of the two-level atom is described by the position of the vector $\boldsymbol{s}(t)$ on the Bloch sphere. They dynamics are such that the vector $\boldsymbol{s}(t)$ precesses around the axis defined by $\boldsymbol{\omega}(t)$. The diagram shows the time-independent case of Rabi-oscillations around a fixed vector $\boldsymbol{\omega}$.

state of the atom is represented by the position of a vector, $\mathbf{s}(t)$, on the unit sphere (Fig. 5.1). The Bloch vector is defined as

$$\boldsymbol{s}(t) = \begin{bmatrix} u(t) \\ v(t) \\ w(t) \end{bmatrix} = \begin{bmatrix} \rho_{12}(t) + \rho_{21}(t) \\ i(\rho_{12}(t) - \rho_{21}(t)) \\ \rho_{11}(t) - \rho_{22}(t) \end{bmatrix}. \tag{5.9}$$

We find the equation of motion for the Bloch vector by substituting the components, $u(t), v(t)$ and $w(t)$, into the density matrix equation of motion (2.34). When we neglect the decay term the dynamics are described the precession equation [26]:

$$\frac{\partial \boldsymbol{s}(t)}{\partial t} = \boldsymbol{\omega}(t) \times \boldsymbol{s}(t). \tag{5.10}$$

Here we have assumed that the Rabi-frequency is real and $\boldsymbol{\omega} = (\Omega(t), 0, -\Delta)$. For a time-independent field the Bloch vector will simply precess around $\boldsymbol{\omega}$ in a manner identical to a magnetic dipole around magnetic field lines. The solution of the problem is straightforward and furnishes the Rabi-oscillations previously discussed.

To solve the time-dependent problem it is first necessary to introduce the concept

of *partial pulse area*, defined by

$$\theta(t) = \int_{-\infty}^{t} \Omega(t')dt'. \tag{5.11}$$

This quantity plays a central role in determining the dynamics of the two-level atom and has more recently been extended to other multi-level systems [79]. We begin our solution by trying an Ansatz of the the following form:

$$v(t, \Delta) = -F(\Delta)\sin[\theta(t)]. \tag{5.12}$$

The form of this is based on the assumption that the Δ-dependence can be taken account of by the term $F(\Delta)$ multiplying the resonant solution. Making this assumption and using the equations of motion for $\dot{v}(t)$ and $\dot{w}(t)$ we find that

$$u(t, \Delta) = \frac{\Omega(t)}{\Delta}\left[F(\Delta) - 1\right], \tag{5.13}$$

$$w(t, \Delta) = F(\Delta)\left\{\cos[\theta(t)] - 1\right\} + 1. \tag{5.14}$$

However, substituting these solutions into the differential equation for $\dot{u}(t, \Delta)$ yields the following restriction on the partial pulse area

$$\frac{\partial^2\theta(t)}{\partial t^2} = \frac{1}{\tau^2}\sin\theta(t). \tag{5.15}$$

Thus, for that Ansatz (5.12) to be valid we are restricted to pulses that satisfy the pendulum equation for $\theta(t)$. The nonlinear differential equation (5.15) occurs frequently in several branches of physics and is particular for possessing solitary-wave solutions. That is, stable localised pulse-like solutions that are undisturbed by collisions with each other, up to a phase shift. The spatially varying version of this equation, the *sine-Gordon* equation, is often studied in the context of nonlinear field theories and arises in the theory of Josephson junctions in superconductors [80]. However, most simply, this equation describes a simple pendulum where the angle θ is made between the radius through the centre of gravity and the vertical.

Given that we want solutions that vanish at $t = \pm\infty$ we find the pulse area is given by

$$\theta(t) = -4\tan^{-1}\left[\exp[(t - t_0)/\tau]\right]. \tag{5.16}$$

By substituting $\theta(t)$ into the solution for $w(t)$ we can see that the population will undergo one cycle as the pulse propagates though the medium, but will be unchanged afterwards. That is $w(-\infty, \Delta) = w(\infty, \Delta) = 1$. This corresponds to one "swing" of the pendulum from $\theta = 0$ to $\theta = 2\pi$. Differentiation yields the solution to the pulse envelope

$$E_0(t) = \frac{2\hbar}{\tau p}\text{sech}[(t - t_0)/\tau]. \tag{5.17}$$

Thus, the pulse envelope is of the well-known hyperbolic secant form often associated with solitons. By saying $t_0 = z/v_p$ and substituting (5.17) into the slowly-varying Maxwell equation (5.5) we find that the pulse velocity through an inhomogeneously broadened medium is given by

$$v_p = \frac{c}{1 + \dfrac{Np^2\omega\tau}{2\hbar\epsilon_0 V\sigma}}. \tag{5.18}$$

Here, N/V is the atomic density and σ is the standard deviation of the normal distribution of detunings Δ. We have also assumed that the pulse bandwidth is much narrower than the inhomogeneous broadening and the pulse is resonant with the distribution peak.

When determining the dynamics of the two-level atom we are limited to a particular class of exactly integrable soliton solutions. However, the pulsed output of a laser will generally not be a secant-shaped pulse. We are therefore still unable to describe how an *arbitrary pulse envelope* will propagate through an ensemble of two-level atoms. Although this is impossible in the general case, we next explore another exactly solvable limit which acts as a very profitable departure point for approximate calculations.

5.2.2 Adiabatic Following

One natural way to proceed when finding the dynamics of pulses is to assume that the pulses are slowly-varying and the atomic dynamics will be closely related to the steady-field Rabi solution. We begin by parameterising the "slowness" of the

variation of the Hamiltonian [81] by introducing the parameter δ, such that

$$i\hbar\frac{\partial}{\partial t}|\psi(t)\rangle = H(\delta t)|\psi(t)\rangle. \tag{5.19}$$

Here the Hamiltonian is a constant as $\delta \to 0$. We can now transform into a "slow-time" $\tau = \delta t$. In this new parameterisation the Schrödinger equation is given by

$$i\epsilon\frac{\partial}{\partial \tau}|\psi(\tau)\rangle = H(\tau)|\psi(\tau)\rangle, \tag{5.20}$$

where $\epsilon = \delta\hbar$. Now, we follow [82] and suppose that the Hamiltonian has the form of the two-level atom is a symmetric trace-zero matrix given by

$$\hat{H}(\tau) = H(\tau)\begin{bmatrix} \cos\theta(\tau) & \sin\theta(\tau) \\ \sin\theta(\tau) & -\cos\theta(\tau) \end{bmatrix}. \tag{5.21}$$

The instantaneous eigenstates of the two-level Hamiltonian are also known as the *adiabatic states*. These are found to be

$$|+(\tau)\rangle = \cos\left[\frac{\theta(\tau)}{2}\right]|1\rangle + \sin\left[\frac{\theta(\tau)}{2}\right]|2\rangle, \tag{5.22}$$

$$|-(\tau)\rangle = \sin\left[\frac{\theta(\tau)}{2}\right]|1\rangle - \cos\left[\frac{\theta(\tau)}{2}\right]|2\rangle. \tag{5.23}$$

Corresponding to the adiabatic states $|\pm(\tau)\rangle$ are the eigenenergies, given by $E_\pm(\tau) = \pm H(\tau)$. The adiabatic states form a basis for the two-level atom. We can therefore write the general solution to the dynamics as:

$$|\psi(\tau)\rangle = d_-(\tau)|-(\tau)\rangle + d_+(\tau)|+(\tau)\rangle. \tag{5.24}$$

Working in this basis we find that the equations of motion for the $d_\pm(\tau)$ coefficients are given by

$$i\epsilon\begin{bmatrix} \dot{d}_+(\tau) \\ \dot{d}_-(\tau) \end{bmatrix} = \begin{bmatrix} H(\tau) & -i\epsilon\dot{\theta}/2 \\ i\epsilon\dot{\theta}/2 & -H(\tau) \end{bmatrix}\begin{bmatrix} d_+(\tau) \\ d_-(\tau) \end{bmatrix}. \tag{5.25}$$

We now suppose that the solutions are of the form

$$d_\pm(\tau) = \exp\left[\mp\frac{i}{\epsilon}\int_0^\tau H(\alpha)d\alpha\right]c_\pm(\tau). \tag{5.26}$$

Due to the finite rate of variation of the field ($\dot{\theta} \neq 0$) we expect non-adiabatic transitions to be induced between the adiabatic states. This manifests itself as

a time-dependence of the coefficients $c_{\pm}(\tau)$. These are determined by solving the equations of motion

$$\dot{c}_{\pm}(\tau) = \mp c_{\mp}(\tau)\frac{\dot{\theta}(\tau)}{2}\exp\left[\pm\frac{2i}{\epsilon}\int_0^{\tau} H(\alpha)d\alpha\right]. \tag{5.27}$$

In the adiabatic limit the term $\dot{\theta}(t)$ is taken to vary sufficiently slowly such that the rapid oscillation in the exponential of (5.27) will cancel out the slow variations of $c_{\pm}(\tau)\dot{\theta}(\tau)$. This causes the coefficients $c_{\pm}(\tau)$ to be constant. The atom is therefore observed to *adiabatically follow the instantaneous eigenstates*. Indeed, this can be generalised to multi-level atoms to give the general solution to the adiabatic dynamics

$$|\psi(t)\rangle = \sum_n d_n(0)\exp\left[-\frac{i}{\hbar}\int_0^t E_n(\alpha)d\alpha\right]|\phi_n(t)\rangle, \tag{5.28}$$

where $|\phi_n(t)\rangle$ are the adiabatic states. To find the lowest-order non-adiabatic correction to the dynamics we begin by assuming that the atom is initially in the $|+(-\infty)\rangle$ state. Throughout the evolution $c_+(\tau) \approx 1$ to zeroth order. This results in the equation of motion for $c_-(\tau)$:

$$c_-(\tau) = \frac{1}{2}\int_{-\infty}^{\tau}\dot{\theta}(\beta)\exp\left[-\frac{2i}{\epsilon}\int_0^{\beta} H(\alpha)d\alpha\right]d\beta. \tag{5.29}$$

However, to solve the above equation poses an essential problem since it cannot be Taylor expanded in terms of the non-adiabatic parameter ϵ. This is because the Laurent expansion of the exponent contains no non-zero positive powers of ϵ. Nonetheless, by transforming the equation into an integral in terms of the action, progress can be made.

5.2.3 Non-adiabatic Corrections

To find a solution of (5.29) we introduce a parameter that is proportional to the action:

$$w(\tau) = 2\int_0^{\tau} d\tau' H(\tau'). \tag{5.30}$$

This transforms the integral into

$$c_-(\tau) = \frac{1}{2}\int_{-\infty}^{w(\tau)}\frac{d\theta}{dw}\exp\left[-\frac{i}{\epsilon}w\right]dw. \tag{5.31}$$

This transformation is analogous to a classical Hamilton-Jacobi transformation into action-angle variables, where the initial momentum in chosen as the energy $H(\tau)$ and the co-ordinate is the slow time τ [23]. The particular benefit of this transformation is seen when we consider the final state transition amplitude.

$$c_-(+\infty) = \frac{1}{2}\int_{-\infty}^{\infty} \frac{d\theta}{dw} \exp\left[-\frac{i}{\epsilon}w\right] dw. \tag{5.32}$$

The form of this integral suggests that it could be evaluated by extending w into the complex plane. The path along the horizontal axis is then replaced by a clockwise semi-circular contour in the lower half plane [82]. For small ϵ, the contribution from the semi-circular path joining $+\infty$ to $-\infty$ will vanish. It is further expected that $\dfrac{d\theta}{dw}$ will be analytic at all points, other than at zeros of the Hamiltonian in the complex-τ plane. At a point τ_c where $H(\tau_c) = 0$ there will be a degeneracy of the eigenvalues in the complex-time plane. Then, the rate of change of $\theta(w)$ with respect to w will be singular. It is therefore possible to push the path along the real axis downwards until we encounter one of the singularities of $\dfrac{d\theta}{dw}$. For a well behaved Hamiltonian, it can be shown that the singularity will be simple and is given by [82]

$$\frac{d\theta}{dw} = \frac{-i}{3(w - w_c)}, \tag{5.33}$$

where w_c is the value of the action at the complex time τ_c. Evaluating (5.32) using Cauchy's integral theorem we find

$$c_-(+\infty) = \frac{\pi}{3} \exp\left[-\frac{iw_c}{\epsilon}\right]. \tag{5.34}$$

This answer is correct to first-order in both $c_+(\tau)$ and adiabaticity parameter ϵ. However, comparison with numerical work suggests that it is very close to being correct to all-orders in $c_+(\tau)$. In particular we find that even when the non-adiabatic loss is large (although ϵ remains small), the exact form of the loss is given by

$$c_-(+\infty) = \exp\left[-\frac{iw_c}{\epsilon}\right]. \tag{5.35}$$

Several authors have calculated this more exact result by various methods [83, 81]. However, the method relevant to my work here is the method of *superadiabatic states* as introduced by Berry [82, 84, 85]. This is examined in the following subsection and will be applied to the Λ- and N-configuration atoms.

5.2.4 Superadiabatic States

In this section we follow Berry [82] and define the superadiabatic state as a solution to the Schrödinger equation of the form

$$|\psi_{\pm}(\tau)\rangle = \exp\left[\mp\frac{i}{\epsilon}\int_0^{\tau} d\tau' H(\tau')\right]\sum_{m=0}^{\infty}\epsilon^m|u_{m\pm}(\tau)\rangle. \tag{5.36}$$

Here we have assumed that the solution can be Taylor expanded in terms of the adiabaticity parameter ϵ. In particular, the n-th order superadiabatic state is defined as the solution (5.36) truncated after the ϵ^n term. To lowest-order this reduces to the adiabatic approximation found earlier

$$|\psi_{\pm}(\tau)\rangle \approx \exp\left[\mp\frac{i}{\epsilon}\int_0^{\tau} d\tau' H(\tau')\right]|u_{0\pm}(\tau)\rangle, \tag{5.37}$$

where $|u_{0\pm}(\tau)\rangle$ are the adiabatic states corresponding to the $E(\tau) = \pm H(\tau)$ eigenenergies. In general the power-series expansion (5.36) will not converge. We can see this intuitively by considering the situation where the Hamiltonian is equal and static at $t = \pm\infty$. In this case the superadiabatic states $|\psi(\tau)_{\pm}\rangle$ will be equal to the adiabatic states $|u_{0\pm}(\tau)\rangle$ at the beginning and end of the evolution (up to a phase factor). However, from experience we know that for an arbitrary time dependence non-adiabatic transitions between the instantaneous eigenstates will occur, although the expansion (5.36) does not allow this possibility.

Nonetheless, the superadiabatic state does form an asymptotic expansion [86] representing the actual state of the atom. This is useful because the error incurred by truncating the superadiabatic state is no greater than the first term neglected. Thus, useful results can be obtained by expanding up to the smallest term, beyond which the series will diverge.

Now let us calculate the form of the superadiabatic state given that the atom is initially in the upper adiabatic state. Hence, $|\psi(-\infty)\rangle = |\psi_+(-\infty)\rangle = |u_{0+}(-\infty)\rangle$. We choose to expand each term $|u_{m+}(\tau)\rangle$ of the superadiabatic state with respect to the adiabatic basis. Thus

$$|u_{m+}(\tau)\rangle = a_m(\tau)|u_{0+}(\tau)\rangle + b_m(\tau)|u_{0-}(\tau)\rangle. \tag{5.38}$$

By substitution of the superadiabatic state (5.36) into the Schrödinger equation, and using the expansion (5.38), we find relationships between the $a_m(\tau)$ and $b_m(\tau)$ coefficients:

$$\dot{a}_m(\tau) = -\frac{i}{2H(\tau)}\left(\ddot{a}_{m-1}(\tau) - \dot{a}_{m-1}(\tau)\frac{\ddot{\theta}(\tau)}{\dot{\theta}(\tau)} + \frac{\dot{\theta}(\tau)^2}{4}a_{m-1}(\tau)\right), \tag{5.39}$$

and

$$b_m(\tau) = -\frac{2\dot{a}_m(\tau)}{\dot{\theta}(\tau)}. \tag{5.40}$$

These recurrence relations are supplemented by the conditions $a_0(\tau) = 1, b_0(\tau) = 0$ and $a_m(-\infty) = b_m(-\infty) = 0, m > 0$. With the initial conditions the recurrence relations completely define the superadiabatic states and give an asymptotic expansion of the dynamics.

As mentioned previously, the value of using the superadiabatic basis is that it is possible to calculate the exact final-state transition amplitude (5.35) by first-order perturbation theory. Working in the n-th order superadiabatic basis the final-state transition amplitude is [82]

$$c_{n-}(+\infty) = 2i\epsilon^n \int_{-\infty}^{\infty} dw \frac{a'_{n+1}(w)}{\theta'(w)} \exp\left[-\frac{iw}{\epsilon}\right]. \tag{5.41}$$

Here the prime denotes a derivate with respect to w. We also transform the recurrence relations into functions of w, and solving these close to the eigenenergy degeneracy at $\tau = \tau_c$ we find

$$2i\frac{a'_{n+1}(w)}{\theta'(w)} = \frac{i^{n+1}(n-1/6)!(n-5/6)!(1+\frac{1}{6n})}{(w-w)^{n+1}(n-1)!(-1/6)!(-5/6)!}. \tag{5.42}$$

Using Cauchy's integral formula for the pole of $(n+1)$-order at $w = w_c$ we obtain the final state transition amplitude. In the nth-order superadiabatic basis this is

$$c_n(+\infty) = A_n \exp\left[-\frac{iw_c}{\epsilon}\right], \tag{5.43}$$

where

$$A_n = \frac{2\pi(n+1/6)!(n-1/6)!}{(-1/6)!(-5/6)!(n!)^2}. \tag{5.44}$$

In particular the for higher-order superadiabatic states

$$A_\infty \to 1. \tag{5.45}$$

It is remarkable that by taking the $n \to \infty$ limit of the superadiabatic basis we have derived the correct result, despite the fact that the superadiabatic states themselves do not converge. Some explanation of this is required. When attempting to calculate the dynamics from $|\psi_{\pm}(\tau)\rangle$ directly, it is indeed necessary to truncate the asymptotic series after the smallest term. However, the final state transition amplitude involves transitions between states. Thus, although the representations of the states themselves do not converge, the relationship between theses states is given correctly. This is confirmed by the fact that the transition amplitude in (5.41) goes as ϵ^n. Higher-order superadiabatic states must therefore cling ever more closely to the actual solution, even if the representations themselves do not converge.

For several examples, the extent of the non-adiabatic loss can be calculated analytically. As an example consider, the Landau-Zener Hamiltonian [87, 84] given by

$$Z(\tau) = \tau, \qquad X(\tau) = 1. \tag{5.46}$$

This results in the action

$$w(\tau) = 2\int_0^{\tau} \sqrt{1+\tau'^2}d\tau' = \tau\sqrt{1+\tau^2} + \text{arcsin}[\tau]. \tag{5.47}$$

The complex degeneracies therefore occur when $H(\tau_c) = 0$ and give $\tau_c = \pm i$. At this point in time the action is found to be $w(\tau_c) = \pm i\pi/2$ and the final-state transition amplitude is

$$c_-(\infty) = \exp\left[-\frac{\pi}{2\epsilon}\right]. \tag{5.48}$$

This result has also been extended into the multi-level case for the Landau-Zener model [88].

5.3 Pulses in the Λ System

We now attempt to apply the method of superadiabatic states to the Λ atom (Fig. 2.2). Unlike previous authors we do not restrict our analysis to an exactly resonant, non-decaying Λ atom [89]. On the other hand, we do simplify matters by solving the problem to only first-order in both the EIT probe field and the non-adiabaticity.

In doing so we will give interesting physical explanations for some familiar results, and develop a method easily generalised to the N-configuration atom.

In the following work we are concerned with the situation where the probe field Ω_a is time-dependent. To first-order in the EIT field the approximate adiabatic states are given by

$$|\phi_1(\tau)\rangle = |1\rangle - \frac{\Omega_a(\tau)\Omega_b}{2N_-\lambda_-}|C_-\rangle - \frac{\Omega_a(\tau)\Omega_b}{2N_+\lambda_+}|C_+\rangle, \tag{5.49}$$

$$|\phi_2(\tau)\rangle = |C_-\rangle + \frac{\Omega_a(\tau)\Omega_b}{2N_-\lambda_-}|1\rangle, \tag{5.50}$$

$$|\phi_3(\tau)\rangle = |C_+\rangle + \frac{\Omega_a(\tau)\Omega_b}{2N_+\lambda_+}|1\rangle. \tag{5.51}$$

Where the states $|C_\pm\rangle$, given by (3.25)-(3.26), are the dressed states of the two-level subsystem composed of the field Ω_b coupling the bare atomic levels $|2\rangle$ and $|3\rangle$. We choose to expand the solution in terms of the approximate adiabatic state basis:

$$|\psi(\tau)\rangle = d_1(\tau)|\phi_1(\tau)\rangle + d_2(\tau)|\phi_2(\tau)\rangle + d_3(\tau)|\phi_3(\tau)\rangle. \tag{5.52}$$

Substitution of (5.52) into the Schrödinger equation (5.20) yields the equation of motion for the adiabatic state coefficients. The adiabatic state coefficients are then found to obey

$$i\epsilon\frac{d}{d\tau}\begin{bmatrix} d_1(\tau) \\ d_2(\tau) \\ d_3(\tau) \end{bmatrix} = \begin{bmatrix} \hbar\lambda_1(\tau) & \epsilon\tilde{\Omega}_-^*(\tau) & \epsilon\tilde{\Omega}_+^*(\tau) \\ \epsilon\tilde{\Omega}_-(\tau) & \hbar\lambda_2(\tau) & 0 \\ \epsilon\tilde{\Omega}_+(\tau) & 0 & \hbar\lambda_3(\tau) \end{bmatrix}\begin{bmatrix} d_1(\tau) \\ d_2(\tau) \\ d_3(\tau) \end{bmatrix}. \tag{5.53}$$

The off-diagonal coupling that gives rise to the mixing of the dressed states is given by

$$\tilde{\Omega}_\pm(\tau) = \frac{i\Omega_b^*}{2N_\pm\lambda_\pm}\frac{d\Omega_a(\tau)}{d\tau}. \tag{5.54}$$

In an analogous way to the two-level atom, we attempt to find solutions to the dynamics by expanding the solution in terms of the adiabaticity parameter ϵ. However, in a slight departure from the method used by Berry [82, 84, 85] we suppose the solution has the general form

$$|\psi(\tau)\rangle = \sum_{s=1}^{3}\exp\left[-\frac{i}{\epsilon}\int_0^\tau \hbar\tilde{\lambda}_s(\tau')d\tau'\right]|\tilde{\phi}_s(\tau)\rangle, \tag{5.55}$$

where $|\tilde{\phi}_s(\tau)\rangle$ and $\hbar\tilde{\lambda}_s(\tau)$ are both asymptotic expansions in ϵ representing the time-dependent superadiabatic state and energy. In the limit $\tau \to \pm\infty$ these are identical to the adiabatic state $|\phi_s(\tau)\rangle$ and eigenenergy $\hbar\lambda_s(\tau)$. By writing the superadiabatic state in this form we are able to calculate it by using standard non-degenerate perturbation theory where the Hamiltonian is split into

$$H_0 = \hbar \begin{bmatrix} \lambda_1(\tau) & 0 & 0 \\ 0 & \lambda(\tau) & 0 \\ 0 & 0 & \lambda_3(\tau) \end{bmatrix} \qquad V = \begin{bmatrix} 0 & \tilde{\Omega}_-^*(\tau) & \tilde{\Omega}_+^*(\tau) \\ \tilde{\Omega}_-(\tau) & 0 & 0 \\ \tilde{\Omega}_+(\tau) & 0 & 0 \end{bmatrix} \tag{5.56}$$

To first-order in the adiabaticity parameter and the EIT field we find that the $|\tilde{\phi}_1(\tau)\rangle$ superadiabatic state is given by

$$|\tilde{\phi}_1(\tau)\rangle = |\phi_1(\tau)\rangle - \epsilon\frac{\tilde{\Omega}_-(\tau)}{\hbar\lambda_-}|\phi_2(\tau)\rangle - \epsilon\frac{\tilde{\Omega}_+(\tau)}{\hbar\lambda_+}|\phi_2(\tau)\rangle. \tag{5.57}$$

Written in terms of the real time we have:

$$|\tilde{\phi}_1(t)\rangle = |\phi_1(t)\rangle - \frac{i\Omega_b^*}{2N_-\lambda_-^2}\frac{d\Omega_a(t)}{dt}|\phi_2(t)\rangle - \frac{i\Omega_b^*}{2N_+\lambda_+^2}\frac{d\Omega_a(t)}{dt}|\phi_3(t)\rangle. \tag{5.58}$$

The eigenenergy corresponding to the superadiabatic state $|\tilde{\phi}_1(t)\rangle$ has the value

$$\tilde{\lambda}_1(t) = -\frac{\delta_2|\Omega_a(t)|^2}{4\delta_1\delta_2 - |\Omega_b|^2} - \frac{4[4\delta_2^3 + (\delta_1 + 2\delta_2)|\Omega_b|^2}{(4\delta_1\delta_2 - |\Omega_b|^2)^3}\left(\frac{d\Omega_a(t)}{dt}\right)^2. \tag{5.59}$$

The first term of $\tilde{\lambda}_1(t)$ represents the adiabatic eigenenergy of the EIT system and the second term is the second-order nonadiabatic correction. When both fields are resonant with the Λ atom, only the nonadiabatic term will contribute. By replacing the superadiabatic state by its adiabatic approximant we find that under the influence of a smoothly varying field the state will evolve as

$$|\psi(t)\rangle \approx c_1(0)\exp\left[-\gamma_1\int_0^t \frac{4\delta_1}{|\Omega_b|^4}\left(\frac{d\Omega_a(t')}{dt'}\right)dt'\right]|\phi_1(t)\rangle. \tag{5.60}$$

We can see that due the gradual variation of the electromagnetic field $\Omega_a(t)$ the population in the adiabatic state will slowly decay. This result was first demonstrated by Fleischhauer and Manka [90] when investigating coherent population transfer in the Λ atom. In this paper they showed that the nonadiabatic loss from the dressed

state was *not* exponentially small in the adiabaticity parameter - quite in contrast to the situation in the two-level atom. However, from the derivation given above we can see that the nature of the adiabatic loss is quite different in the two situation. For the two-level atom the loss is caused by non-adiabatic but coherent transition between the dressed states. On their own, the dressed states are radiatively stable. However, for the Λ atom described above the loss arises due to the radiative decay of the superadiabatic state itself. In the model used, the population is simply "lost" to the environment and does not transfer into one of the other adiabatic states. The strikingly different behaviour of the nonadiabatic loss is therefore due to quite different loss mechanisms operating in both situations.

Of particular interest in the work that follows is the off-diagonal density matrix elements of the EIT transition:

$$\rho_{21}(t) = \frac{-2\Omega_a(t)\delta_2}{4\delta_1\delta_2 - |\Omega_b|^2} - \frac{2i(4\delta_2^2 + |\Omega_b|^2)^2}{(4\delta_1\delta_2 - |\Omega_b|^2)}\frac{d\Omega_a}{dt}, \tag{5.61}$$

From here on we assume that the loss from the superadiabatic state is negligible. When operating close to Raman resonance, and for a slowly varying field this approximation is quite appropriate for most purposes (except when studying coherent population transfer of course). From this off-diagonal element, the nonadiabatic linear electric susceptibility can be calculated:

$$\chi^{(1)}(\omega_a;\omega_a,t) = \frac{|p_{12}|^2}{\hbar\epsilon_0 E_a(t)}\left[\frac{4E_a(t)\delta_2}{4\delta_1\delta_2 - |\Omega_b|^2} + \frac{4i(4\delta_2^2+\Omega_b^2)}{(4\delta_1\delta_2 - |\Omega_b|^2)^2}\frac{dE_a(t)}{dt}\right]. \tag{5.62}$$

We note that the susceptibility now has an imaginary term that is proportional to the rate of change on the electric field. Thus, a rapid increase in the field will give rise to a large absorption and vice-versa. Shortly we will see that this term generates slow-light propagation in the Λ atom.

As shown in appendix B the first-order nonadiabatic susceptibility is essentially the temporal representation of the linear susceptibility (2.48) Taylor expanded around the frequency ω_a. On resonance of the probe and control fields we have

$$\chi^{(1)}(\omega_a;\omega_a,t)E_a(t) = i\frac{d\chi^{(1)}}{d\omega_a}\bigg|_{\Delta_a=0}\frac{dE_a(t)}{dt} = \frac{4i|p_{12}|^2}{\hbar\epsilon_0|\Omega_b|^2}\frac{dE_a(t)}{dt} \tag{5.63}$$

The significance of this can be appreciated by substitution of the polarisation $P(\omega_a, t) = \epsilon_0 \hat{\chi}^{(1)}(t) E_a(z,t)$ into the wave equation for the slowly varying envelope (5.5). Rearrangement of this equation gives

$$\left(\frac{d}{dt} + c_g \frac{d}{dz}\right) E_a(z,t) = 0, \tag{5.64}$$

where the group velocity is given by

$$c_g = \frac{c}{1 + \dfrac{\omega_a}{2} \left.\dfrac{d\chi^{(1)}}{d\omega_a}\right|_{\Delta_a=0}} = \frac{c}{n_g}. \tag{5.65}$$

Here, $n_g = 1 + \omega_a \left.\dfrac{d\eta}{d\omega_a}\right|_{\Delta_a=0}$ is the group refractive index and $\eta(\omega_a)$ is the phase refractive index introduced in chapter 1. By transforming into the temporal representation of the susceptibility we gain an insight into the non-adiabatic origin of slow light. Essentially, the reduced group velocity is caused due to polarisation acting to coherently absorb the front of the pulse, but amplify the tail. It is this "Lenz-law" type behaviour that causes the remarkable reductions in group velocity that have been demonstrated [48].

5.4 Pulses in the N System

The calculations performed in the previous section can quite easily be extended to the N-configuration atom, as was done in the candidate's publication [61]. Again we assume that only the field Ω_a is slowly varied. We begin by writing down the adiabatic states of the N-configuration atom, as determined in section 4.2. These are

$$|\phi_1(\tau)\rangle = |1\rangle - \frac{\Omega_a(\tau)\Omega_b^*}{2\bar{N}_-\bar{\lambda}_-}|C_-\rangle - \frac{\Omega_a(\tau)\Omega_b^*}{2\bar{N}_+\lambda_+} - \frac{\Omega_a(\tau)\Omega^*\Omega_c}{2\delta_3(4\delta_1\delta_2 - |\Omega_b|^2)}|4\rangle, \tag{5.66}$$

$$|\phi_2(\tau)\rangle = |C_-\rangle + \frac{\Omega_a^*(\tau)\Omega_b}{2\bar{N}_-\bar{\lambda}_-}|1\rangle - \frac{\Omega_c(\lambda_- - \delta_1)}{\bar{N}_-\delta_3}|4\rangle, \tag{5.67}$$

$$|\phi_3(\tau)\rangle = |C_+\rangle + \frac{\Omega_a^*(\tau)\Omega_b}{2\bar{N}_+\bar{\lambda}_+}|1\rangle - \frac{\Omega_c(\lambda_+ - \delta_1)}{\bar{N}_+\delta_3}|4\rangle, \tag{5.68}$$

$$|\phi_4(\tau)\rangle = |4\rangle + \frac{\Omega_c^*(\lambda_- - \delta_1)}{\delta_3\bar{N}_-}|C_-\rangle + \frac{\Omega_c^*(\lambda_+ - \delta_1)}{\delta_3\bar{N}_+}|C_+\rangle. \tag{5.69}$$

We note that only the field $\Omega_a(\tau)$ is time-dependent. All other quantities, such as the normalisations $N_\pm$, are functions of the static fields Ω_b, Ω_c or static detunings $\delta_1, \delta_2, \delta_3$. When taking the time-derivative of the states, this makes the calculations much more straightforward than would be the case if the control field was pulsed. When the time-derivatives of the adiabatic states are expressed in terms of the adiabatic basis we find that

$$|\dot{\phi}_1(\tau)\rangle = -\frac{\Omega_b^*}{2\bar{N}_-\bar{\lambda}_-}\frac{d\Omega_a(\tau)}{d\tau}|\phi_2(\tau)\rangle - \frac{\Omega_b^*}{2\bar{N}_+\bar{\lambda}_+}\frac{d\Omega_a(\tau)}{d\tau}|\phi_3(t)\rangle, \tag{5.70}$$

$$|\dot{\phi}_2(\tau)\rangle = \frac{\Omega_b}{2\bar{N}_-\bar{\lambda}_-}\frac{d\Omega_a(\tau)}{d\tau}|\phi_1(\tau)\rangle, \tag{5.71}$$

$$|\dot{\phi}_3(\tau)\rangle = \frac{\Omega_b}{2\bar{N}_+\bar{\lambda}_+}\frac{d\Omega_a(\tau)}{d\tau}|\phi_1(\tau)\rangle, \tag{5.72}$$

$$|\dot{\phi}_4(\tau)\rangle = 0. \tag{5.73}$$

It is notable that to first-order in the probe fields there is no non-adiabatic coupling between the Λ-atom dressed states and the state $|\phi_4(\tau)\rangle$. This is because second-order the terms of the form $\Omega_a\Omega_c$ have been neglected from the approximate eigenstates.

Since the instantaneous eigenstates form a basis we may express the solution to dynamics as

$$|\psi(\tau)\rangle = d_1(\tau)|\phi_1(\tau)\rangle + d_2(\tau)|\phi_2(\tau)\rangle + d_3(\tau)|\phi_3(\tau)\rangle + d_4(\tau)|\phi_4(\tau)\rangle. \tag{5.74}$$

By substitution of this solution into the Schrödinger equation we find that the adiabatic state coefficients obey the differential equation

$$i\epsilon\frac{d}{d\tau}\begin{bmatrix} d_1(\tau) \\ d_2(\tau) \\ d_3(\tau) \\ d_4(\tau) \end{bmatrix} = \begin{bmatrix} \hbar\lambda_1(\tau) & \epsilon\tilde{\Omega}_-^*(\tau) & \epsilon\tilde{\Omega}_+^*(\tau) & 0 \\ \epsilon\tilde{\Omega}_-(\tau) & \hbar\lambda_2(\tau) & 0 & 0 \\ \epsilon\tilde{\Omega}_+(\tau) & 0 & \hbar\lambda_3(\tau) & 0 \\ 0 & 0 & 0 & \lambda_4(\tau) \end{bmatrix}\begin{bmatrix} d_1(\tau) \\ d_2(\tau) \\ d_3(\tau) \\ d_4(\tau) \end{bmatrix}. \tag{5.75}$$

This matrix equation of motion has exactly the same structure as for the Λ atom, and therefore we expect the non-adiabatic behaviour of the N-configuration atom to be qualitatively identical. It should be noted however that the definitions of the dressed states $|\phi_1(\tau)\rangle, |\phi_2(\tau)\rangle$ and $|\phi_3(\tau)\rangle$ contain components of the bare state $|4\rangle$.

This is obviously not present in the Λ atom, and will lead to a quantitative, if not qualitative change in behaviour between the two systems. Nonetheless the dynamics are essentially very similar.

By the process of first-order perturbation theory described previously we deduce the first-order nonadiabatic state and second-order energy. For the nonadiabatic eigenenergy of the state $|\tilde{\phi}_1(\tau)\rangle$ we have

$$\begin{aligned}\tilde{\lambda}_1(\tau) &= -\frac{\delta_2|\Omega_a(\tau)|^2}{4\delta_1\delta_2-|\Omega_b|^2} - \epsilon^2\frac{4[4\delta_2^3+(\delta_1+2\delta_2)|\Omega_b|^2}{(4\delta_1\delta_2-|\Omega_b|^2)^3}\left(\frac{d\Omega_a(\tau)}{d\tau}\right)^2 - \\ &\quad \epsilon^2\frac{2|\Omega_b|^2|\Omega_c|^2[6\delta_1^2+8\delta_1\delta_2+6\delta_2^2|\Omega_b|^2]}{\delta_3(4\delta_1\delta_2-|\Omega_b|^2)^4}\left(\frac{d\Omega_a(\tau)}{d\tau}\right)^2. \qquad (5.76)\end{aligned}$$

And, the first-order superadiabatic state is found to be given by

$$|\tilde{\phi}_1(\tau)\rangle = |\phi_1(\tau)\rangle - \epsilon\frac{\tilde{\Omega}_-(\tau)}{\hbar\bar{\lambda}_-}|\phi_2(\tau)\rangle - \epsilon\frac{\tilde{\Omega}_+(\tau)}{\hbar\bar{\lambda}_+}|\phi_2(\tau)\rangle, \qquad (5.77)$$

which is identical to the superadiabatic state of the Λ atom although we recall that the instantaneous dressed states are now defined by (5.66)-(5.69).

From the approximate superadiabatic state we can also determine the off-diagonal density matrix elements. For the sake of clarity we again consider the case where the fields are Raman-resonant, $\delta_2 = 0$, and the radiative decay is very small (non-depletion approximation). Thus, we obtain the coherence elements:

$$\begin{aligned}\rho_{21}(t) &= -\frac{\Omega_a|\Omega_c|^2}{2\delta_3|\Omega_b|^2} - \frac{2i}{|\Omega_b|^2}\frac{d\Omega_a}{dt} + \frac{4i|\Omega_c|^2\delta_1}{\delta_3|\Omega_b|^4}\frac{d\Omega_a}{dt}, \qquad (5.78)\\ \rho_{43}(t) &= -\frac{\Omega_a(t)\Omega_c}{2\delta_3|\Omega_b|^2}\left[\Omega_a(t) - \frac{4\Gamma_2}{|\Omega_b|^2}\frac{d\Omega_a}{dt}\right]. \qquad (5.79)\end{aligned}$$

Considering only the cross-phase modulation terms we note that the adiabatic and nonadiabatic terms can be written in the form of a retarded "steady state" response to the fields. That is

$$\begin{aligned}\rho_{21}^{XPM}(t) &= -\frac{\Omega_a(t+\Delta t)|\Omega_c|^2}{2\delta_3|\Omega_b|^2}. \qquad (5.80)\\ \rho_{43}^{XPM}(t) &= -\frac{|\Omega_a(t+\Delta t/2)|^2\Omega_c}{2\delta_3|\Omega_b|^2}, \qquad (5.81)\end{aligned}$$

where $\Delta t = -2\Gamma_2/|\Omega_b|^2$. The XPM responses of the atom are therefore retarded by a period on the order of the GSC and bright-state relaxation times. Thus, the

bright-state relaxation time is again seen to dominate the lag of the nonadiabatic XPM experienced by a pulse, just as it determines the transient rise-time.

In an identical manner to that performed for the Λ atom, the time-dependent nonadiabatic susceptibility experienced by the fields Ω_a and Ω_c can be calculated. On Raman resonance, the susceptibilities experienced by both the Ω_a and Ω_c fields are found to be identical and are

$$\chi^{(3)}_{a,c}(t) = \frac{2|p_{12}|^2|p_{34}|^2}{3\epsilon_0\hbar^3\delta_3|\Omega_b|^2} - \frac{8|p_{12}|^2|p_{34}|^2\Gamma_2\dot{E}_a(t)}{3\epsilon_0\hbar^3|\Omega_b|^4\delta_3 E_a(t)} \tag{5.82}$$

To see how this form of susceptibility effects the propagation of optical pulse, we use (5.82) to construct the polarisation terms for the fields Ω_a and Ω_c:

$$P_a(z,t) = \epsilon\chi^{(1)}(t)E_a(z,t) + \frac{3}{2}\epsilon_0\chi^{(3)}(t)E_a(z,t)|E_c(z,t)|^2, \tag{5.83}$$

$$P_c(z,t) = \frac{3}{2}\epsilon_0\chi^{(3)}(t)E_c(z,t)|E_a(z,t)|^2. \tag{5.84}$$

These polarisation terms will give rise to a pair of coupled wave equations for the fields $E_a(z,t)$ and $E_c(z,t)$. To solve these we first suppose that the field $E_c(z,t)$ is constant in time and is not appreciably absorbed by propagation through the medium in Eq. (5.83). The wave equation for $E_a(z,t)$ can then reduces to the linear partial differential equation

$$\left(\frac{d}{dt} + c\frac{d}{dz}\right)E_a(z,t) = -\frac{\omega_a}{2}\mathrm{Img}\left[\chi^{(1)} + \frac{3}{2}\chi^{(3)}|E_c|^2\right]E_a(z,t). \tag{5.85}$$

The solution to this equation is found to be of the form

$$E_a(z,t) = \exp(-\gamma z)E_a(z - c_g t, 0). \tag{5.86}$$

This solution describes the propagation of an initial pulse profile $E_a(z,0)$ at the group velocity c_g. As the pulse propagates through the medium the small absorptive component of the cross-phase modulation gives rise to a Beer's Law form decay [42] of the pulse at the rate γ. On resonance the absorption coefficient is proportional to the imaginary part of the XPM susceptibility multiplied by the intensity of the constant field $E_c(0,0)$:

$$\gamma = \frac{3\omega_a}{4c}\mathrm{Img}\left[\chi^{(3)}(\omega_{21})\right]|E_c(0,0)|^2. \tag{5.87}$$

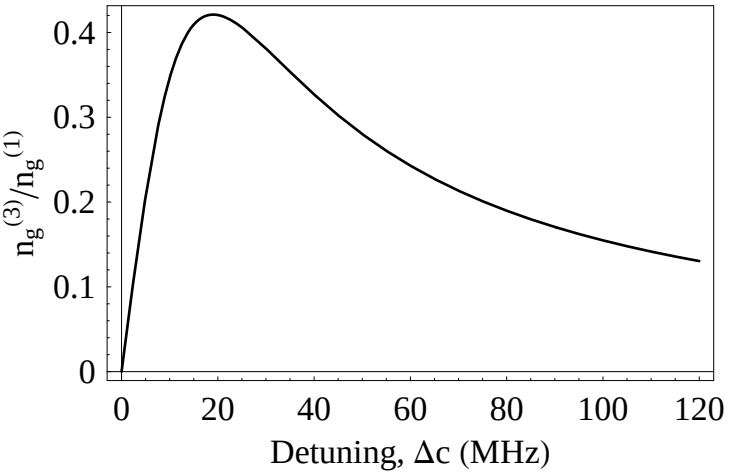

Figure 5.2: The ratio of the cross-phase modulation induced group refractive index $n_g^{(2)}$ to the Λ subsystem group refractive index $n_g^{(0)}$. Plotted for $\Omega_a = 0.5$ MHz, $\Omega_b = 3$ MHz and $\Omega_c = 2$ MHz in ^{87}Rb.

The group velocity is given by $c_g = c/n_g$ where n_g is the group index of refraction, found to be

$$n_g = 1 + n_g^{(0)} + n_g^{(2)}. \tag{5.88}$$

Here the group refractive index is the sum of two terms: $n_g^{(0)}$, the linear term associated with slow light in the Λ subsystem and $n_g^{(2)}$, a contribution due to the nonadiabatic cross-phase modulation:

$$n_g^{(0)} = \frac{\omega_a}{2}\left.\frac{d\chi^{(1)}}{d\omega_a}\right|_{\Delta_a=\Delta_b=0}, \qquad n_g^{(2)} = \frac{3}{2}|E_c|^2 \mathrm{Img}\left[\frac{d\chi^{(3)}}{d\omega_a}\right]\Bigg|_{\Delta_a=\Delta_b=0}. \tag{5.89}$$

The effect of the nonadiabatic XPM makes a significant contribution to the group velocity [91, 61], as is plotted in figure 5.2. Here we see that for values typical of experiments undertaken in rubidium-87 a group velocity reduction of up 40% is possible. This is as we expect. Due to the identical pattern of nonadiabatic coupling between the dressed states we expect a quantitative, although not qualitative difference between pulse propagation in the Λ- and N-configuration atoms. For the phase of the EIT prove field we solve the decoupled wave equation:

$$c\frac{d}{dz}\phi_a(z) = \frac{3}{4}\omega_a|E_c|^2 \mathrm{Re}\left[\chi^{(3)}(\omega_{21})\right], \tag{5.90}$$

This has the straightforward solution

$$\phi(z) = \varphi z + \phi(0). \tag{5.91}$$

where

$$\varphi = \frac{3\omega_a}{4c}|E_c(0,0)|^2 \mathrm{Re}\left[\chi^{(3)}(\omega_{21})\right]. \tag{5.92}$$

Thus, the field accumulates phase at a rate proportional to the XPM refractive index. The existence of a nonadiabatic (slow-light) response makes no difference to the phase refractive index.

For the $E_c(z,t)$ field the wave equation for the field amplitude is given by

$$\left(\frac{d}{dt} + c\frac{d}{dz}\right) E_c(z,t) = -\frac{\omega_c}{2}\left\{\frac{3}{2}\mathrm{Img}[\chi^{(3)}]E_a(z,t)|E_c(z,t)|^2\right\}. \tag{5.93}$$

Here $E_a(z,t)$ is the solution (5.86), which is correct to zeroth-order in $E_c(z,t)$. This gives rise to a solution of the form

$$E_c(z,t) = E_c(0,0)\exp\left[-\frac{3\omega_c \mathrm{Img}\left[\chi^{(3)}\right]}{4(c-c_g)}\int_0^{z-c_g t}|E_a(z',0)|^2 dz'\right]. \tag{5.94}$$

This is best interpreted in the stationary frame of reference of the pulse $\zeta = z - c_g t$. In this frame, the field $E_c(z,t)$ is seen to propagate at a velocity $c - c_g$ and suffer a decay proportional to the XPM induced absorption. Thus the absorption is proportional to the integral of the intensity of the EIT pulse, past which $E_c(z,t)$ has propagated.

For completeness we include the solution for the phase of the field $E_c(z,t)$:

$$\phi_c(z,t) = \phi(0,0)\exp\left[\frac{3\omega_c \mathrm{Re}\left[\chi_c^{(3)}(\omega_c)\right]}{4(c-c_g)}\int_0^{z-c_g t} E_a(z')dz'\right], \tag{5.95}$$

where

$$\mathrm{Re}\left[\chi_c^{(3)}(\omega_c)\right] = \frac{2N|p_{12}|^2|p_{34}|^2\Gamma_3}{3\epsilon_0 V(\Delta_c^2+\gamma_3^2)|\Omega_b|^2}. \tag{5.96}$$

Again, the form of this is best understood in the stationary frame of reference of the pulse $E_a(z,t)$. In this case, the phase is seen to depend on the total XPM induced "refractive depth" that the field $E_c(z,t)$ has propagated through.

5.5 Chapter Summary

In this chapter we have explored the time-dependent behaviour of the N-configuration atom when the EIT probe field is slowly varied. We have shown that by examining the system in terms of the superadiabatic basis, a method originally employed for the two-level atom, we can gain a deeper understanding of the nonadiabatic behaviour. In particular, we have shown that the nonadiabatic response of the cross-phase-modulation can be written as a retarded version of the steady-state behaviour. The period of retardation, the "atomic lag" to changes in the applied field, is equal to the relaxation time of the bright superposition of the ground states. As in the case of the transient XPM response, the relaxation of the bright state plays a central role in determining the time-dependent behaviour of the atom; although in the steady state only the dark state is of significance.

The introduction of the XPM probe field Ω_c is also observed to have a significant influence on slow-light propagation. For fairly typical values in a rubidium-87 experiment one could expect to obtain changes in the group refractive index of up to 40 %.

Conclusions

The work presented in this thesis has explored the generation of cross-phase modulation in the N-configuration atom. Particular emphasis has been placed on the experimental applicability of the theory to a vapour of cold rubidium-87. In chapter 3 we first explored cross-phase modulation in the steady-state regime. A general expression was obtained for the magnitude of the linear, self-Kerr and cross-Kerr responses of the N-configuration atom. As hoped, we found that a very large and pure cross-phase modulation can be produced. This occurs so long as the detunings of the electromagnetic fields are adjusted to produce coherent population trapping in the Λ subsystem and an off-resonant coupling to the fourth level of the N system by a weak probe. By examining the system in terms of the partly dressed basis we saw that the generation of the steady-state XPM arises due to the perturbation of the Λ-atom dark state produced by the parametric coupling to the fourth level of the N system.

Chapter 4 investigated transient cross-phase modulation induced by the sudden turn-on of the EIT probe field. It was shown that the decay rate of the bright state superposition of the Λ-atom ground states dominates the transient dynamics of the N-configuration atom. Indeed, the rise time of XPM on both probe transitions was shown to occur on a time scale equal to the relaxation of the atom into the dark state. In addition, it was shown that the EIT probe field will also experience a very large transient absorption when suddenly turned-on.

Remarkably, by working in the partly dressed basis it was shown that the transient XPM experienced on the non-EIT probe transition arises due to contributions from both the bright and dark states. Thus, although it is coupling between the

dark state and fourth state that produced XPM with steady fields, a significant contribution also arises due to coupling between the bright and fourth states in the transient regime.

Finally, chapter 5 explored the effect of slowly varying the intensity of the EIT probe field. The theory was developed by constructing the first-order superadiabatic state of the N-configuration atom. By doing so it was shown that XPM can have a significant effect on the propagation of slow light through an atomic ensemble. Again, the response of the atoms to changes in the EIT probe field intensity was show to "lag" by a period equal to the bright state relaxation time.

Throughout this thesis it has been shown that the greatest physical insight into atomic dynamics is obtained by working in the dressed (or partly) dressed picture of the atom. The utility of such an approach is however limited when considering the dynamics of atoms driven by continuously varying electromagnetic fields. Nonetheless, by introducing the concept of superadiabatic states it was shown that similar insight can be obtained even when the Hamiltonian is a continuous function of time.

Appendix A

Perturbation Theory

In general it is possible to diagonalise any matrix of dimension up to 4×4. However, in practice the expressions rapidly become unwieldy. Nonetheless, if an exact solution is not required then non-degenerate time-independent perturbation theory can be used to determine the eigensystem. Indeed, for systems of dimension higher than four, exact diagonalisation is generally impossible. Nonetheless, several important Hamiltonians, such as the simple harmonic oscillator, can be put in diagonal form.

Non-degenerate time-independent perturbation theory is covered extensively in several undergraduate text books on quantum mechanics [92]. However, the form developed here will follow a slightly modified approach that makes it more suitable to our applications. Namely, we will consider the effect of two independent perturbations on the eigenstates of the system.

The underlying assumption of perturbation theory is that the system we are attempting to solve is very similar to one for which exact solutions are already known. The difference between the Hamiltonian $\hat{H}$ of the system of interest and the exactly solvable Hamiltonian $\hat{H}_0$ can be parameterised by some small variables ξ_i. We therefore expect to be able to expand the eigenvectors and eigenvalues of $\hat{H}$ as a power series in terms of the ξ_i's, as expressed in (3.32) and (3.33).

Using the expressions (3.35) and (3.36) formulae for the low-order corrections to the energy eigenvalues and eigenvectors can be found. However, for a particular type of "layered perturbation" a large number of eigenvalue and eigenstate expansion

coefficients will vanish. Indeed, the type of perturbation used in this these (that of two electromagnetic fields coupling opposite parity states by the dipole interaction) will be of the layer type. Up to forth-order the non-vanishing eigenvalue terms are given by

$$E_n^{(2,0)} = \langle\phi_n^{(0,0)}|\hat{V}_a|\phi_n^{(1,0)}\rangle, \tag{A.1}$$

$$E_n^{(0,2)} = \langle\phi_n^{(0,0)}|\hat{V}_c|\phi_n^{(0,1)}\rangle, \tag{A.2}$$

$$E_n^{(4,0)} = \langle\phi_n^{(0,0)}|\hat{V}_a|\phi_n^{(3,0)}\rangle - E_n^{(2,0)}a_n^{n(0,2)}, \tag{A.3}$$

$$E_n^{(0,4)} = \langle\phi_n^{(0,0)}|\hat{V}_c|\phi_n^{(0,3)}\rangle - E_n^{(0,2)}a_n^{n(0,2)}, \tag{A.4}$$

$$E_n^{(2,2)} = \langle\phi_n^{(0,0)}|\hat{V}_a|\phi_n^{(1,2)}\rangle + \langle\phi_n^{(0,0)}|\hat{V}_c|\phi_n^{(2,1)}\rangle - E_n^{(0,2)}a_n^{n(2,0)} - E_n^{(2,0)}a_n^{n(0,2)}. \tag{A.5}$$

And, up to third-order the non-vanishing eigenstate expansion coefficient terms are (where $n \neq m$)

$$a_n^{m(1,0)} = \frac{\langle\phi_m^{(0,0)}|\hat{V}_a|\phi_n^{(0,0)}\rangle}{E_n^{(0,0)} - E_m^{(0,0)}}, \tag{A.6}$$

$$a_n^{m(0,1)} = \frac{\langle\phi_m^{(0,0)}|\hat{V}_c|\phi_n^{(0,0)}\rangle}{E_n^{(0,0)} - E_m^{(0,0)}}, \tag{A.7}$$

$$a_n^{m(2,0)} = \frac{\langle\phi_m^{(0,0)}|\hat{V}_a|\phi_n^{(1,0)}\rangle}{E_n^{(0,0)} - E_m^{(0,0)}}, \tag{A.8}$$

$$a_n^{m(0,2)} = \frac{\langle\phi_m^{(0,0)}|\hat{V}_c|\phi_n^{(0,1)}\rangle}{E_n^{(0,0)} - E_m^{(0,0)}}, \tag{A.9}$$

$$a_n^{n(2,0)} = -\frac{1}{2}\sum_{s=1}^{d}|a_n^{s(1,0)}|^2, \tag{A.10}$$

$$a_n^{n(0,2)} = -\frac{1}{2}\sum_{s=1}^{d}|a_n^{s(0,1)}|^2, \tag{A.11}$$

$$a_n^{m(1,1)} = \frac{\langle\phi_m^{(0,0)}|\hat{V}_a|\phi_n^{(0,1)}\rangle + \langle\phi_m^{(0,0)}|\hat{V}_b|\phi_n^{(1,0)}\rangle}{E_n^{(0,0)} - E_m^{(0,0)}}, \tag{A.12}$$

$$a_n^{m(3,0)} = \frac{\phi_m^{(0,0)}|\hat{V}_a|\phi_n^{(2,0)}\rangle - E_n^{(2,0)}a_n^{m(1,0)}}{E_n^{(0,0)} - E_m^{(0,0)}}, \tag{A.13}$$

$$a_n^{m(0,3)} = \frac{\phi_m^{(0,0)}|\hat{V}_c|\phi_n^{(0,2)}\rangle - E_n^{(0,2)} a_n^{m(0,1)}}{E_n^{(0,0)} - E_m^{(0,0)}}, \tag{A.14}$$

$$a_n^{m(2,1)} = \frac{\langle\phi_m^{(0,0)}|\hat{V}_a|\phi_n^{(1,1)}\rangle + \langle\phi_m^{(0,0)}|\hat{V}_c|\phi_n^{(2,0)}\rangle - E_n^{(2,0)} a_n^{m(0,1)}}{E_n^{(0,0)} - E_m^{(0,0)}}, \tag{A.15}$$

$$a_n^{m(1,2)} = \frac{\langle\phi_m^{(0,0)}|\hat{V}_a|\phi_n^{(0,2)}\rangle + \langle\phi_m^{(0,0)}|\hat{V}_c|\phi_n^{(1,1)}\rangle - E_n^{(0,2)} a_n^{m(1,0)}}{E_n^{(0,0)} - E_m^{(0,0)}}. \tag{A.16}$$

Appendix B

Operator Representations

B.1 Position and Momentum Operators

In elementary quantum mechanics we are commonly concerned with determining the properties of the wavefunction represented in real space. That is, the squared magnitude of the wavefunction gives the probability density of detecting a particle in a certain region of space (the domain, e.g. $-\infty < x < \infty$). When using the real space representation of the wavefunction, the conjugate position and momentum operators are given by

$$\hat{x} = x, \qquad \hat{p} = -i\hbar\frac{d}{dx}. \tag{B.1}$$

However, by Fourier transforming the real-space wavefunction it is possible to construct its momentum-space counterpart. That is, a function whose squared magnitude defines the probability density of detecting a particle with a given momentum (at any point in the domain). For some arbitrary function of the momentum operator $\hat{f} = f(\hat{p})$ we determine the representation in momentum space by considering the Fourier transform of its action on a wavefunction in real space.

$$\frac{1}{\sqrt{2\pi\hbar}}\int_{-\infty}^{\infty} f\left(-i\hbar\frac{d}{dx}\right)\psi(x)\exp(-ipx/\hbar)dx. \tag{B.2}$$

However, since the operator $f(\hat{p})$ can be Taylor expanded we can write the integral as sum of terms of the form

$$\frac{1}{\sqrt{2\pi\hbar}}\int_{-\infty}^{\infty} \left(-i\hbar\frac{d}{dx}\right)^n\psi(x)\exp(-ipx/\hbar)dx. \tag{B.3}$$

After n integration by parts, and assuming that the wavefunction and all of its derivatives vanish as $x \to \pm\infty$ we find that the above is equal to

$$p^n \tilde{\psi}(p), \tag{B.4}$$

where $\tilde{\psi}(p)$ is the momentum space wavefunction. Therefore, the real and momentum-space representation of an operator are related by

$$f(\hat{p}) = \begin{cases} f\left(-i\hbar\dfrac{d}{dx}\right), & \text{in real space} \\ f(p), & \text{in momentum space} \end{cases} \tag{B.5}$$

Similarly, for the position operator we find $\hat{x} = x$ in real space and $\hat{x} = i\hbar\dfrac{d}{dp}$ in momentum space.

B.2 Susceptibility Operator

The result above is a general property of any operators acting on functions that can be Fourier transformed. Consider the polarisation of a linear dielectric material:

$$\tilde{P}(\omega) = \epsilon_0 \chi(\omega) \tilde{E}(\omega). \tag{B.6}$$

Here, $\tilde{E}(\omega)$ is the Fourier transform of the time-dependent electromagnetic field and the susceptibility is the frequency space representation. Again, by Taylor expanding the electric susceptibility in terms of ω, we find the corresponding temporal-space representation:

$$\chi(\hat{\omega}) = \begin{cases} \chi(\omega), & \text{in frequency space} \\ \chi\left(i\dfrac{d}{dt}\right), & \text{in temporal space} \end{cases} \tag{B.7}$$

We note that we rely on the linearity of the dielectric medium to make this transformation. Furthermore, we stress that the description of the susceptibility as an operator is valid for classical as well as quantum mechanical fields. The use of the operator formalism is a mathematical device, rather than of physical significance.

As an example, let us consider EIT in the Λ atom. From Eq. (2.48) we can see that for a resonant control field we can Taylor expand the linear susceptibility to

first-order in ω_a to give

$$\chi^{(1)}(\omega_a;\omega_a) = \frac{4\Delta_a|p_{12}|^2}{\hbar\epsilon_0[4\Delta_a(\Delta_a - i\gamma_1) - |\Omega_b|^2]} \approx \frac{4|p_{12}|^2}{\hbar\epsilon|\Omega_b|^2}(\omega_a - \omega_{21}) \tag{B.8}$$

Then, by making the substitution $\omega_a \rightarrow i\dfrac{d}{dt}$ we get the temporal representation of the Taylor expanded linear susceptibility:

$$\hat{\chi}^{(1)}(t) = \frac{4|p_{12}|^2}{\hbar\epsilon_0|\Omega_b|^2}(i\frac{d}{dt} - \omega_{21}). \tag{B.9}$$

Let us suppose that the susceptibility operator is acting on an *almost* monochromatic field. That is, we work in the slowly-varying envelope approximation so that $E(t) = E_a(t)\exp(-i\omega_a t)$. Then, the susceptibility operator *acting on the field envelope only* is given by

$$\hat{\chi}^{(1)}(t) = i\frac{d\chi^{(1)}}{d\omega_a}\bigg|_{\Delta_a=0}\frac{d}{dt} = \frac{4i|p_{12}|^2}{\hbar\epsilon_0|\Omega_b|^2}\frac{d}{dt}. \tag{B.10}$$

It is seen that the derivative of the susceptibility around resonance is directly related to the non-adiabatic response of the atom.

A similar process can be undertaken to derive the non-adiabatic cross-Kerr susceptibility of the Ω_a transition in the N-configuration atom. We begin by noting that the XPM susceptibility can be calculated in the steady state to be

$$\chi^{(3)}(\omega_a;\omega_a,\omega_c,-\omega_c) = \frac{2N|p_{12}|^2|p_{34}|^2|\Omega_b|^2}{3\epsilon_0\hbar^3V(\delta_3 - i\gamma_3)[4\delta_2(i\gamma_1 - \delta_1) + |\Omega_b|^2]^2}. \tag{B.11}$$

If we assume that the control field is resonant ($\Delta_b = 0$) and Taylor expand around resonance of the probe field we find

$$\hat{\chi}^{(3)}(t) = \frac{2N|p_{12}|^2|p_{34}|^2}{3\epsilon_0\hbar^3V\delta_3|\Omega_b|^2} - 8N|p_{12}|^2|p_{34}|^2\Gamma_2 3V\epsilon_0\hbar^3\delta_3|\Omega_b|^4\frac{d}{dt}. \tag{B.12}$$

Here we have employed the condition that δ_3 is very large and the derivative operator is taken to be acting on the slowly varying field $\Omega_a(t)$. Again, this is identical to that calculated by using the first-order superadiabatic state method in chapter 5. However, we note that using this method it is not possible to calculate the nonlinear susceptibility experienced by the Ω_c field, due to the nonlinearity with respect to the pulsed field Ω_a. Although, it should be noted that when $\Delta_a = \Delta_b = 0$ the nonadiabatic XPM experienced by both fields is actually identical.

Bibliography

[1] I. Newton. *Opticks*. William Innys, 1704.

[2] C. Huygens. *Traité de la lumiere*. Chez Pierre van der Aa, 1690.

[3] T. Young. The bakerian lecture. experiments and calculations relative to physical optics. *Phil. Trans. R. Soc.*, 94:1, 1803.

[4] P.A.M Dirac. The quantum theory of the emission and absorption of radiation. *Proc. Roy. Soc.*, A114(243), 1927.

[5] V. Weisskopf and E. Wigner. Berechnung der natürlichen linienbreite auf grund der diracschen lichttheorie. *Z. Phys.*, 63:54, 1930.

[6] W.E. Lamb and R.C. Retherford. Fine structure of the hydrogen atom by a microwave method. *Phys. Rev.*, 72(3):241, 1947.

[7] H.B.G. Casimir and D. Polder. The influence of retardation on the london-van der waals forces. *Phys. Rev.*, 73(4):360, 1948.

[8] S.F. Pereira J.-Ph. Poizat S. Schiller G. Breitenbach, T. Müller and J. Mlynek. Squeezed vacuum from a monolithic optical parametric oscillator. *J. Opt. Soc. Am. B*, 12(11):2304, 1995.

[9] R. Short and L. Mandel. Observation of sub-poissonian photon statistics. *Phys. Rev. Lett.*, 51(5):384, 1983.

[10] G. Brassard C.H. Bennett and C. Crépeau. Teleporting and unknown quantum state via dual classical and einstein-podolsky-rosen channels. *Phys. Rev. Lett.*, 70(13):1895, 1993.

[11] B.I. Erkmen and J.H Shapiro. Unified theory of ghost imaging with gaussian-state light. *Phys. Rev. A*, 77:043809, 2008.

[12] D.S. Abrams A.N. Boto, P. Kok and S.L. Braunstein. Quantum interferometric optical lithography: exploiting entanglement to beat the diffraction limit. *Phys. Rev. Lett.*, 85(13), 2000.

[13] A.K. Ekert. Quantum cryptography based on bell's theorem. *Phys. Rev. Lett.*, 67(6):661, 1991.

[14] W.J. Munro, K. Nemoto, and T.P. Spiller. Weak nonlinearities: a new route to optical quantum computation. *New J. Phys.*, 7(137), 2007.

[15] J.H. Shapiro and M. Razavi. Continuous-time cross-phase modulation and quantum computation. *New J.Phys.*, 9(16), 2007.

[16] J.D. Jackson. *Classical Electrodynamics*. John Wiley & Sons, Inc., third edition, 1999.

[17] L. Allen and J.H Eberly. *Optical Resonance and Two-Level Atoms*. John Wiley & Sons, Inc., 1975.

[18] R.L. Walsworth M. Fleischhauer, S.F. Yelin. Tunable negative refraction without absorption via electromagnetically induced chirality. *Phys. Rev. Lett.*, 99:073602, 2007.

[19] J.B. Pendry. A chiral route to negative refraction. *Science*, 306:1353, 2004.

[20] R.W. Boyd. *Nonlinear Optics*. Academic Press, second edition, 2003.

[21] A. Imamoğlu K.-J. Boller and S.E. Harris. Observation of electromagnetically induced transparency. *Phys. Rev. Lett.*, 66(20):2593, 1991.

[22] R. Louden. *The Quantum Theory of Light*. Oxford University Press, second edition, 1983.

[23] H. Goldstein. *Classical Mechanics*. Addison-Wesely Publishing Company, Inc., second edition, 1981.

[24] S.K. Lamoreaux. Demonstration of casimir force in the 0.6 to 6 μ m range. *Phys. Rev. Lett.*, 78(1):5, 1997.

[25] U. Leonhardt and T. Philbin. Quantum levitation by left-handed metamaterials. *New J. Phys.*, 9:254, 1997.

[26] C.C. Gerry and P.L. Knight. *Introductory Quantum Optics*. Cambridge University Press, 2005.

[27] P. Carruthers and M.M. Neito. Coherent states and the number-phase uncertainty relation. *Phys. Rev. Lett.*, 14(11):387, 1965.

[28] T.H. Maiman. Stimulated optical radiation in ruby. *Nature*, 187(493), 1960.

[29] J. Kerr. A new relation between electricity and light; dielectric media birefringence. *Philosophical Magazine and Journal of Science*, 50:332–348, 1875.

[30] G.P. Agrawal. *Nonlinear Fiber Optics*. Academic Press, third edition, 2001.

[31] R. Leonhardt J.D. Harvey J.C. Knight W.J. Wadsworth P. St. J. Russell S. Coen, A.H. Lun. Supercontinuum generation by stimulated raman scattering and parametric four-wave mixing in photonic crystal fibers. *J. Opt. Soc. Am. B*, 19(4):753, 200.

[32] P.G. Drazin and R.S. Johnson. *Solitons: an introduction*. Cambridge Uninversity Press, 1989.

[33] A. Hasegawa and F. Tappert. Transmission of stationary nonlinear optcial pulses in dispersive dielectric fibers. i. anonalous dispersion. *Appl. Phys. Lett.*, 23(3):142–144, 1973.

[34] A. Hasegawa and F. Tappert. Transmission of stationary nonlinear optical pulses in dispersive dielectric fibers. ii. normal dispersion. *Appl. Phys. Lett.*, 23(4):171–172, 1973.

[35] H.A. Haus N. Imoto and Y.Yamamoto. Quantum nondemolition measurement of the photon number via the optical kerr effect. *Phys. Rev. A*, 32(4):2287, 1985.

[36] S.M. Barnett and P.M. Radmore. *Methods in theoretical quantum optics*. Oxford University Press, 2002.

[37] U. Litzén A. Thorne and S. Johansson. *Spectrophysics: principles and applications*. Springer Verlag, 1999.

[38] R.G. Beausoleil, W.J. Munro, and T.P. Spiller. Applications of coherent population transfer to quantum information processing. *Phys. Rev. A*, 51(11):1559–1601, 2004.

[39] M.O. Scully and S. Zubairy. *Quantum Optics*. Cambridge University Press, 1997.

[40] N.B. Narozhny J.H. Eberly and J.J. Sanchez-Mondragon. Periodic spontaneous collapse and revival in a simple quantum model. *Phys. Rev. Lett.*, 1980.

[41] A. Maali J. Dreyer E. Hagley J.M. Raimond M. Brune, F. Schmidt-Kaler and S. Haroche. Quantum rabi oscillations: a direct test of field quantization in a cavity. *Phys. Rev. Lett.*, 76(11):1800, 1996.

[42] P. Meystre and M. Sargent III. *Elements of Quantum Optics*. Springer-Verlag, fourth edition, 2007.

[43] T. Matsuda A. Tonomura, J. Endo and T. Kawasaki. Demonstration of single-electron buildup of an interference pattern. *Am. J. Phys.*, 57(2):117, 1989.

[44] U. Fano. Effects of configuration interaction on intensities and phase shifts. *Phys. Rev.*, 124(6):1866, 1961.

[45] E. Arimondo. In E. Wolf, editor, *Progress in Optics*, volume XXXV, chapter V. Elsevier, 1996.

[46] A. Imamoğlu and S.E. Harris. Lasers without inversion: interference of dressed lifetime-broadened states. *Opt. Lett.*, 14(24):1344, 1989.

[47] S.H. Autler and C.H. Townes. Stark effect in rapidly varying fields. *Phys. Rev.*, 100(2):703, 1955.

[48] Z. Dutton L.V. Hau, S.E. Harris and C.H. Behroozi. Light speed reduction to 17 meters per second in an ultracold atomic gas. *Nature*, 397:594, 1999.

[49] M. Fleischhauer and M.D. Lukin. Dark-state polaritons in electromagnetically induced transparency. *Phys. Rev. Lett.*, 84(22):5094, 2000.

[50] M. Fleischhauer and M.D. Lukin. Quantum memory for photons: dark-state polaritons. *Phys. Rev. A*, 65:022314, 2002.

[51] A. Mair D.F. Phillips, A. Fleischhauer and R.L. Walsworth. Storage of light in atomic vapor. *Phys. Rev. Lett.*, 86(5):783, 2001.

[52] M.J. Sellars J.J. Longdell, E. Fraval and N.B. Manson. Stopped light with storage times greater than one second using electromagnetically induced transparency in a solid. *Phys. Rev. Lett.*, 95:063601, 2005.

[53] F. Massou M. Fleischhauer A.S. Zibrov M.D. Eisaman, A. Andre and M.D. Lukin. Electromagnetically induced transparency with tunable single-photon pulses. *Nature*, 438(8):837, 2005.

[54] H. Schmidt and A. Imamoğlu. Giant kerr nonlinearities obtained by electromagnetically induced transparency. *Opt. Lett.*, 21(23), 1996.

[55] Z.B. Wang, K.P. Marzlin, and B.C. Sanders. Large cross-phase modulation between slow copropagating weak pulses in ^{87}rb. *Phys. Rev. Lett.*, 97:063901, 2006.

[56] J. Fiurášek, L. Mišta, and R. Filip. Entanglement concentration of continuous-variable quantum states. *Phys. Rev. A*, 67(2):022304, Feb 2003.

[57] D. Menzies and N. Korolkova. Procrustean entanglement concentration of continuous-variable states of light. *Phys. Rev. A*, 74:042315, 2006.

[58] I.L. Chuang and Y. Yamamoto. Simple quantum computer. *Phys. Rev. A*, 52(5), 1995.

[59] G.F. Sinclair and N. Korolkova. Cross-kerr interaction in a four-level atomic system. *Phys. Rev. A*, 76:033803, 2007.

[60] G.F. Sinclair and N. Korolkova. Effective cross-kerr hamiltonian for a nonresonant four-level atom. *Phys. Rev. A*, 77:033843, 2008.

[61] G. Sinclair. Time-dependent cross-phase modulation in rubdium-87. *Phys. Rev. A*, 79:023815, 2009.

[62] M.J. Hartmann F.G.S.L Branão and M.B. Plenio. Light-shift-induced photonic nonlinearities. *New J. Phys.*, 10:043010, 2008.

[63] J. Yao C. Xie H. Chang, Y. Du and H. Wang. Observation of cross-phase shift in hot atoms with quantum coherence. *Europhys. Lett.*, 65(4):485, 2004.

[64] H. Kang and Y. Zhu. Observation of large kerr nonlinearity at low light intensities. *Phys. Rev. Lett.*, 91(9):093601, Aug 2003.

[65] Robert W. Boyd. *Nonlinear Optics*. Academic Press, 2003.

[66] D.A. Steck. Rubidium 87 d line data. Technical report, Theoretical Division (T8), MS B285, Los Alamos National Laboratory, 2001.

[67] Chris Candler. *Atomic Spectra*. Hilger & Watts Ltd., second edition, 1964.

[68] P.R. Berman and R. Salomaa. Comparison of dressed-atom and bare-atom pictures in laser spectroscopy. *Phys. Rev. A*, 25(5):2667, 1982.

[69] G-C. Pan Y-F. Chen and I.A. Ye. Frequency modulation-induced transient oscillation in the spectra of electromagnetically induced transparency. *J. Opt. Soc. Am. B*, 21(9):1647, 2004.

[70] T.Y. Kwon S. Park, H. Cho and H.S. Lee. Transient coherence oscillation induced by a detuned raman field in a rubidium λ-system. *Phys. Rev. A*, 69:023806, 2004.

[71] S.R. de Echaniz A.V. Durrant J.P. Marangos D.M. Segal A.D. Greentree, T.B. Smith and J.A. Vaccaro. Resonant and off-resonant transients in electromagnetically induced transparency: Turn-on and turn-off dynamics.

[72] A.V. Durrant D.M. Segal J.P. Marangos J.A. Vaccaro S.R. Echaniz, A.D. Greentree. Observation of transient gain without population inversion in a laser-cooled rubidium λ system. *Phys. Rev. A*, 64:055801, 2001.

[73] D. Nikonov G.G. Padmabandu M.O. Scully A.V. Smith F.K. Tittle C. Wang S.R. Wilkinson E.S. Fry, X. Li. Atomic coherence effects within the sodium d_1 line: Lasing without inversion via population trapping. *Phys. Rev. Lett.*, 70(21):3235, 1993.

[74] R.M. Camacho M.V. Pack and J.C. Howell. Transients of the electromagnetically-induced transparency-enhanced refractive kerr nonlinearity: Theory. *Phys. Rev. A*, 74:013812, 2006.

[75] R.M. Camacho M.V. Pack and J.C. Howell. Transients of the electromagnetically-induced-transparency-enhanced refractive kerr nonlinearity. *Phys. Rev. A*, 76:033835, 2007.

[76] H. Failache P. Valente and A. Lezama. Temporal buildup of electromagnetically induced transparency and absorption resonances in degenerate two-level transitions. *Phys. Rev. A*, 67:013806, 2003.

[77] F.X. Kärtner L. Boivin and H.A. Haus. Analytic solution to the quantum field theory of self-phase modulation with a finite response time. *Phys. Rev. Lett.*, 73(2):240, 1994.

[78] S.L. McCall and E.L. Hahn. Self-induced transparency. *Phys. Rev.*, 183(2):457, 1969.

[79] B.D. Calder E. Groves and J.H. Eberly. Pulse areas in multi-soliton propagation. *arXiv*, 2008.

[80] J.B. Ketterson and S.N. Song. *Superconductivity*. Cambridge University Press, 1999.

[81] J.P. Davis and P. Pechukas. Nonadiabatic transitions induced by a time-dependent hamiltonian in the semi-classical/adiabatic limit: the two-state case. *J. Chem. Phys.*, 64(8):3129, 1976.

[82] M.V. Berry. Histories of adiabatic quantum transitions. *Proc. R. Soc. Lond. A*, 429:61–72, 1990.

[83] A.M. Dykhne. *Sov. Phys. JETP*, 14:941, 1962.

[84] R. Lim and M.V. Berry. Superadiabatic tracking of quantum evolution. *J. Phys. A: Math. Gen.*, 24:3255, 1991.

[85] M.V. Berry and R. Lim. Universal transition prefactors derived by superadiabatic renormalization. *J. Phys. A: Math. Gen.*, 26:4737, 1993.

[86] E.T. Copson. *Asymptotic Expansions*. Cambridge University Press, 1965.

[87] C. Zener. Non-adiabatic crossing of energy levels. *Proc. R. Soc. A*, 137:696, 1932.

[88] A.V. Shytov. Landau-zener transitions in a multilevel system: an exact result. *Phys. Rev. A*, 70:052708, 2004.

[89] M. Elk. Adiabatic transition histories of population transfer in the λ system. *Phys. Rev. A*, 52(5):4017, 1995.

[90] M. Fleischhauer and A.S. Manka. Propagation of laser pulses and coherent population transfer in dissipative three-level systems: an adiabatic dressed-state picture. *Phys. Rev. A*, 54(1):784, 1996.

[91] T.N. Dey and G.S. Agarwal. Observable effects of kerr nonlinearity on slow light. *Phys. Rev. A*, 76:015802, 2007.

[92] F. Mandl. *Quantum Mechanics*. Butterworths, second edition, 1957.